

AALBORG UNIVERSITY

Mobile Communication Master
Department of Electronic Systems



Modelling of the base station radiation pattern in practical urban deployment

Sergio Flores Poveda Master Thesis / 2011-2012
Miguel Miñano Belvis Master Thesis / 2011-2012

Long Master Thesis Information

TITLE:

Modelling of the base station radiation
pattern in practical urban deployment

PROJECT PERIOD:

September 2011 – May 2012

PROJECT GROUP:

Mobile Communication - group 1013

AUTHOR:

Sergio Flores Poveda
Miguel Miñano Belvis

SUPERVISORS:

Troels B. Sørensen
Patrick C. F. Eggers

Number of pages in report: 69

Number of pages in appendix: 55

Total number of pages: 124

Number of copies printed: 5

ABSTRACT

It is well-known that when antennas are placed, it changes its performance due to environmental effects or interactions with the mounting structure.

As a first step, simulations will lead us to quantify the impacts of effects mentioned before on antenna radiation pattern and as a consequence of this, the impact on network parameters performance.

Finally, it will be compared simulations results with the results obtained for a realistic deployment by means of a measurement campaign performed in the urban area of Aalborg.

This report must not be modified, published or reproduced without express permission from the authors. Sergio Flores Poveda and Miguel Miñano Belvis, Aalborg University. 2011.

Preface

This Long Master Thesis has been written by Sergio Flores Poveda and Miguel Miñano Belvis (group 1013, Mobile Communication) from September 2011 to May 2012 at Aalborg University.

It has been written in L^AT_EX and consists of the following chapters: Introduction, Theoretical Background, Modelling antenna deployment, Measurement Campaign, Measurement Campaign Processing and Conclusions. In addition, all the technical details in the report are supported by appendices.

MATLAB has been used to create graphics and give support to the different calculations performed.

Literature references follow IEEE recommendations. Texts, figures and tables are referenced using a number in brackets, as next list show, to indicate the position in the reference list:

Quoted text [Reference Number]

Figure number: Figure Description Reference Number

Table number: Table Description Reference Number

Equation number: Equation Description (Reference Number)

Sergio Flores Poveda - Mobile Communication
Miguel Miñano Belvis - Mobile Communication
Aalborg University, 31st May, 2012

Acknowledgments

We, the authors, would like to express our gratitude to our home university (UMH) for giving us the opportunity of writing our master thesis at Aalborg university.

We would also like to thank our supervisors, Patrick C.F. Eggers and Troels B. Sørensen for their continuous feedback and advices during the supervision and their patience in the beginning of the project.

Thank to our friends in Aalborg, Jan, Ivan, Michael, Zdravko and Emil for making our stay here the best experience of our lives. Also thank to our friends from our department, Carmen, Pablo, Nacho and Victor for all those moments in the university and coffees in the afternoon.

We would like to make a special mention to Ignacio Rodríguez Larrad (Nacho) for his disinterested help and support to our project. He is a real professional.

We will continue in Spanish for our last acknowledgements.

De parte de Miguel:

Por encima de todo, quiero dar las gracias a mi familia, especialmente a mis padres Miguel y Cloti y mi hermano Víctor, por la educación que he recibido todos estos años y su apoyo incondicional durante mi estancia en Aalborg. Mención especial merecen también mi tía Mayte y mi abuelo Alfonso por lo unido que me siento a ellos.

A Amanda, por haber permanecido a mi lado todo este tiempo y por haber sido la luz que me ha alumbrado en los malos momentos.

Gracias también a mis amigos de Alicante por su apoyo.

De parte de Sergio:

El agradecimiento más grande se lo tengo que dar a mi familia. Os debo todo lo que

soy y pueda llegar a ser. Nunca os podré devolver todo lo que me disteis para conseguir ser quien soy. Sé que siempre estareis a mi lado para apoyarme en mis decisiones y etapas de mi vida.

No menos especial es el agradecimiento que siento hacia mi novia, Sara, gracias por todas las conversaciones y ánimos que me has dado a lo largo de esta experiencia y la que llevamos viviendo juntos. Sin tí, nada de esto hubiese sido posible.

Por último, agradecer a todos los amigos que en mi país esperan y mandan apoyos. Y además, a todos los nuevos amigos que aquí he encontrado, Nacho, Pablo, Carmen y todos aquellos que se den por aludidos. También quiero nombrar a Miguel, por aguantarme pacientemente durante todos estos meses tantas horas diarias.

Contents

Information	i
Preface	ii
Acknowledgements	iii
Contents	v
List of Figures	ix
List of Tables	xii
List of Abbreviations	xiii
List of Symbols	xv
Chapter I	
Introduction	1
1.1 Introduction	1
1.2 The problem definition	4
1.3 Methodology	4
1.4 Delimitations	5
Chapter II	
Theoretical Background	6
2.1 Antennas	6
2.1.1 Radiation properties	7
2.1.2 Antennas for Base Station in Mobile communication	8
2.1.3 Impact of antenna features on cellular systems	10
2.2 RF propagation	11
2.2.1 Path loss models	12
2.2.2 Shadowing fading	15
2.2.3 Multipath	17
2.2.4 Angular dispersion	18

Chapter III

Modelling antenna deployment	19
3.1 System Deployment	19
3.2 Angular dispersion	20
3.2.1 State of the art	20
3.2.2 Results	22
3.3 Mounting structure	27
3.3.1 State of the art	28
3.3.2 Results	31
3.4 Angular dispersion & Mounting structure	34
3.5 Summary	37

Chapter IV

Measurement Campaign	39
4.1 Objectives	39
4.2 Measurement planning	39
4.3 Campaign Execution	40
4.4 Results	41

Chapter V

Measurement Campaign Processing	43
5.1 Measurements reliability	43
5.2 Signal Drop Outs	47
5.3 Procedure	49
5.3.1 Data processing	50
5.3.2 Algorithm application	52
5.4 Real deployment analysis	55
5.4.1 Effective pattern simulation	56
5.4.2 Impact on Network parameters	56
5.4.2.1 Simulation results	56
5.5 Explanation about difference between results from measurements and sim- ulations	61
5.5.1 Antenna tilting	61
5.5.2 Non stationary value of Angular Spread along the area	62
5.6 Summary	64

Chapter VI

Conclusions	65
6.1 Conclusions about simulations	65
6.2 Conclusions about effective radiation pattern	65
6.3 General conclusions	65

References	67
-------------------	-----------

Appendix A

Antenna pattern processing	70
A.1 Discretize	70
A.2 Difference	72
A.3 Evaluation	73
A.4 Network parameters performance	75

Appendix B

Effective pattern algorithm	81
B.1 Objectives	81
B.2 Methodology	81
B.2.1 Routes	82
B.2.2 Log-normal fading	86
B.2.3 Uncorrelated noise	87
B.3 Results	90
B.4 Conclusions	93

Appendix C

Measured Signal	94
C.1 UMTS Basics	94
C.2 WCDMA FDD parameters	94
C.2.1 RSCP	95
C.2.2 ISCP	95
C.2.3 SIR	95
C.3 TELENOR	96

Appendix D

Measurements Campaign Routes	97
D.1 Route 1 Data	98
D.2 Route 2 Data	100
D.3 Route 3 Data	102
D.4 Route 4 Data	104
D.5 Route 5 Data	106
D.6 Route 6 Data	108

Appendix E

Equipment Information	110
E.1 Measurement Equipment	110
E.1.1 HUBER&SUHNER SWA-0859/360/4/10/V	110
E.1.2 R&S TSMW	111
E.1.3 Cables	112
E.2 Measurement Setup	112

Appendix F

Data sheets	115
F.1 katherin-scala 742215 Antenna	116
F.2 Panel accessory mounting hardware 738546	118
F.3 Rfd world 206516L Antenna	119
F.4 Panel accessory mounting hardware APM40-2	120
F.5 HUBER&SUHNER	122
F.6 R&S TSMW Universal Network Radio Scanner	123

List of Figures

1.1	Example frequency reuse	2
1.2	Coverage area	3
2.1	Antenna pattern example	7
2.2	Example BSs antennas for outdoor coverage.	9
2.3	Example BSs radiation pattern for outdoor coverage[24].	9
2.4	Antenna downtilt	11
2.5	Path loss definition[3].	12
2.6	example of propagation parameters	13
2.7	Log-normal distribution function with x-axis expressed in dB, see equation (2.8).	16
2.8	Multipath propagation[2].	17
2.9	Signal propagation profile[2].	17
2.10	Multipath direction of arrival[4].	18
3.1	Radiation pattern used for simulations.	20
3.2	Laplacian distribution.	21
3.3	Convolved radiation pattern.	22
3.4	Convolved pattern 180° shifted	23
3.5	Zoom of Figure 3.4	23
3.6	DBC affected	25
3.7	Network parameters calculated for the reference pattern.	26
3.8	SINR and SIR comparison	26
3.9	CDF of $\Delta SINR(x, y)$ and ΔSIR within the total covered area.	27
3.10	Mast distortion at a Omnantenna[11]	28
3.11	Graphic definition of <i>aperture angle</i> α	29
3.12	Simulated mast distortion at a Omnantenna	30
3.13	Linear representation of the different distortion.	30
3.14	Distortions applied to the real antenna pattern.	31
3.15	Power received calculated with different antenna distorted patterns.	32
3.16	Cdf Function of every ΔPr defined by (A.10).	32
3.17	Cdf Function of every $\Delta SINR$ defined by (3.5).	33
3.18	SINR modification after new antenna distorted parameter.	34
3.19	DBC affected	35
3.20	Network parameters comparison between distorted and reference pattern.	35
3.21	CDF of $\Delta SINR$ and ΔSIR	36

3.22 CDF of absolute values of SIR and SINR including distortions within the total covered area.	37
4.1 Aalborg aerial view[3].	40
5.1 WCDMA decoding, [28].	44
5.2 E_c/I_o measured by Network scanner.	44
5.3 Comparison between 8 highest power sum and Single sector Received Power.	45
5.4 Comparison between 8 highest power sum and Single sector Received Power after mean value for each Azimuthal angle.	46
5.5 Route1a for BS, the one which was done twice.	47
5.6 Information for route1a.	48
5.7 Signal drop outs for Route1a.	49
5.8 Interesting points at same Base Station for both routes.	49
5.9 Algorithm divided into steps.	50
5.10 Received signal profile from one of the sectors for route 3a and 3b.	50
5.11 Red lines represent the mean value for each degree.	51
5.12 Performance of ΔP_r for both routes.	52
5.13 Effective radiation pattern from route 3.	53
5.14 Route 6.	54
5.15 Effective radiation pattern from route 6.	54
5.16 Route 1.	55
5.17 Effective radiation pattern from 1.	55
5.18 Simulated effective radiation pattern.	56
5.19 Variation of covered DBC compare with manufacturer pattern.	57
5.20 Absolute SIR and SINR values for affected DBC.	58
5.21 Absolute values of SIR and SINR within DBC affected for effective pattern.	58
5.22 Relative result for most characteristic parameters between both patterns.	59
5.23 Increment value for SIR and SINR within affected DBC.	60
5.24 Plane where radiation pattern is measured.	61
5.25 Comparison between manufacturer patterns with 0 and 8°	62
5.26 Angular spread results from ray-tracing tool.	62
5.27 Angular spread values along route 3.	63
5.28 Comparison between patterns.	63
A.1 Received signal power level	71
A.2 Discretizing error	72
A.3 Algorithm example	74
A.4 Zoom of Figure A.3	74
A.5 CDF of increment of power (ΔP_r)	75
A.6 SIR level into the footprint	76
A.7 SINR level into the footprint	78
A.8 CDF of the SINR value into the footprint.	78
A.9 Received power in a three-sector footprint	79
A.10 SIR level for a three-sector BS.	79

A.11 SINR level for a three-sector BS.	80
B.1 Different reference antenna radiation pattern.	82
B.2 Different routes around BS site.	83
B.3 Different Received Power for each method.	84
B.4 ΔP_r obtained for each different method.	84
B.5 ΔP_r for each route calculated by P_r sector sum method.	85
B.6 Error between antenna pattern and effective antenna pattern, ΔG	86
B.7 Received power including shadowing effect.	87
B.8 Normal distribution function with $\mu = 0$ and $\sigma = 3$	88
B.9 Signals created to model our correlated noise.	89
B.10 Received power including shadowing effect and both different noise signal, equations (B.11).	90
B.11 Comparison between $G_{eff}(\phi)$ and $G_{manufacturer}(\phi)$ when $\rho = 0.9$	91
B.12 Comparison between $G_{eff}(\phi)$ and $G_{manufacturer}(\phi)$ for different values of ρ	92
B.13 DBC affected within network performance due to $\rho = 0.2$	92
B.14 Network parameters analysis when $\rho = 0.2$	93
D.1 Diferent routes and deployment specification for route 1.	98
D.2 Received power points along the route 1-A.	99
D.3 Received power points along the route 1-B.	99
D.4 Diferent routes and deployment specification for route 2.	100
D.5 Received power points along the route 2-A.	101
D.6 Received power points along the route 2-B.	101
D.7 Diferent routes and deployment specification for route 3.	102
D.8 Received power points along the route 3-A.	103
D.9 Received power points along the route 3-B.	103
D.10 Diferent routes and deployment specification for route 4.	104
D.11 Received power points along the route 4-A.	105
D.12 Received power points along the route 4-B.	105
D.13 Diferent routes and deployment specification for route 5.	106
D.14 Received power points along the route 5-A.	107
D.15 Received power points along the route 5-B.	107
D.16 Diferent routes and deployment specification for route 6.	108
D.17 Received power points along the route 6-A.	109
D.18 Received power points along the route 6-B.	109
E.1 SWA-0859 Omnidirectional Antenna.	111
E.2 TSMW radio networ scanner.	112
E.3 Antenna layout on the van.	112
E.4 Schematic connection for measurement equipment.	113
E.5 Real van which we carried out the measurement campaign.	113
E.6 Connections between the equipment.	114

List of Tables

2.1	COST-231-HATA propagation restrictions [1].	14
2.2	COST-231-HATA parameters descriptions [1].	14
2.3	Typical values for shadowing standard deviation[3].	16
3.1	Parameters used for simulations.	19
3.2	Typical values for angular spread for different scenarios[1].	22
3.3	Results obtained for the simulation.	24
3.4	Summary of general parameters defined by [11] represented in Figure 3.13. .	29
A.1	Summary of the general parameters in the simulation and colour.	73
A.2	Summary of the general parameters defined by [21]	77
B.1	Gain tolerances obtained by [13] and UE datasheet (Appendix E).	87
B.2	Correlation factor values.	91
C.1	Telenor UMTS parameter specifications, UMTS2100 band I.	96
E.1	Equipment description used for the measurements.	110
E.2	SWA-0859 data specifications.	111
E.3	TSMW specifications.	111

List of Abbreviations

2D	Two Dimensions
3D	Three Dimensions
BS	Base Station
BW	Band Width
CDF	Cummulative Distribution Function
CDMA	Code Division Multiple Access
COST	European Cooperation in Science and Technology
CPICH	Common Pilot CHannel
DBC	Data Base Cell
FDD	Frequency Division Duplex
GPS	Global Positioning System
GSM	Global System for Mobile Communications
ISCP	Interference Signal Code Power
LAN	Local Area Network
LOS	Line Of Sight
LTE	Long Term Evolution
MS	Mobile Station
NDL	Null Depth Level
NF	Noise Figure
NLOS	Non Line Of Sight
NPSD	Noise Power Spectral Density
P-CPICH	Primary Common Pilot CHannel

PAS	Power Azimuthal Spectrum
PL	Path loss model
RF	Radio Frequency
RSSI	Received Signal Strength Indicator
S-CPICH	Secondary-Common Pilot CHannel
SINR	Signal to Interference Noise Ratio
SIR	Signal to Interference Ratio
SLL	Side Lobe Level
UE	User Equipment
UMTS	Universal Mobile Telecommunications System
WCDMA	Wideband Code Division Multiple Access
WIFI	WIreless Fidelity
WiMax	Worldwide Interoperability for Microwave Access
WLAN	Wireless Local Area Network

List of Symbols

- $a(hr)$: correction factor path loss model [dB].
 $a(\phi)$: free space antenna pattern.
 C_M : correction factor path loss model [dB].
 $C(x, y)$: coverage [discrete].
 d : distance [m].
 dB : decibels.
 dB_i : isotropic decibels.
 dB_m : milliwatts decibels.
 $d_{mast-antenna}$: distance between antenna mast and antenna [cm].
 $e(\phi)$: environment response.
 E_b/N_o : SIR after despreading [dB].
 E_c/I_o : SIR before despreading [dB].
 f_c : carrier frequency [Hz].
 G_p : processing gain [dB].
 G_{eff} : gain effective pattern [dB].
 $G_{Sum-manuf-ref}$: gain manufacturer reference [dB].
 $G_{ref}(\phi)$: gain reference pattern [dB].
 $G_{sect}(\phi)$: gain from a sector [dB].
 G_{tx} : transmitter gain [dB].
 GHz : Giga Hertz.
 ht : BS height [m].
 hr : MS height [m].
 $I_{S_x-S_n}$: Interference level [dBm].
 Km : Kilometres.
 m : metres.
 $m(\phi)$: angular response.
 MHz : Mega Hertz.
 N : noise [dBm].
 P_r : received power [dBm].
 P_t : transmitted power [dBm].
 R : Range [m].
 R_{mast} : mast radius [cm].
 X_{1-2} : random variable.

α : aperture parameter [$^{\circ}$].

μ : median value of a probability distribution.

σ : standard deviation of a probability distribution.

ϕ : angular domain variable [$^{\circ}$].

φ : angular domain variable [$^{\circ}$].

Δ : subtraction.

ρ : correlation factor.

Chapter I

Introduction

1.1 Introduction

Wireless communication is one of the most active researching areas of our time. Nowadays, it is enjoying its fastest growth period in history, due to enabling technologies which permit widespread deployment. This development in mobile communication has been a slow process and is related to technological advances, but it was not until the 60s and the 70s when Bell Laboratories developed the cellular concept to provide a whole population with wireless communications[14].

These initial systems consisted of a base station with a high power transmitter placed on tall buildings or mountains which served an entire metropolitan area. Since wireless resources are shared by all users located in the same area and radio spectrum is scarce, an inefficient use of such resources could be a problem. In the beginning, these initial system designers did not foresee that the number of users would grow rapidly, that, the system design had to be adapted as a function of this growth. Therefore, they needed to find a better way of providing their subscribers with resources. Nowadays, cellular systems mostly use smaller cells with lower transmitting power. Depending on the size, these cells are called macro, micro or picocells. The use of these smaller cells occurred because of the need of a higher capacity in areas with a high density users, as well as the size and cost reduction of base station electronics.

The basic premise of cellular system design is frequency reuse in which signal power falls off with distance to reuse the same frequency spectrum at spatially-separated locations[1]. This allows a more efficient use of the system spectrum so that a bigger number of users can be accommodated.

Neighboring base stations are given different groups of frequencies in order to minimize the interference between base stations, see Figure 1.1. By symmetrically spacing base stations and their channel groups throughout a service area, the available frequencies are distributed all around the area and may be reused as many times as necessary, as long as the interference between co-channel stations is kept below acceptable levels[14]. The minimum allowable distance between nearby co-channel base stations involves receivers

tolerance to co-channel interferences which allow a dense frequency reuse and thus, a higher capacity. This frequency reuse factor is the rate in which the same frequency can be used in a network cluster, that is to say, the number of cells in which available spectrum is divided (see Figure 1.1).

Another way to increase capacity in a cell and reduce interferences is called sectorization. When this technique is carried out, the channels used in a particular cell are divided into sectorized groups and are used only within a particular sector. By the use of sectorization, it is not only possible to increase the system performance but also the number of overlaps between cells, which causes an increment of traffic load due to an increasing number of handover. The most typical sectorized cells for mobile communication systems are three-sector and six-sector cells.

Interference treatment changes between systems or different deployments. For instance, systems like GSM allocate different frequencies for different cells to avoid co-channel interferences. This means that there can be a quite large cell overlap without causing significant interference. Other systems like WCDMA use the same frequency band in all cells which implies that large overlap could cause significant interference[16]. The planning activity of

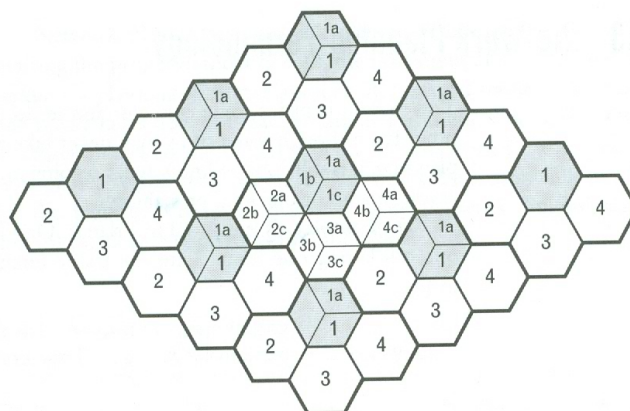


Figure 1.1: Example of a frequency reuse and sectorized network.[6]

a mobile network is a continuous process in which operators consider an optimum trade-off between equipment and installation costs, performance, reliability and user satisfaction as well. In the dimensioning phase an approximate number of base station sites, base stations and their configurations and other network elements are estimated, considering the operators requirements and the radio propagation in the area[5]. Following this line of thought, the main issue for wireless systems can be summarized in one word: coverage.

The cell coverage area in a cellular system is defined as the expected percentage of area within a cell which is received given a minimum power level. All mobile users within a cell require a minimum received SINR for acceptable performance. Assuming some reasonable noise and an interference model, SINR turns into a minimum received power through the

cell. The transmitted power at the base station is designed for an average received power in the cell boundary[1]. This would be a first assumption to make the coverage estimation area easier given by a BS . Although it is known that coverage area is not considered a well defined circle, it can be a good approach for the planning. Nevertheless, variations due to propagation can cause either more received power or sometimes less than the average expected. This fact is what makes the idealistic model different from the realistic one (see Figure1.2).

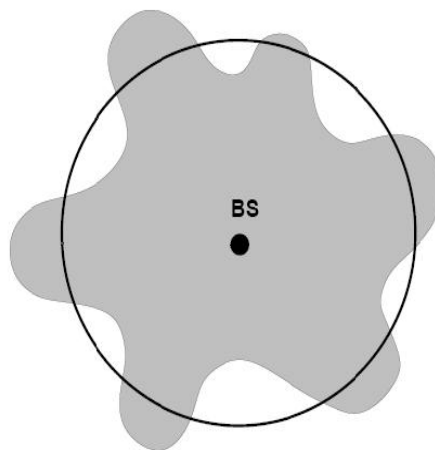


Figure 1.2: Black circle represents expected coverage, while grey spot represents how coverage can vary hypothetically from the expected one[1].

Several models are used by network operators in order to estimate coverage area in the planning activity. Normally, these planning tools are based on received signal strength within BS site in which a database for the survey area is required. One of them consists of constant antenna configuration fixing transmission power and radiation pattern. They apply propagation models, according to the significance of validation survey data, by estimating the received signal strength at a particular location. However, only path loss is predicted without taking into account multipath or shadowing fading.

Other model which is used by network operators is done through a computer simulation process. A software planning tool uses a terrain digital model which is divided into squared pixels. This tool estimates the percentage of the covered area by a signal strength threshold specified, calculating path loss and additional diffraction loss.

Once network operators have done the planning task, the next step is to verify their estimations by taking measures in the desired area and analyse whether predictions correspond with the real process or not.

Antennas are one of the most important elements in cellular systems and are strongly related to coverage. Antenna radiation properties and RF propagation are key factors on

which network operators base their network planning and design. This network planning is carried out by using the antenna manufacturer specifications where radiation properties are measured for free space; what means that, the specific environment and propagation effects are not included in the survey. Nevertheless, radiation properties could change as a consequence of environmental interactions or propagation phenomena.

Hence, if antenna environment and propagation have such an impact on antenna features, should these effects be taken into account by network operators in a network design?

1.2 The problem definition

The aim of this project is firstly, as far as operators are concerned, whether it can be useful to get an antenna pattern which includes not only manufacturer's specifications but also the impact of immediate surroundings and the mounting structure of an urban base station deployment. And secondly, whether it can give us a more accurate understanding of the network performance.

Before having done a research about surrounding effects or mounting structure influence, there are some questions that we would like to consider:

- How can interference level be affected by these distortions?
- Could the influence of these factors be modelled before network deployment?
- In which magnitude do the different factors modify free space radiation pattern?

1.3 Methodology

In order to find a solution, there are some methods which could help us to approach the problem given. These methods are:

- **Theoretical research.** Search for references about the problem to get information, then this information is analysed and, finally, conclusions from this analysis can be reached concerning the problem.

Moreover, it is a good way of providing an overall view of the problem and understand its magnitude by doing a study of what other people wrote about it and try to offer new aspects. Probably the method that takes more time because the research needs to be as precise as possible so that we can totally rely on the information selected.

- **Empirical data.** Taking measurements in the desired area is another method of estimating the effects which affects the coverage and BS deployment. It is a way of seeing what impact immediate surroundings and other source of distortions have on electromagnetic-signals. It involves measuring the signal strength within a cell and

evaluate the footprint shape specially on the cell boundary. From these measurements a coverage estimation can be carried out and they will help to analyse weak points in the system performance.

This method could be regarded as the most accurate. Accuracy of the method depends on the number of measurements taken in the desired area. Only a small number of them and with more or less error can be taken due to physical limitations and the tool used.

- **Numerical data.** By the use of software tools, a coverage prediction survey can also be done. Database whose content is characteristics of the area such as building density, building height, building structure or antenna emplacement that could help us to understand how the system performance in a specific deployment works. This task could be subdivided into two. Firstly, a task related to antenna or antenna mounting (near field) and secondly related to electromagnetic propagation and environmental interactions (far field).

Good way of simulating the impact of mounting structure on the radiation pattern. For this project section, MATLAB will be used to carry out the simulations. This software is well-known and precise enough for our purpose.

To study the existing problem, we will combine the three above mentioned methods. By doing so we will be able to compare as far as our possibilities are concerned to what extent simulations differ from empirical measurements.

As a starting point we will do a research by reading references and articles about antenna performance on cellular systems, and the effect that surroundings and mounting structure have on coverage prediction. The following step we will take is to combine the data extracted from literatures with numerical simulations and empirical measurements to see how the simulated results can change in comparison with the realistic results. We will attempt to evaluate how big is the impact of certain changes on the system performance is and if these changes should be taken into account.

1.4 Delimitations

Since we are limited by time and resources, we will focus on horizontal plane which is the most significant plane referred to coverage and vertical plane in relation to antenna downtilt but always analysing both patterns in 2D .

We will conduct our research in some base stations in the city of Aalborg, Denmark. The number of base stations to analyse is also conditioned to time and resources. There are many types of antenna for base station but we will focus on base station antennas from different models and structures founded in Aalborg University.

Chapter II

Theoretical Background

In this chapter we will explain all theoretical basis which concerns our project. Antennas play a very important role in wireless communication being the main issue for signal propagation. Regarding antennas, it will be also talked about their parameters and how they interact with environment. Moreover, it will be explained the effect of these parameters in network planning and how to control them for a better performance.

Another important issue about wireless propagation is how electromagnetic signals are transmitted through the space and which effects they suffer. Hence, propagation phenomena will be explained and possible consequences they have into the transmitter and receiver signals.

2.1 Antennas

The most important device in wireless communication is the antenna. An antenna is used to transmit or receive electromagnetic signals through the space. They are frequency dependent, what means that they are designed for a certain frequency. Therefore, they can be seen as a bandpass filter, that is to say, they reject signals beyond operating frequency.

Antennas are essential elements within mobile communication systems. Antenna parameters should be taken into account by network designers because network performance depends on these parameters and they should be able to adjust them according to the needs of the system.

There are many factors that can be involved in a BS design like the type of antenna to choose, which radiation properties have, how antenna parameters interact with the environment, where it will be mounted...

Hence, following sections will explain basic antenna parameters and RF propagation properties in order to have a better view within network performance and how they impair on it.

2.1.1 Radiation properties

Radiation properties of antennas are shown on the antenna radiation pattern which graphically represents radiation intensity as a space function[17]. Radiation patterns are usually represented in a 3D graph or by means of the azimuthal (horizontal) or elevation (vertical) pattern. Figure 2.1 shows antenna parameters in an azimuthal radiation pattern which will be the one we will focus on as it is stated at methodology.

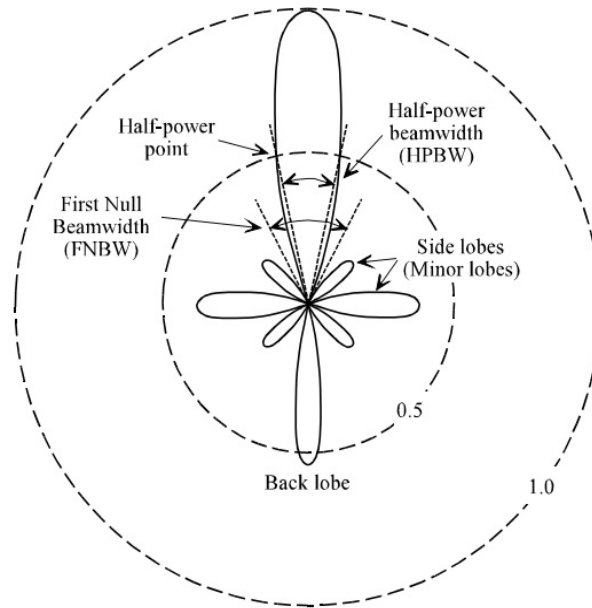


Figure 2.1: Example of an antenna radiation pattern[27].

Antenna radiation pattern is usually plotted in a polar graph in which some quantitative aspects are appreciated. These aspects include the beamwidth, side lobe level, front-to-back level and directivity.

On the one hand directivity expresses the relative level of how well an antenna radiates or directs the energy radiated. There is always a direction for practical antennas which refers to the maximum directivity. On the other hand, antenna gain describes how efficiency an antenna is, that is to say, if an antenna was 100% efficient, its gain would be equal to its directivity. Thus, directivity and gain are linked between them in dependence of factors that can reduce or affect antenna efficiency, like antenna impedance, material losses or matching network losses[20].

Following with parameters description, beamwidth expresses the angular width where most of the power is radiated. It is usually referred as 3dB beamwidth, considered the half radiated power which is 3dB below the main peak of the radiation pattern. This parameter is frequently referred to both patterns separately.

Antennas are not able to radiate all power in one single direction, inevitably some of the power is radiated in other directions. These peaks are called side lobes and have a lower magnitude than main lobe.

Besides these parameters, there are more that should be taken into account and have also influence on the design. One of these parameters are the nulls, which are referred to the radiated power at minimum value. For instance, this parameter can be useful to suppress interfering signals in some directions. Another parameter is the front-to-back ratio which is the difference between the value in the front direction and back direction.

In general terms, influence of these parameters will depend on system requirements. Antennas can be used for many implementations in the field of wireless communications, thus, each of them will need different antenna aspects to be taken into account. This report will be focused on antenna requirements for mobile communication and more specifically, on BS antennas for urban/suburban environment macrocells.

2.1.2 Antennas for Base Station in Mobile communication

Requirements for BS designing differ greatly from MS antennas. Cost is not such an important issue due to expensive cost of BS antennas. Also, size restrictions are less strict since it is only required for macrocells that antenna mast can bear wind forces or impact of environment should be small. Nevertheless, regarding pico and microcells antennas, they need to be much smaller because they are mounted on building surfaces, street lanterns or office walls[7].

Different requirements are imposed on BS antennas for indoor and outdoor coverage. Our report will be focused on BS for outdoor coverage since our research was stated for urban and suburban BSs.

Performance characteristics requirement of outdoor antennas are not easy to achieve and, depending on the deployment, a variety of beamwidth, gain and downtilt will be laid out according to deployment scenarios in urban, suburban or rural environments.

Figure 2.2 shows different BS deployment for urban, suburban or rural environment and mounted differently. Differences between horizontal and vertical pattern for BS can be also seen in Figure 2.3. It is appreciated that 3dB beamwidth is much wider at the horizontal since it is the pattern which provides coverage within the desired area boundaries. Moreover, this pattern does not have such high level of side and back lobes in comparison to the vertical one. With respect to vertical pattern, it is responsible for confining coverage into the service area. In contrast, it has a narrower 3dB beamwidth which leads to the appearance of more sidelobes.

In general, before choosing a specific antenna, a research about BS site surrounding should

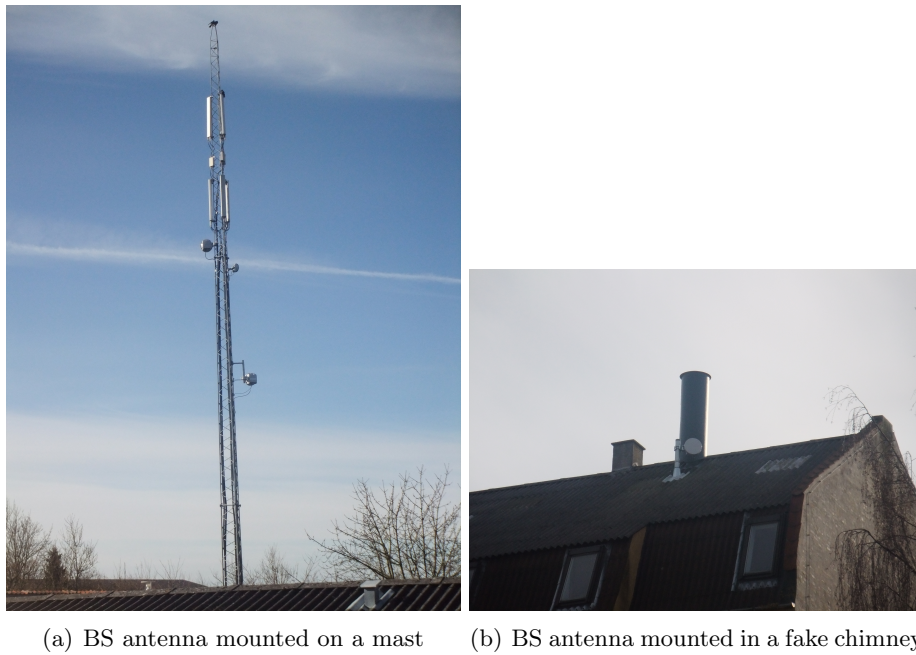


Figure 2.2: Example BSs antennas for outdoor coverage.

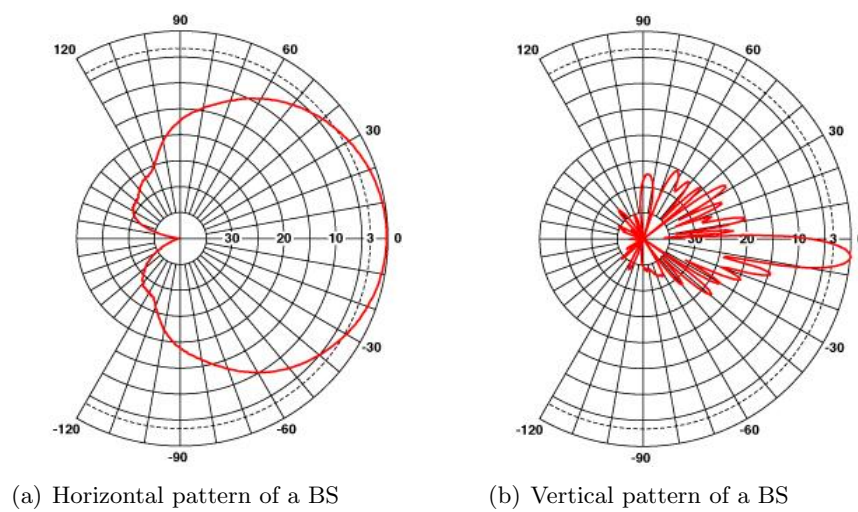


Figure 2.3: Example BSs radiation pattern for outdoor coverage[24].

be carried out in order to obtain the most suitable design. However, it is well known that antenna characteristics will interact with the environment and may change the performance. These interactions will be explained in the following sections.

2.1.3 Impact of antenna features on cellular systems

Since the first demonstration of wireless technology in 1886 by Heinrich Hertz and its first practical radio application by Guglielmo Marconi in 1901, the antenna has been a key factor in the construction of wireless communication system design[20].

Besides, it is known that antennas provide a link between BS and MS, BSs are fundamental parts in a wireless network since they control frequency reuse and optimization of channel capacity. In the design and planning of wireless systems, it is necessary to have a fundamental knowledge of the antenna as well as RF characteristics. A properly selected antenna can make the design improve system performance and coverage.

As it was already above mentioned, antenna pattern parameters such as side lobes, front to back ratio, antenna tilting and antenna height play a very important role on cellular design (see Figure 2.1).

Antenna side lobe and front-to-back ratio are measures of how energy is radiated by the antenna outside of its main beam. These levels should be as low as possible since they reduce the directivity and efficiency of main beam. Presence of side lobe and back lobe can also cause interference to other nearby receive sites and to the receive system from surrounding transmissions.

Azimuth beamwidth of a BS is chosen in function of frequency re-use plan for the network. The typical configuration for BSs would be three sectors spaced 120° in azimuth plane with 65° 3dB beamwidth, but this is not considered a strict configuration because coverage needs will depend on buildings or hills around.

Considering vertical plane, antenna tilting is a technique which allows the operator to adjust sector coverage. By using antenna downtilting, the side lobes are also redirected, this fact may cause interference in neighbouring cells and nulls below the main lobe, that will lead to areas of poor coverage close to BS. In contrast, antenna downtilting is also an effective way to reduce inter-cell interference and consequently increase the capacity but if it is too aggressive, it may result in insufficient coverage and mobility support (see Figure 2.4).

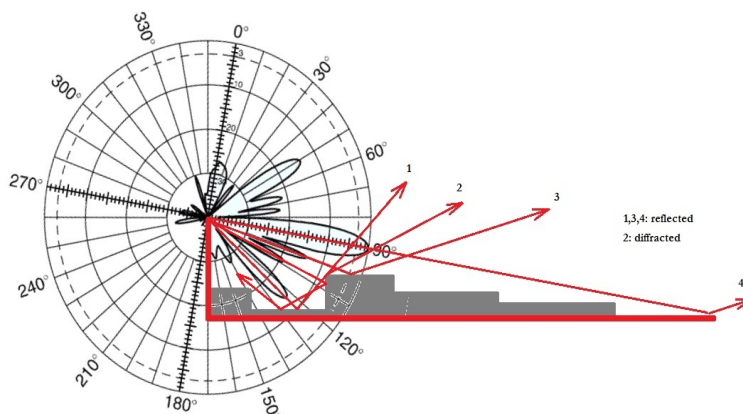


Figure 2.4: Antenna downtilt performance[26].

Most of all antenna performance characteristics are specified under free space conditions[17]. However, once the antenna is placed on the urban or suburban environment, this pattern may change because of the influence of immediate surroundings. Due to the aspects mentioned, specific parameters in a radiation pattern may suffer modifications in a realistic deployment and such modifications can lead to changes in essential parameters in a mobile network such as received power, SIR, SINR, coverage and so on. For instance, a front-to-back ratio measured for free space conditions (manufacturer's) will change once antenna is placed.

The purpose of evaluating these parameters in a realistic environment is to analyse how these antenna parameters modifications affect network parameters and how significant they are for the design.

2.2 RF propagation

In addition to antenna properties described, other factors have an impact on system performance. These factors are those which affect electromagnetic signals propagation.

Design of wireless networks differs fundamentally from wired network design due to the nature of the wireless channel. This channel is unpredictable and a difficult communications medium.

In order to estimate signal parameters accurately, it is necessary to estimate propagation characteristics. The ability to predict radio-propagation behaviour for wireless systems like cell communications has gained importance.

Many researches have been done over the past few years on improving propagation predic-

tion techniques, and many different models have been developed which take into account the effect of various types of terrain and other obstructions in the far field. These models have become in a low-cost and convenient alternative since site measurements are costly. It becomes necessary to understand how RF signals will be attenuated as they pass through objects such as foliage, walls and buildings. The signals suffer random fluctuations in time if the transmitter, receiver or surrounding objects are moving due to changing reflections. It is more complicated to determine the signal level because of the influence of the mounting structure or the nature of immediate surroundings which are complex and may unknown. Hence, it is more difficult to quantify variations of the signal inside the propagation model.

There are also significant impacts of scattering in the near field of the antenna (mast, mountings, other objects in the vicinity, such as roof-top, etc.) and diffraction. These near-field scatterers and diffractions are not accounted for by the propagation models. Therefore they need to be included in an effective radiation pattern[19].

Generally, antenna selection and location are not arbitrary. It requires an evaluation of system coverage and range requirements, a review of station locations and a review of surroundings objects that may become a source of interference[20].

In the following lines, propagation phenomena will be briefly explained and their impact on system performance. Propagation and propagation effects can be estimated mathematically in order to take a previous overview of the environment impact which will be also explained.

2.2.1 Path loss models

Propagation path loss models play an important role in the design of cellular systems as they are used in the typical initial network design to determine the number of sites necessary to provide enough coverage and predict possible interference problems. Path loss is reduction in power density level of an electromagnetic wave through the space[3].



Figure 2.5: Path loss definition[3].

In the design of a wireless system, one of the most important issues is to predict the coverage in a desired area. In order to carry out this important task, many approaches have been designed by using propagation models. Propagation models are useful to estimate

As it was said before, propagation models only give a good approach for path loss within a geographical area characterized by terrain parameters. There is still a lack of propagation mechanisms which are not represented in a propagation model. Therefore, this is one of the main reasons to find out whether an effective radiation pattern makes network planning more accurate or, however, it can contribute to give more details about propagation phenomena.

Each empirical propagation model has its own restrictions to operate with it. In principle it is applicable to scenarios which are similar to the one in which measurements were taken. We will not explain every propagation model and their restrictions in detail but we will introduce the one we choose for simulations according to the sites and Aalborg relief.

COST-231-HATA

COST-231 is an extension to Hata model which was designed in the beginning for frequencies from 150 to 1500 MHz. Hata model was good for first generation cellular systems, but does not model propagation well in current cellular systems with smaller cell sizes and higher frequencies[1]. This is the reason why European scientific COST group decided to extend Hata model with some modifications. It is recommended for large and small cells when BSs are placed above rooftop level of buildings adjacent to the BS.

Restrictions for COST-231-HATA are:

$$\begin{aligned} 1.5\text{GHz} &\leq f_c \leq 2 \text{ GHz} \\ 30\text{m} &\leq ht \leq 200 \text{ m} \\ 1\text{m} &\leq hr \leq 10 \text{ m} \\ 1\text{Km} &\leq d \leq 20 \text{ Km} \end{aligned}$$

Table 2.1: COST-231-HATA propagation restrictions [1].

PARAMETER	DESCRIPTION
f_c	Frequency [Mhz]
ht	BS height [m]
hr	UE height [m]
d	Distance [Km]
$a(hr)$	Correction factor [dB]
C_M	Cutter correction factor [dB]

Table 2.2: COST-231-HATA parameters descriptions [1].

Therefore, taking into account all previous parameters and the type of environment, path loss is calculated as follows [15]:

Urban area:

$$PL_U = 46.3 - 33.9 \log_{10}(f_c) - 13.82 \log_{10}(h_t) - a(hr) + [44.9 - 6.55 \log_{10}(h_t)] \log_{10}(d) \quad (2.1)$$

$$a(hr) = (1.1 \log_{10}(f_c) - 0.7) * hr - (1.56 \log_{10}(f_c) - 0.8) + C_M \quad (2.2)$$

$$C_M = \begin{cases} 0\text{dB} & \text{medium sized cities/suburban centres} \\ 3\text{dB} & \text{metropolitan centres} \end{cases} \quad (2.3)$$

Suburban area:

$$PL_S = PL_U - 2 * \left[\log\left(\frac{f_c}{28}\right) \right]^2 - 5.4 \quad (2.4)$$

Quasi-open area:

$$PL_q = PL_U - 4.78 * [\log(f_c)]^2 + 18.33 * \log(f_c) - 35.94 \quad (2.5)$$

Rural area:

$$PL_R = PL_U - 4.78 * [\log(f_c)]^2 + 18.33 * \log(f_c) - 40.94 \quad (2.6)$$

2.2.2 Shadowing fading

A signal transmitted in a wireless environment will suffer random fluctuations due to blockage, introducing some variations in the received signal. These variations may be caused by signals which reflects in surfaces or in scattering objects. A model to explain such random fluctuations in the received signal should be an statistical model since the location, size, and dielectric properties of the blocking objects as well as the changes in reflecting surfaces and scattering objects are generally unknown[1].

The most common model for shadowing fading is a log-normal distribution (2.7). Figure 2.7 shows a log-normal distribution with zero mean and standard deviation value of 3dB.

$$f(x; \mu, \sigma^2) = \frac{1}{x\sigma\sqrt{2\pi}} e^{-\frac{(\ln(x)-\mu)^2}{2\sigma^2}} \quad (2.7)$$

Where:

x : dependent variable.

μ : mean of the log-normal distribution.

σ : standard deviation.

If $x \sim \text{log-N}(\mu, \sigma^2)$ then $\rightarrow \ln(x) \sim \mathcal{N}(\mu, \sigma^2)$. This property represents that a log-normal variable follows a normal distribution function in terms of logarithmic value. Therefore,

$$\text{”Shadowing”} \rightarrow f(x[\text{dB}]; \mu, \sigma^2) = \frac{1}{\sigma\sqrt{2\pi}} e^{-\frac{(x-\mu)^2}{2\sigma^2}} \quad (2.8)$$

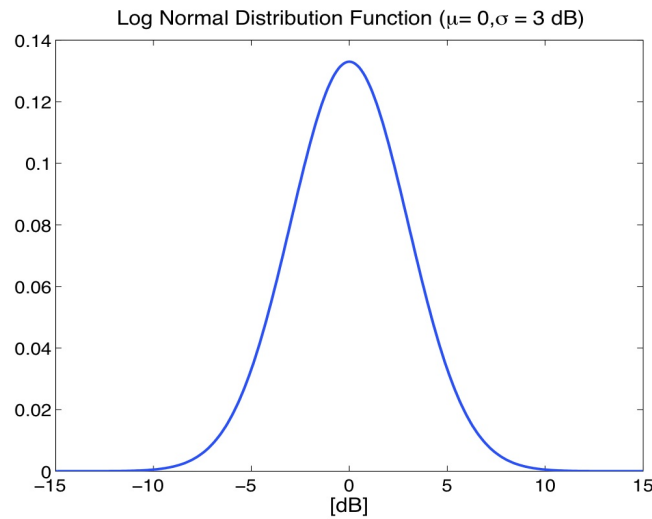


Figure 2.7: Log-normal distribution function with x-axis expressed in dB, see equation (2.8).

Table 2.3 shows different values for shadowing standard deviation:

ENVIRONMENT	σ_{dB} [dB]
Outdoors	4 to 12
Office, hard partition	7
Office, soft partition	9.6
Factory, line of sight	3 to 6
Factory, obstructed	6.8

Table 2.3: Typical values for shadowing standard deviation[3].

2.2.3 Multipath

Multipath effect is a serious problem for the system performance since it is the result of multiple signals from the same RF source arriving to the receiver via many different paths, due to natural or artificial obstructions such as buildings, trees, posts, etc. These multiple signals are time delayed, attenuated, refracted or reflected obstructions and arrive at the receiver with different amplitude and phase. Depending on how these multiple signals interact between each other, the overall signal can be slightly affected or it might be even cancelled. This effect also happens when the receiver is static.

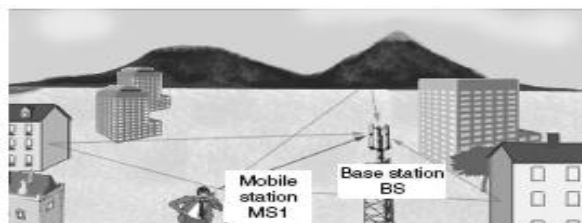


Figure 2.8: Multipath propagation[2].

As far as antennas are concerned, it is a difficult task to remove multipath fading. Depending on the kind of antenna, it would be possible to minimize impact of multipath, what is to say; the more directive antenna is, the less multipath impact has. Most effective techniques to reduce multipath effect are laid on system designers like optimizing antenna location or applying diversity techniques.

Variations in the signal due to multipath can occur over short distances and cause what it is called small-scale fading (fast fading) (Figure 2.9). Although multipath effect can be seen as a problem in signal reception, it could provide coverage to areas which are surrounded by obstructions.

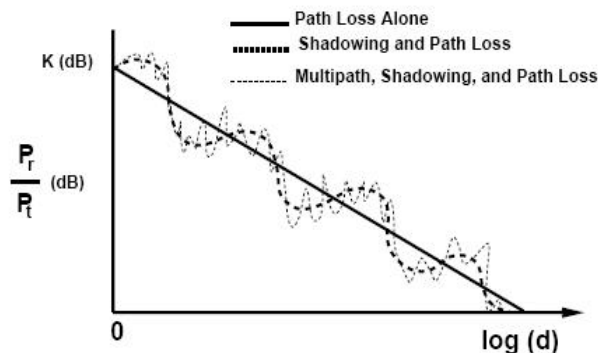


Figure 2.9: Signal propagation profile[2].

2.2.4 Angular dispersion

Angular properties have become recently necessary to understand and improve interference and multipath situation. The angular domain seen from a base station is important for the proper understanding and determination of the correlation of antenna properties. Angular spread is an important parameter to understand properties in angular domain. It is a measure of how multipath concentrates about a single azimuthal direction of arrival.

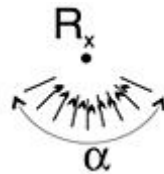


Figure 2.10: Multipath direction of arrival[4].

Angular spread behaviour and its impact on the network performance will be shown by means of practical simulations in the following chapters.

CHAPTER III

Modelling antenna deployment

This chapter is divided into three well differentiated sections. The first section introduces a deployment defined by observing BSs in the city of Aalborg and taking into account geographical characteristics such as BS height or distance covered. In the second section, the impact of environment on reception is explained, what is to say, the changes caused by surroundings into the horizontal antenna pattern. To conclude the chapter, the last section is related to distortions produced in reception due to mounting structure.

This chapter is mainly focused on modelling the type of distortions mentioned above by means of software tools. Once simulations are done, we will compare them with real measurements to evaluate the reliability of both methods.

3.1 System Deployment

Antenna parameters are usually defined as free space conditions, but this model is not suitable to represent how antenna parameters are modified by environment response or surroundings. By means of these simulations, we will try to quantify these modifications and find out whether they are of great importance for the system performance or not.

After reviewing available BSs for our research, we will proceed to simulate a possible scenario. According to COST-231-HATA parameters (equation (2.3)) and Aalborg geographical characteristics, the chosen deployment will be:

PARAMETER	VALUE
Frequency (f_c)	2100 MHz
BS height (ht)	30 m
UE height (hr)	2.6 m
Tilting	8°
Gain	18 dBi
P_t	33 dBm

Table 3.1: Parameters used for simulations.

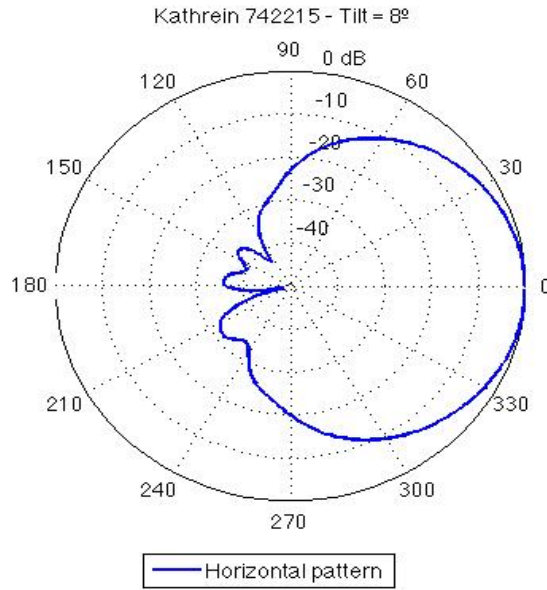


Figure 3.1: Radiation pattern used for simulations.

3.2 Angular dispersion

3.2.1 State of the art

Angular domain dispersion was already previously introduced in the theoretical background chapter. It could be interesting to represent BS spatial characteristics using angular domain descriptions. The expression for angular response $m(\varphi)$ relates antenna pattern $a(\varphi)$ and environment response $e(\varphi)$ as a complex correlation between them [10].

$$m(\varphi) = \oint_{\phi} e(\phi)a(\phi - \varphi)d\phi = R_{e,a^*}(\varphi) \quad (3.1)$$

Where:

$a(\varphi)$: antenna radiation pattern measured in free space conditions.

$e(\varphi)$: environment response.

$m(\varphi)$: angular response.

An antenna can also be regarded as an angular filter causing interferences within the angular partial components, if the beamwidth is wider than the angular spreading of the environment[8]. A good spreading parameter should reflect a measure of the extension of the effective source environment, thus angular spread parameter is useful to describe the azimuthal spatial spreading of the environment seen from BS[9].

In order to represent the environment response and according to [12], a laplacian distribution function (3.2) which better fits in order to represent the shape of the Power

Azimuthal Spectrum (PAS) at the BS for urban and rural outdoor environment. The laplacian distribution will be centred at μ and b is the value for the angular spread.

$$f(x|\mu, b) = \frac{1}{2b} \exp\left(-\frac{|x - \mu|}{b}\right) \quad (3.2)$$

Where:

x : independent variable.

μ : mean of the distribution.

b : standard deviation.

Figure 3.2 shows different environment responses for different values of angular spread, specifically, 5° , 10° and 15° .

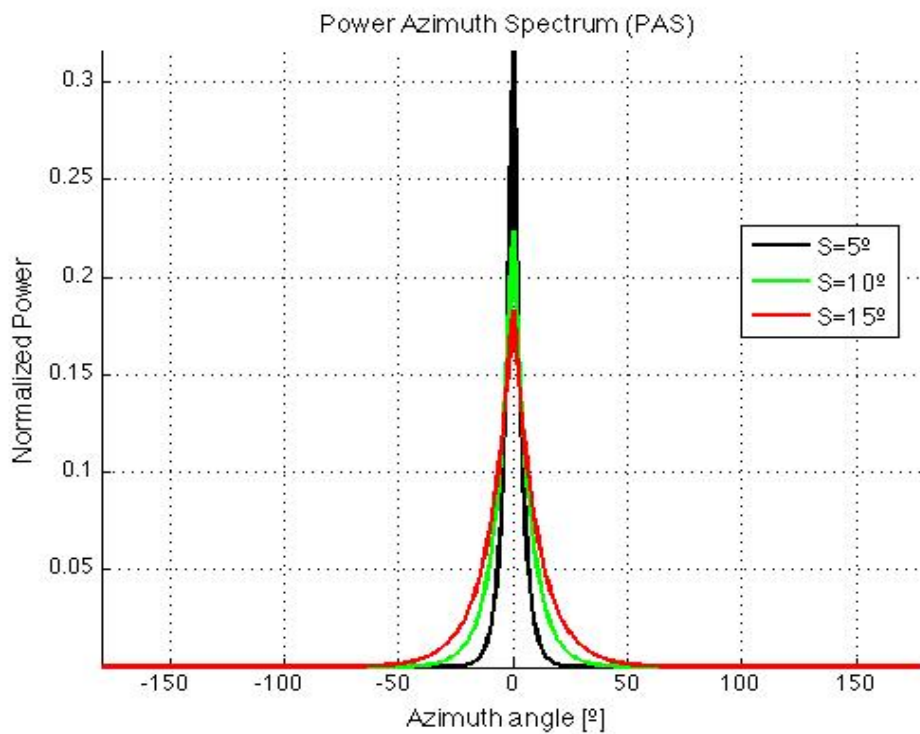


Figure 3.2: Different values of angular spread for a Laplacian distribution.

Angular spread parameter varies depending on the environment. Table 3.2 shows different values of angular spread for different environment conditions.

Environment	Value[°]	
	NLOS	LOS
Indoor office	10-20	≈5
Industrial	20-30	not specified
Microcells	10-40	5-20
Typical urban	not specified	3-20
Typical suburban	not specified	smaller range than urban
Bad urban and hilly terrain	20 or larger	20 or larger
Rural	1-5	1-5

Table 3.2: Typical values for angular spread for different scenarios[1].

3.2.2 Results

According to Table 3.2, values of angular spread range can vary from 1 to 40 within all types of scenarios. Our study will be focused on representing values for urban and suburban deployment, hence, different values of angular spread have been chosen to see how our radiation pattern changes supposing it was modelled as an urban or suburban deployment, specifically, for 5°, 10° and 15°. We will not consider the worst case for angular spread since Aalborg downtown is not considered as an strong urban environment or outskirts either.

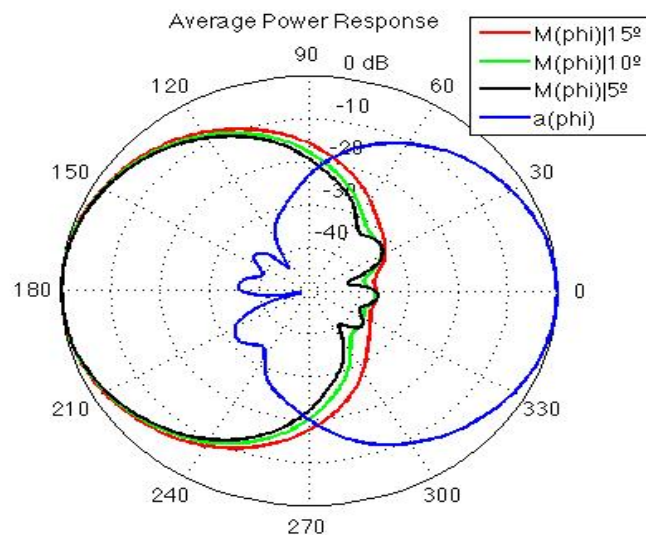


Figure 3.3: Antenna radiation pattern convoluted with different environment responses for different values of angular spread.

By means of convolution between antenna pattern $a(\varphi)$ and angular environmental response $e(\varphi)$ we obtain the angular response $m(\varphi)$, Figure 3.3. It can be observed that, once the convolution is done, angular response pattern has been shifted 180° due to cir-

cular convolution properties. In order to compare distorted radiation pattern with the original one, another 180° phase shift is applied, Figure 3.4.

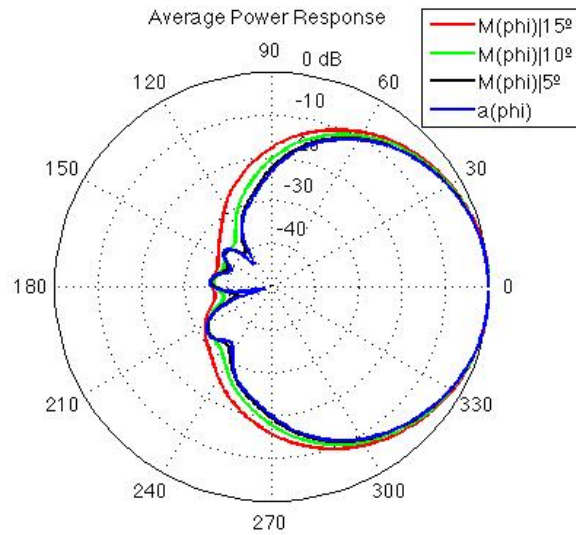


Figure 3.4: 180° shift phase to compare with original radiation pattern.

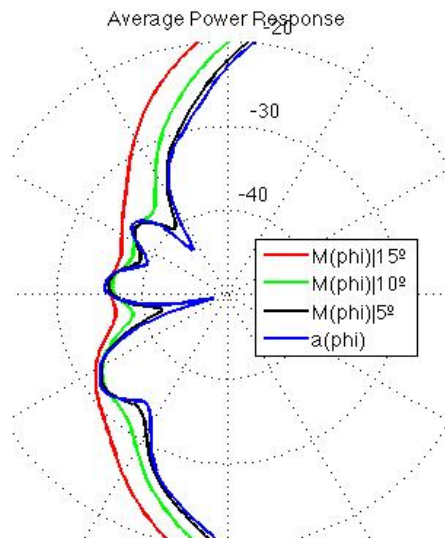


Figure 3.5: Zoom of Figure 3.4.

It can be seen from Figure 3.5 that, the impact of angular spread on the angular response has a greater influence in nulls and sidelobes than on the mainlobe.

To avoid ambiguities, ordinary antenna parameters can be applied if they are based on

measurement response $m(\varphi)$ instead of on antenna free space $a(\varphi)$ [10]. Side Lobe Level (SLL) and Null Depth Level (NDL) are defined to evaluate angular spreading, (3.3) (3.4).

$$SLL(\varphi)_{\text{test}} = \frac{M(\varphi)|_{\varphi = \text{mainlobe}}}{M(\varphi)|_{\varphi = \text{sidelobe}}} \quad (3.3)$$

$$NDL(\varphi)_{\text{test}} = \frac{M(\varphi)|_{\varphi = \text{mainlobe}}}{M(\varphi)|_{\varphi = \text{mainlobenullridge}}} \quad (3.4)$$

These results are collected in Table 3.3. As it may be seen from the results shown in the table, Side Lobe Level (SLL) increases when angular spread value is also increased due to difference between main lobe and side lobe.

Angular Spread[°]	0	5	10	15
SLL[dB]	32	32	32.5	33
NDL[dB]	49	42.5	39	36

Table 3.3: Results obtained for the simulation.

As far as these results are concerned, they are basically values in order to give a quantitative description of how sidelobes and nulls are affected by angular spread. It is important to quantify these distortions of the pattern within a BS context in order to appreciate how one single sector has influence on the others. Before carrying out the research, a procedure has been designed (Appendix A) in which, the footprint covered by BS radiation pattern is discretized in DBCs (Data Base Cells) and a comparison between the reference pattern and the distorted one is made to evaluate the number of DBCs affected.

Once this comparison is made, we will translate the number of DBCs affected into changes in the network parameters such as P_r , SIR or SINR. For the following simulations we will only focus on a value for angular spread of 15° because it is the worst case in our urban environment.

First results extracted from the procedure in Appendix A are shown in Figure 3.6. The color code is also explained in Appendix A. For example, DBCs in red mean that they are not covered by the reference pattern but by the distorted one. It can be seen that distortions are concentrated on the sidelobes and backlobe of the antenna.

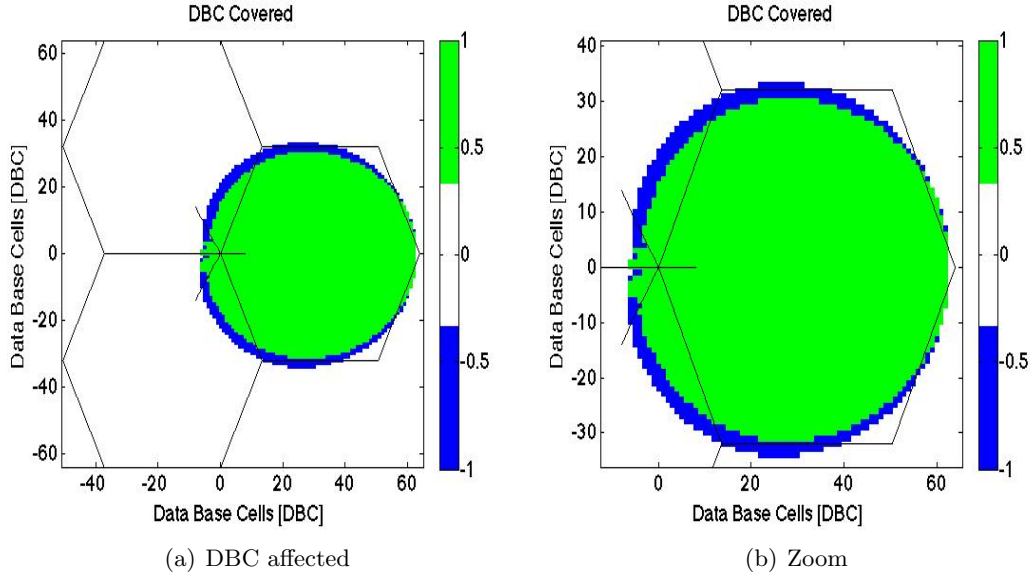


Figure 3.6: View of the comparison between reference and distorted one applying the procedure in Appendix A.

In Figure 3.7, absolute network parameters are represented in relation a three sector BS which are made up of the manufacturer's radiation pattern. In the graphic below, we will focus on SINR and SIR to see how distortions affect the network performance. Thus, $\Delta SINR(x, y)$ is defined in equation 3.5 to show the variation between patterns, presented in Figure 3.8. It is appreciated that the distorted pattern differs from the reference one between $[-6$ to $0]$ dB and the most affected areas are located at the vicinities of the BS.

$$\Delta SINR(x, y) = SINR(x, y)|_{distorted} - SINR(x, y)|_{reference} \quad (3.5)$$

Where:

$SINR(x, y)|_{distorted}$: SINR calculated for the distorted pattern [dB].

$SINR(x, y)|_{reference}$: SINR calculated for the reference pattern [dB].

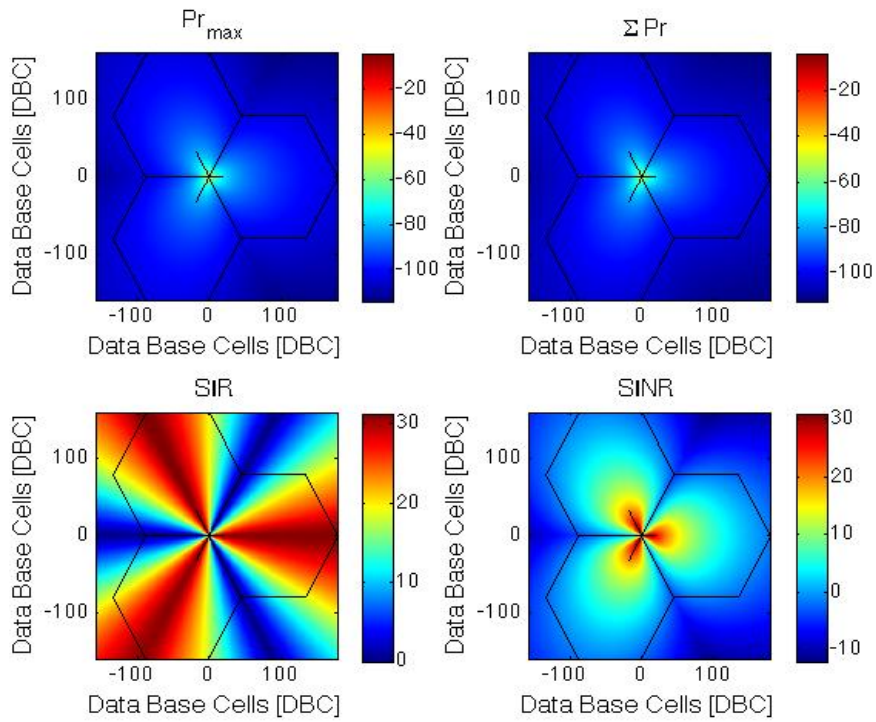


Figure 3.7: Network parameters calculated for the reference pattern.

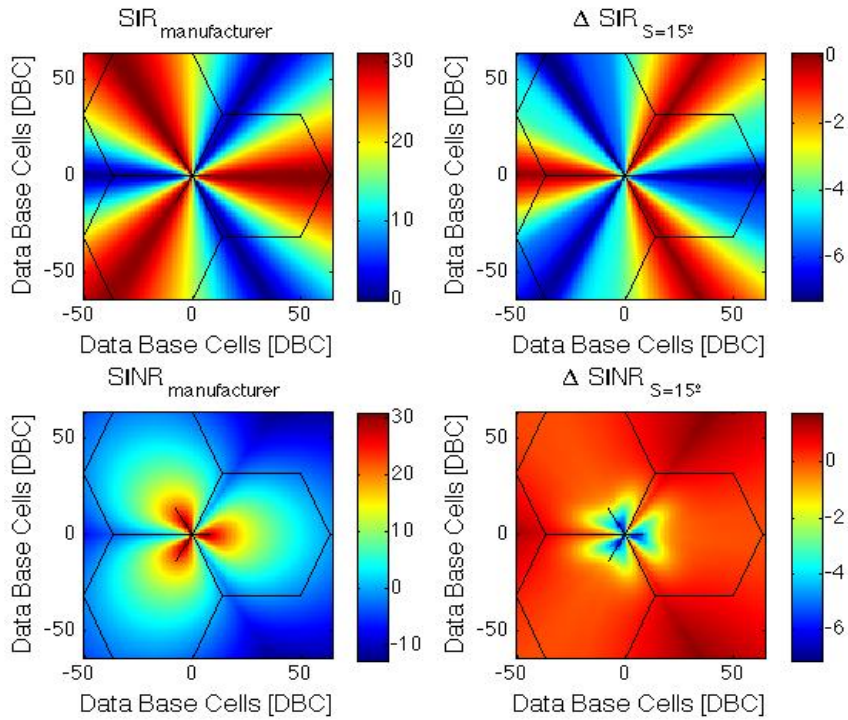


Figure 3.8: SINR and SIR absolute reference values and difference with respect to the same distorted parameters.

With the purpose of having an overview of the results, a statistical study has been done. Figure 3.9 shows the result of CDF of $\Delta SINR(x, y)$ over the covered area. Observing the worst case, an angular spread of 15° , the 1% of DBC inside the total covered area differed at least 2dB with respect to the reference, which is not very significant.

Considering the amount of DBCs distorted in one single sector over the total amount of DBCs within the covered area, the percentage of DBC affected is 5% (3.6).

$$DBC_{distorted} = \frac{DBC_{distorted}|_{onesector}}{DBC_{affected}|_{totalcoveredarea}} = \frac{425}{8603} = 4.94\% \approx 5\% \quad (3.6)$$

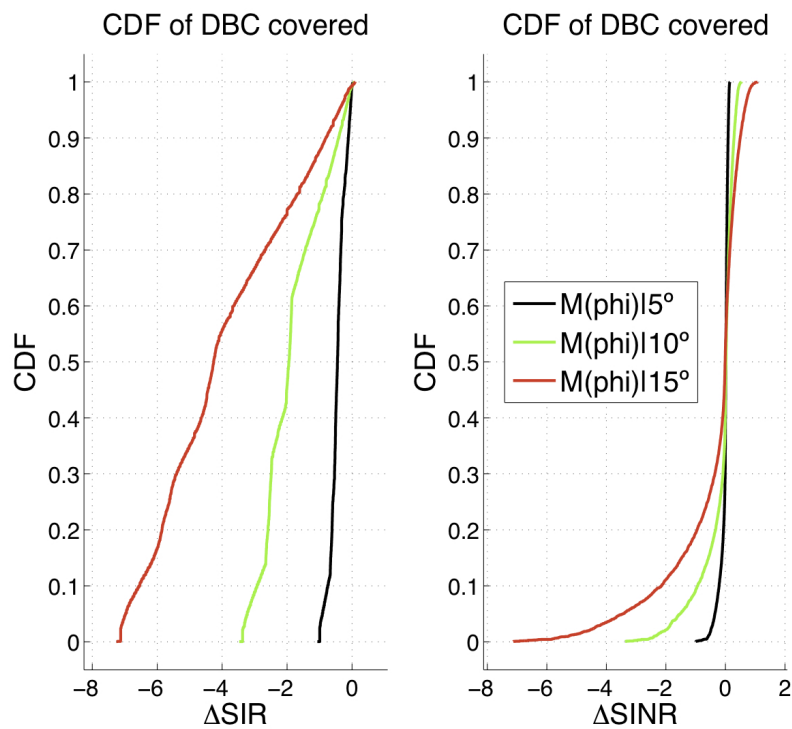


Figure 3.9: CDF of $\Delta SINR(x, y)$ and ΔSIR within the total covered area.

3.3 Mounting structure

It is well known that when an antenna is placed, it may change its performance due to many reasons such as propagation phenomena, environmental interactions or the structure where it is mounted.

Distortions on a radiation pattern due to environment were studied in previous sections. In this section we will analyse the influence of antenna mast, bar between antenna-mast and antenna mast conductivity to find out to what extent the mounting structure of a BS antenna affects the radiation pattern and, consequently, how the performance of the

network is affected.

In order to carry out the simulations, the same deployment characteristics and antennas are applied in this section.

3.3.1 State of the art

There are some scientific investigations about how mounting structure can have an influence on antenna radiation pattern, but not all of them are suitable to achieve the purpose of this project. However, reference [11], summarizes the interaction of different distortions evaluated in an Omni antenna of 19.2 dBi gain. The results were summarized for both radiation patterns, vertical and horizontal plane.

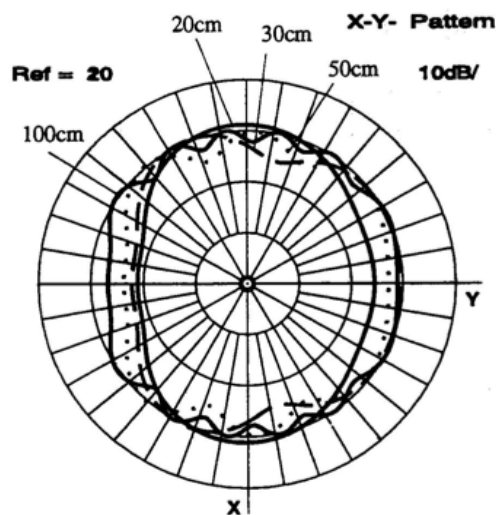


Figure 3.10: Antenna pattern distortion due to Mounting structure studied at an Omnidirectional antenna[11].

As it was already explained in the methodology, this project will fundamentally be focused on horizontal plane because it gives the coverage area in terms of received power at the Base Station Cell coverage.

Figure 3.10 represents the variation in the Azimuthal plane of an omniantenna of 19.2 dBi gain varying the distance between the antenna mast when the radius is fixed (in this case $R_{mast}=10$ cm). It is also possible to study this variation by implementing the opposite procedure, that is to say, by fixing the distance between mast-antenna ($d_{mast-antenna}$) and modify the mast radius.

In order to represent these variations, we will define our procedure as shown in Figure 3.11. Thus, we can translate every modification of these both parameters into an angle called *aperture angle* which is represented by symbol ' α ' defined by (3.7).

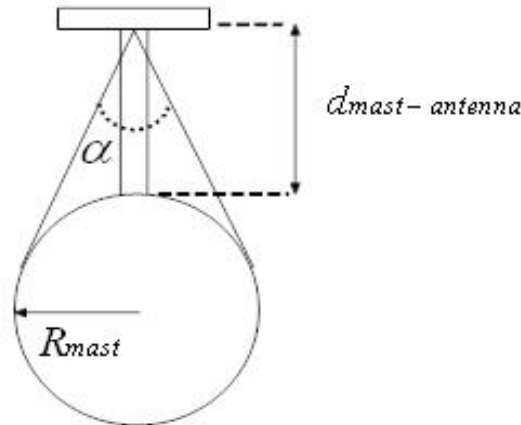


Figure 3.11: Graphic definition of *aperture angle* α .

$$\alpha = 2 * \arctan \left(\frac{R_{mast}}{d_{mast-antenna}} \right) \quad (3.7)$$

Therefore, Table 3.4 represents the tabulated maximum values for distortions as a consequence of mounting structure on each range of α . Hence, our first assumption is based on the idea that every configuration of mounting structure deployment has to be affected by the same distortion as long as its aperture angle is located within the same α range. A reason to explain our assumption is that, the three antenna sectors are supposed to be mounted on the same mast as well as the same mounting.

GENERAL DISTORTION PARAMETERS				
Aperture angle	Mainlobe [dB]	Sidelobe [dB]	backlobe [dB]	Name
$50 < \alpha \leq 90$	-5	+1	-8	Pat_{dist1}
$36 < \alpha \leq 50$	0	-5	7	Pat_{dist2}
$22 < \alpha \leq 36$	-2	-3	-6	Pat_{dist3}
$0 < \alpha \leq 22$	0	-2	-2	Pat_{dist4}

Table 3.4: Summary of general parameters defined by [11] represented in Figure 3.13.

Although we know the maximum distortion value, we need to design how distortions work around different directions as well. By doing so, we will be able to include distortions in every antenna of our deployments. The results for the distortions extracted from [11] are shown in Figure 3.13 and, specifically, in Figure 3.12 applied to an Omni antenna of 19.2 dBi gain. The resemblance with the original can be easily seen.

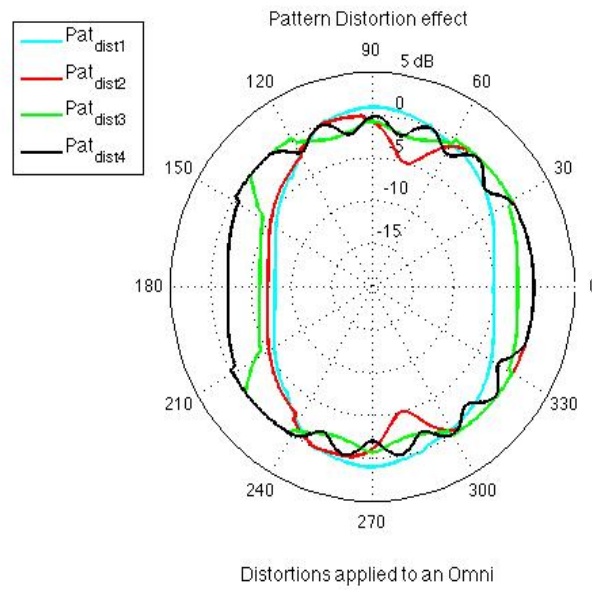


Figure 3.12: Simulated antenna distorted pattern due to Mounting structure deployment.

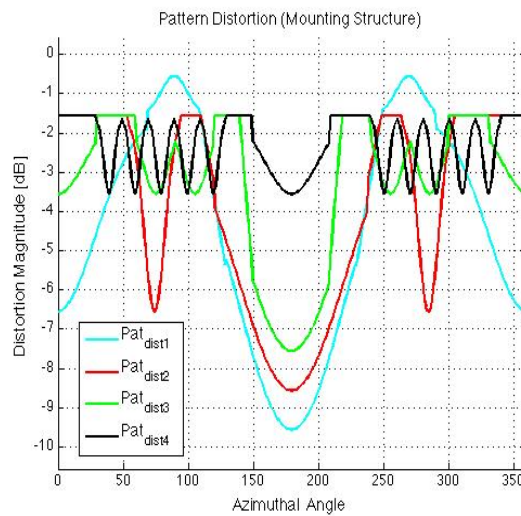


Figure 3.13: Linear representation of the different distortion.

Despite these distortions refer to an omnidirectional antenna, we will extrapolate these results to our own directional antennas. Furthermore, we assume that distortions caused by mounting structure are the same for omnidirectional antenna obtained by [11].

Hence, thanks to the result of combining distortions calculated previously with the antenna radiation pattern of Kahterin 742215 model (Figure 3.1) it is possible to obtain the supposed pattern after the antenna device was mounted. Figure 3.14 represents the simulated antenna patterns where we can see the distortions.

These antenna radiation patterns imply an important modification into the reference

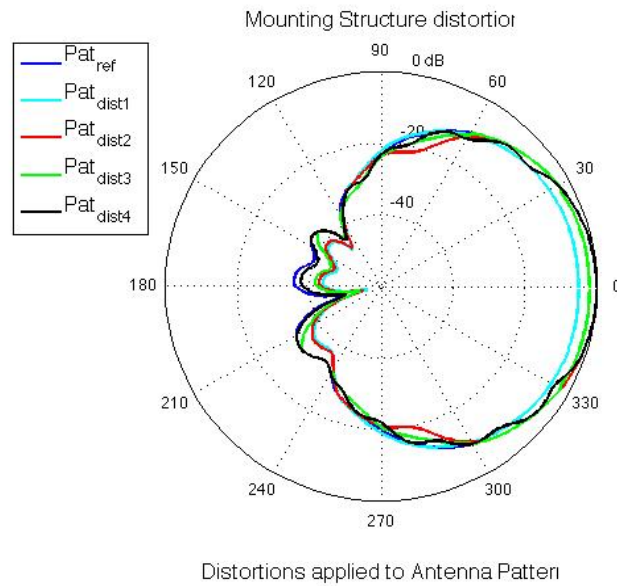


Figure 3.14: Distortions applied to the real antenna pattern.

pattern given by manufacturers. Moreover, if some operators want to be as precise as possible, these effects must be taken into consideration in the cell planning for mobile radio communications networks.

3.3.2 Results

All distortions in an antenna radiation pattern modify network parameters such as received power or SINR which are the identity of a Wireless Network. There is no doubt that, the bigger the magnitude of distortion is, the greater the change into these parameters is. However, what we would like to discover is how they vary within the coverage area.

Thus, we need to define a procedure to determine and interpret these changes. Hence, we follow the procedure explained in Appendix A by which by equation (A.10) we obtain the difference in received power (ΔP_r) inside the cell relative to the received power by manufacturer antenna pattern.

As we can see in Figure 3.15 received power within the area in terms of antenna mast distortion does not follow any kind of linear behaviour. Furthermore, the change into this received power varies from one distortion of mounting structure to another. To understand the importance of these distortions in a global meaning, it is necessary to obtain their cdf of them (see Figure 3.16).

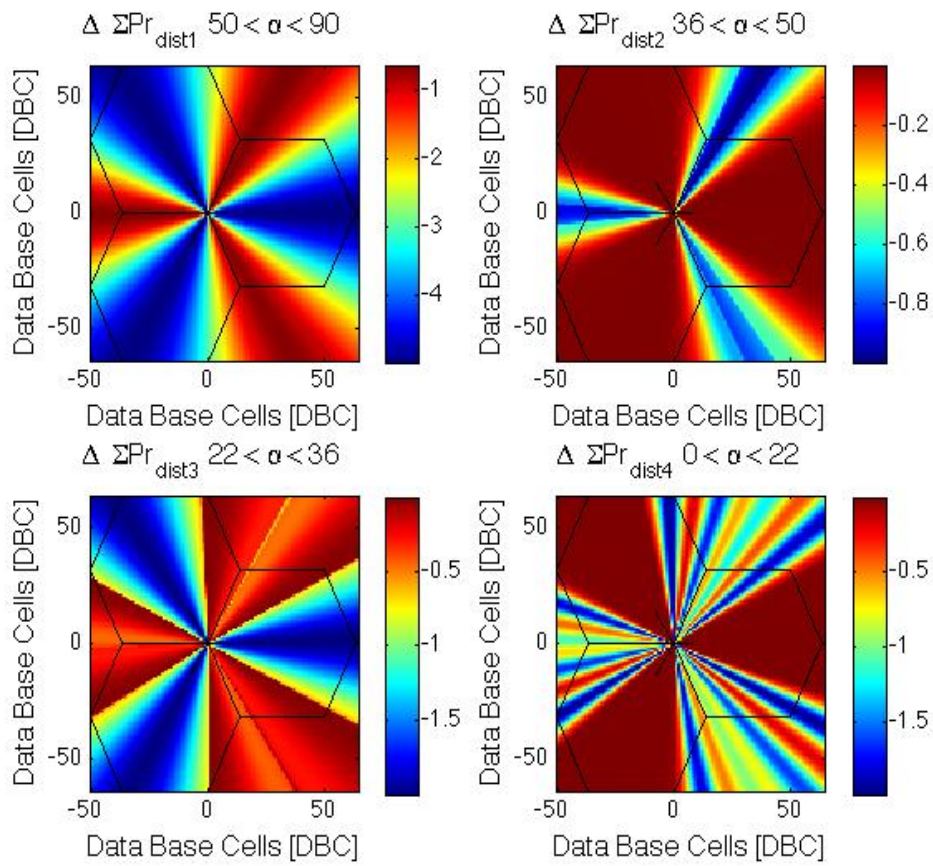


Figure 3.15: Power received calculated with different antenna distorted patterns.

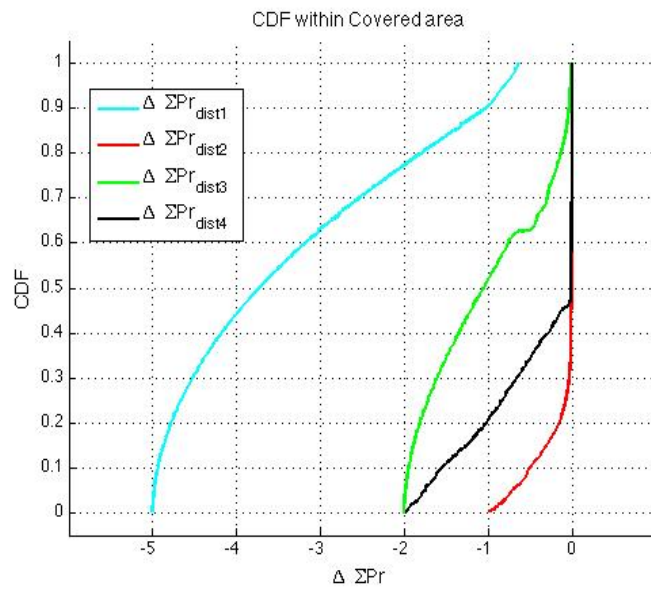


Figure 3.16: Cdf Function of every ΔPr defined by (A.10).

By observing Figure 3.16, it is possible to extract some basic ideas. The most repre-

sentative is that none of these distortions increase the received power in a cell. Indeed, they can reduce maximum value in order of -2 dB to -5 dB the total power received in particular places of the coverage area.

Other interesting point is that cdf function does not provide any information about the angular behaviour. Since, simply by observing this function we are not able to find out in which positions the ΔP_r has a greater influence than others, we will simulate the response of these increases of power and this is how we obtained the result represented in Figure 3.15. Hence, the result of this variation has a strong dependence on the angular direction.

Another idea is related to the response in function of SINR parameter inside the covered area. Thus, following the same procedure as the one for the received power, we can use equation 3.5 to obtain the increment value in terms of SINR in relation to the reference pattern calculated by the manufacturer antenna pattern.

In Figures 3.17 and 3.18 the variations of this parameter are represented. Observing the cdf function, the SINR can be reduced or increased between range of -6 dB and +2 dB.

There is no doubt that, due to the fact that received power has a strong dependence on the angular direction, SINR response should follow the same performance because it is function of the first one.

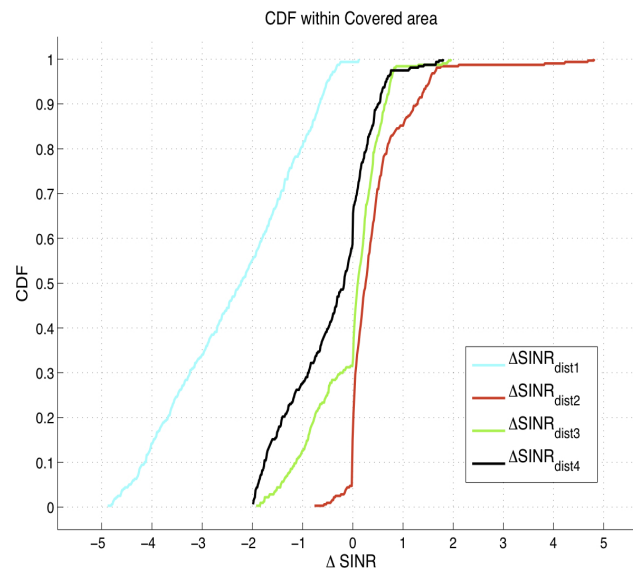


Figure 3.17: Cdf Function of every $\Delta SINR$ defined by (3.5).

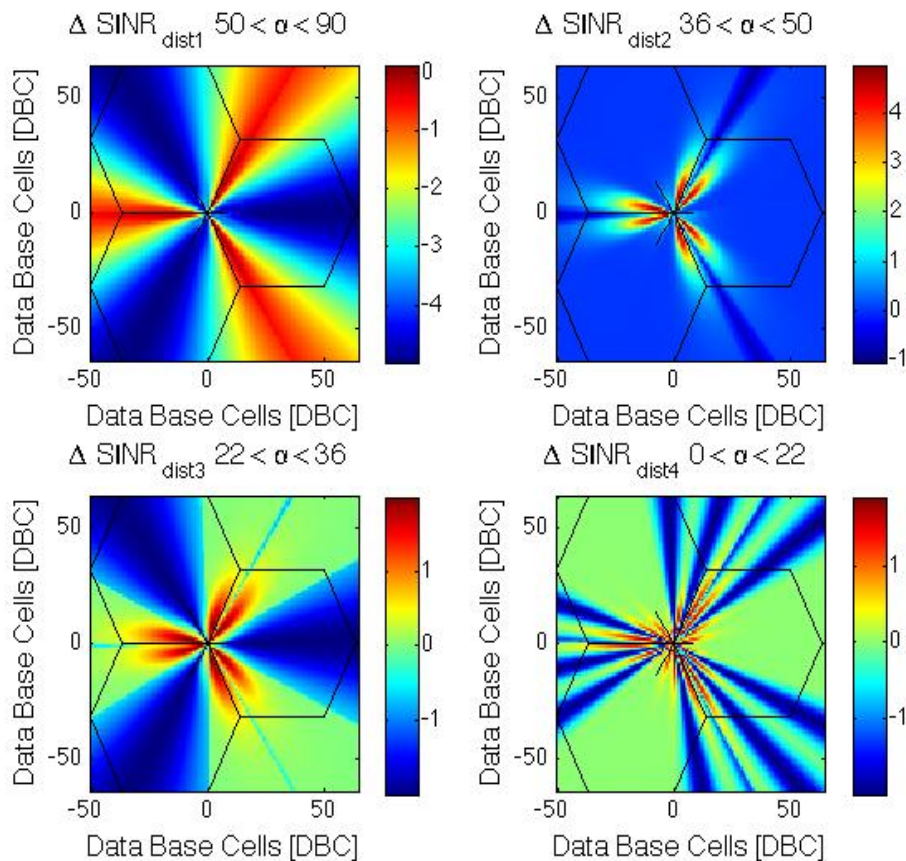


Figure 3.18: SINR modification after new antenna distorted parameter.

3.4 Angular dispersion & Mounting structure

Once we have analysed both effects separately and their impact on a BS deployment, we will proceed to combine both distortions effects in order to see what influence they have on the network parameters.

We will follow, the same previous line. We will simulate the amount of DBCs projected into the footprint of one single sector and the DBCs affected (Figure 3.19) according to Appendix A. It can be seen some DBCs in red, what means, they were covered by the reference but not by the distorted pattern.

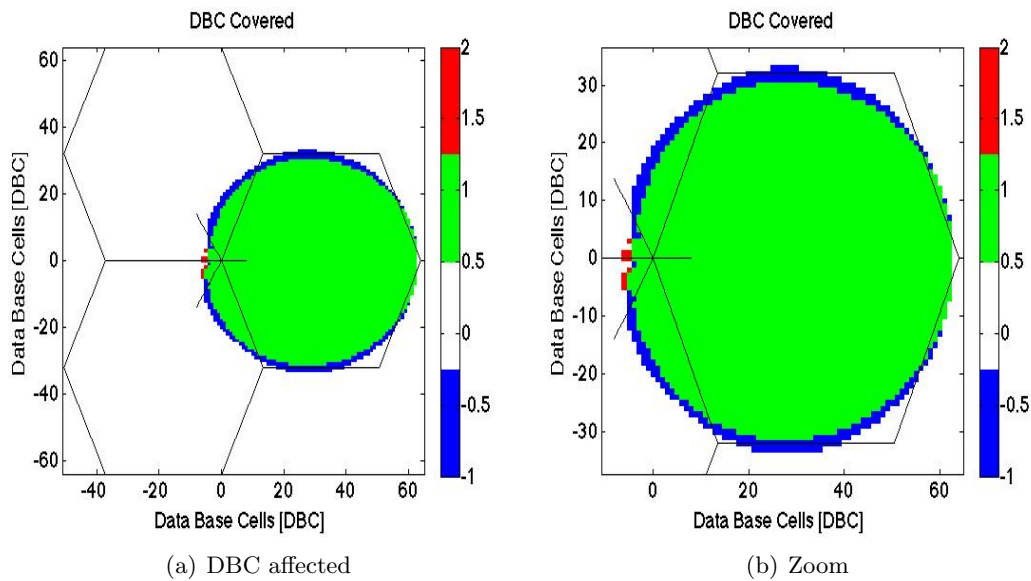


Figure 3.19: DBC affected in one sector combining angular spread of 15° and mounting structure with $36^\circ < \alpha < 50^\circ$.

Figure 3.20 shows the comparison made between the reference and the new network parameters. ΔSIR varies between $[-5$ to $0]$ dB while $\Delta SINR$ varies between $[0$ to $-5]$ dB. These values are lower than the values for an angular spread of 15° because the distortion of mounting structure applied reduces the back lobe.

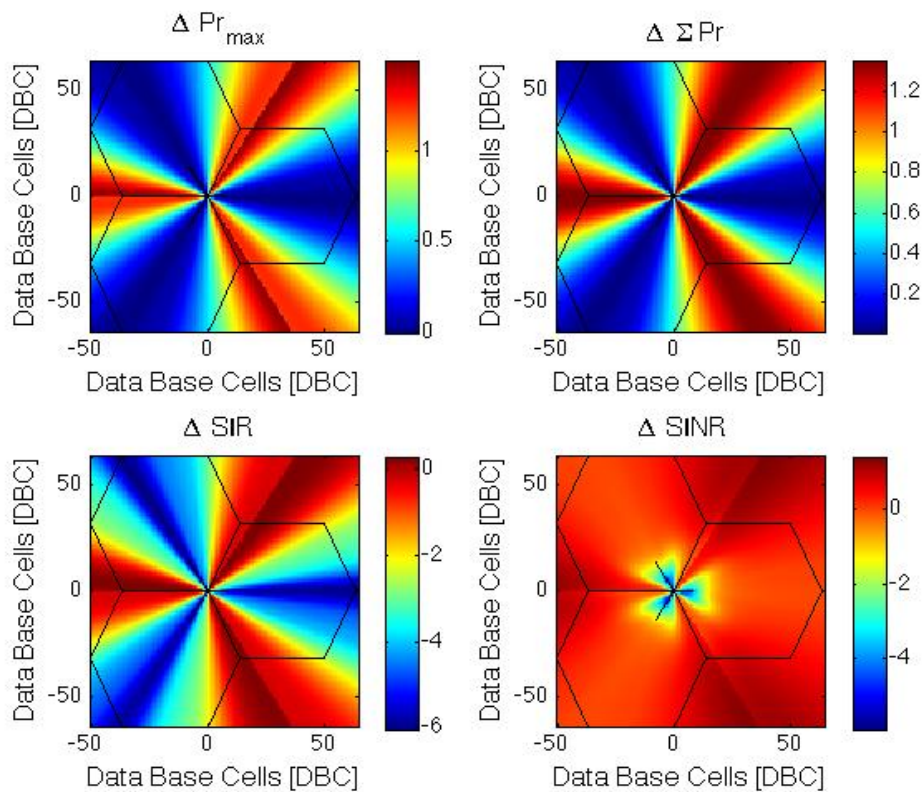


Figure 3.20: Network parameters comparison between distorted and reference pattern.

Considering the CDFs in Figure 3.21, there is a low percentage of DBCs affected by distortions; specifically around the 2% of the DBCs affected reduce their SINR between 1 and 4 dB. Regarding the number of DBCs[%] affected in one sector compared to the total DBCs covered within the BS is:

$$DBC_{affected}[\%] = \frac{DBC_{distorted|onesector}}{DBC_{totalcovered}} = \frac{317}{8603} = 3.7\% \quad (3.8)$$

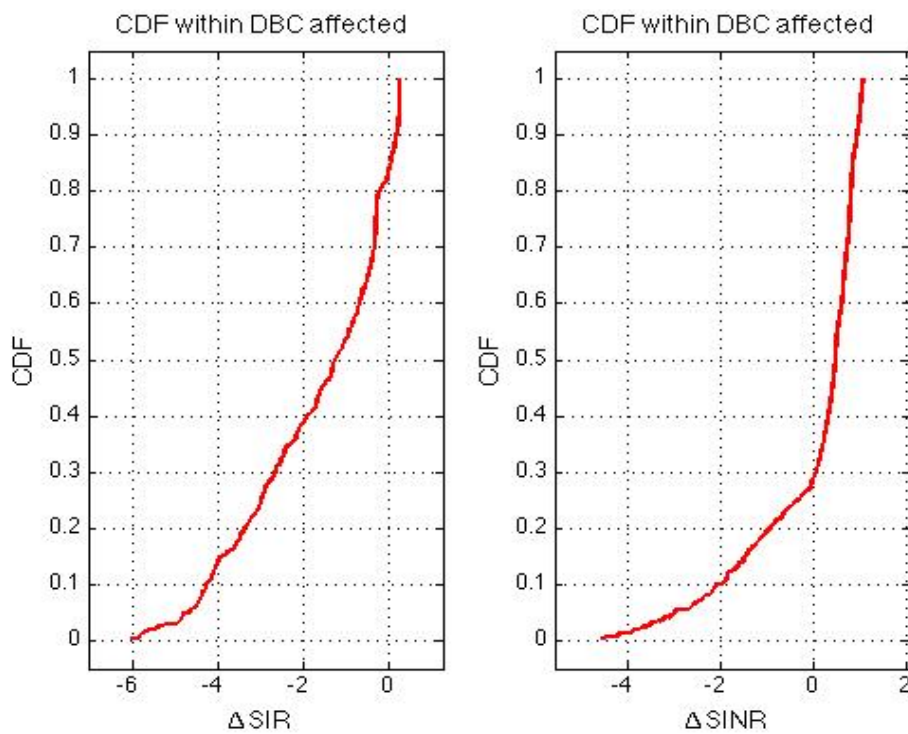


Figure 3.21: CDF of $\Delta SINR$ and ΔSIR .

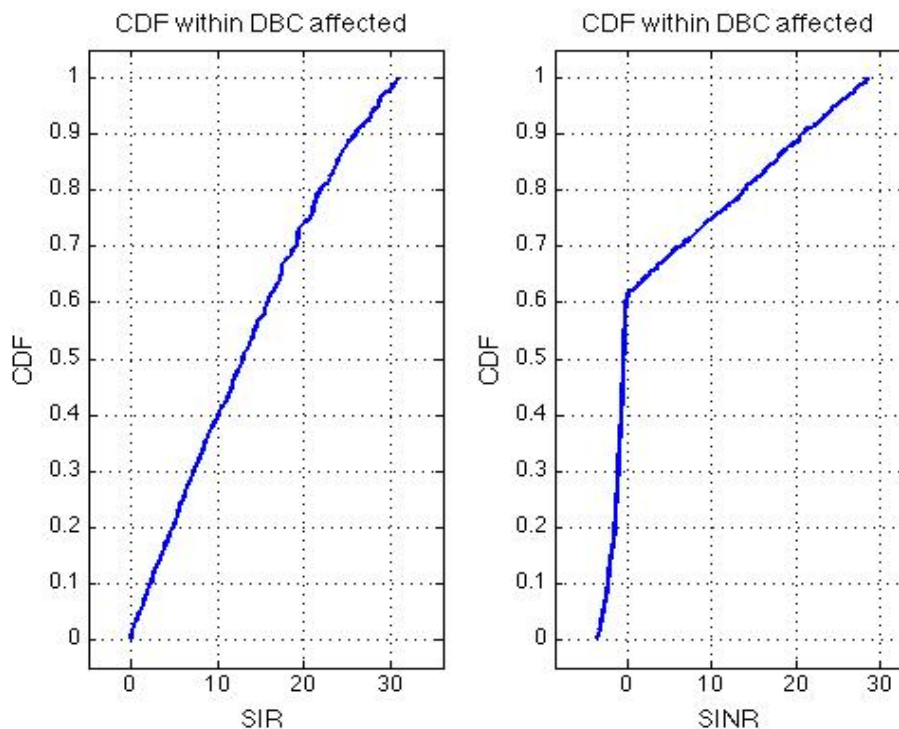


Figure 3.22: CDF of absolute values of SIR and SINR including distortions within the total covered area.

3.5 Summary

We will proceed to summarize this chapter by providing conclusions related to each section separately.

Angular dispersion statements

It is appreciated that angular dispersion characteristics have more influence inside the main beam. The more the value of angular spread increases, the more the level of sidelobes increases as well, while null depth level is reduced, Table 3.3. Since antenna pattern is modified, these distortions might affect network performance in terms of interferences with adjacent cells or sectors within the same base station.

The distortions shown in this chapter are not of great importance regarding the network performance. Even if we focus on the worst case for angular spread which is 15° , the impact on network parameters is not critical.

Mounting Structure statements

First of all, it is totally necessary to carry out a measurement campaign to check the validity of the simulated results before reaching any.

It is observed that this kind of distortion can lead to several changes in the BS covered area such as a reduction in received power within a range from 0 to -6dB. Furthermore, without taking into account these distortions, predicted coverage area can modify the behaviour of the BS to some significant point, for instance, the strongest distortion ($dist_{pat1}$) which reduces SINR 3dB for the 50% of the DBCs covered by the BS.

Received power explains how the coverage is affected but it does not give us any new information about the SINR response. In fact, from this research we have obtained strong distortion in the SINR within the coverage area. Hence, this variation can lead to a completely different behaviour compared with the predicted behaviour.

Our main conclusion is that, Wireless Network operators must consider these distortions in mobile radio communications networks. To support this idea, we have carried out some simulations to compare a real deployment.

Angular dispersion & Mounting structure statements

This combination of effects concludes that, they introduce similar values of distortions, and sometimes, they are reduced due to the randomly behaviour of the mounting structure.

Chapter IV

Measurement Campaign

This chapter is related to the measurement campaign carried out. It will be focused on how the campaign was planned, choosing the potential routes to analyse in Aalborg provided by Telenor, which data from each route is possible to be evaluated or previous calculations about measurement equipment.

The campaign was done with the purpose of contrasting the results obtained by means of simulations with the ones obtained in a real urban deployment. We will evaluate the changes in the antenna parameters such as sidelobes, nulls, front-to-back or mainlobe, as well as, how they impact on network parameters.

4.1 Objectives

The main purpose of the measurement campaign is, firstly, to extract an effective radiation pattern so that operators are able to carry out a more precise network plan, providing an overview of the propagation phenomena effects on the network. Secondly, it would be also useful to compare the effective pattern taken from simulations with the one from measurements, in order to study whether the expected results come true.

4.2 Measurement planning

To begin with, some BSs in the city of Aalborg were the object of study. The information, characteristics and location about them was provided by Telenor to perform the campaign. Figure 4.1 shows an aerial view of Aalborg downtown to get an idea about building height, density, width of the streets and so on. BSs in Aalborg are usually placed above rooftops at 18m height in average.

Before planning the measurement campaign, a procedure was carried out with purpose of extracting the effective radiation pattern from the measurements, as well as, how to deal with data from them. This procedure is explained and proved in Appendix B and further consists of removing range dependence and environment propagation influence by means of getting a reference pattern taken also from references. This way, we will be able to extract the effective pattern from any different route at the same BS.



Figure 4.1: Aalborg aerial view[3].

Therefore, we can trust our procedure to treat measurements as we prove in Appendix B. For more information about the procedure, see appendix mentioned.

4.3 Campaign Execution

At first place, it should be known the equipment which will be used to take measurements. This equipment will be mounted on a van, thus, we will have to find a trade-off between all factors which involve the measurement equipment performance, such as:

- Receive antenna: omnidirectional SWA-0589 (7dBi)
- Scanner: R&S TSMW (UMTS PNS mode)
- Scanner measurement mode:
 - High Dynamic \rightarrow 12 samples/seg (max. 12 samples/seg)
 - High Speed \rightarrow 25 samples/seg
 - Sensitivity: -121dBm (High Speed)/-123dBm (High Dynamic)

It would be suitable to have approximately 40 samples/5m, but in order to reach that amount of samples per meter we would have to use High Speed mode. However, if we use

that mode we will lose sensitivity in reception and it would be more difficult to measure power from the side and backlobes. As it is interesting to have as much sensitivity as possible in order to take samples of the parts of the antenna mentioned before, we will use High Dynamic mode in spite of having less samples per metre rate.

$$f=2162.6\text{MHz} \rightarrow \lambda = 0.139\text{m}$$

$$15 \text{ Km/h} = 4.17 \text{ m/s}$$

$$\text{@12 samples/s (high dynamic)} \rightarrow 2.88 \text{ samples/m}$$

$$\text{@25 samples/s (high speed)} \rightarrow 6 \text{ samples/m}$$

$$\text{@33.33 samples/s (high speed)} \rightarrow 8 \text{ samples/m}$$

Therefore, we will use High Dynamic mode to carry out the measurement campaign. This mode will allow us to have more range to measure the power from side and back lobes. Everything related to measurement equipment is explained in Appendix E.

4.4 Results

Everything in regard to results and routes is written in Appendix D where all graphics from all routes are shown. A brief description is given about the environment around the BS, mounting, and corresponding samples for every sector.

In this section, we will focus on the proper routes that we chose in order to carry out our study from the measurements. There are some requirements that potential study routes should achieve, so that we are able to apply the process explained in Appendix B. The main requirement is to have power samples from the three sectors at the desired parts of the route in order that the process can be put into practice.

The chosen routes to study the BS performance are explained below, as well as, what we can analyse from them.

Route1 - Kristinevej

This route was the only in which route1a (blue route) was done twice, thus, it would be useful to prove whether the signal drop outs are at the same points in the route. It would be also interesting whether it is possible to extract the same piece of radiation pattern from the different routes done (blue and red).

Route3 - Handsundvej

This is an interesting route due to its unconventional configuration. It is not the typical 120° three sector BS since its sectors have T shape. In addition and the most important issue about this route is that, it presents many power samples from the three sectors at the same time along the route. Hence, we can get almost the whole effective pattern.

Route6 - Absalongsgade

The object of study in this route is similar to route1. It is possible to prove whether we can extract the same pattern from different routes, but it is even better than route1 because we have more samples.

Chapter V

Measurement Campaign Processing

Data processing would be an interesting task to carry out after the measurement campaign. This chapter summarizes the data analysis performed in Appendix D and, specifically, the routes explained in the previous chapter with the purpose of obtaining results from a real network.

As it was stated in Chapter one, the project is focused on BS radiation patterns and it is necessary to find out how they are affected by external factors. Considering this, we will analyse and work with data from measurement campaign. Moreover, we will provide an explanation as to whether they are reliable or not.

5.1 Measurements reliability

Before working with any kind of data processing, we need to define under which conditions the measurements were taken. In this section, we will confirm if we can rely on measurements and data from user equipment, according to its specifications in Appendices E and F.

These specifications are related to the mode selected to execute measurements. As it was already mentioned in the previous chapter, the mode was high dynamic range, what means that, a 30dB dynamic range is set for (E_c/I_0) . Firstly, what we would like to find out is whether this parameter is fixed or varies.

Another task we will carry out is to know if the network scanner is accurate enough to measure data even under worst possible technological conditions at the time of measuring it.

As we are working with UMTS/HSPA, E_c/I_0 refers to signal to interference level before despreading the received signal as Figure 5.1 shows.

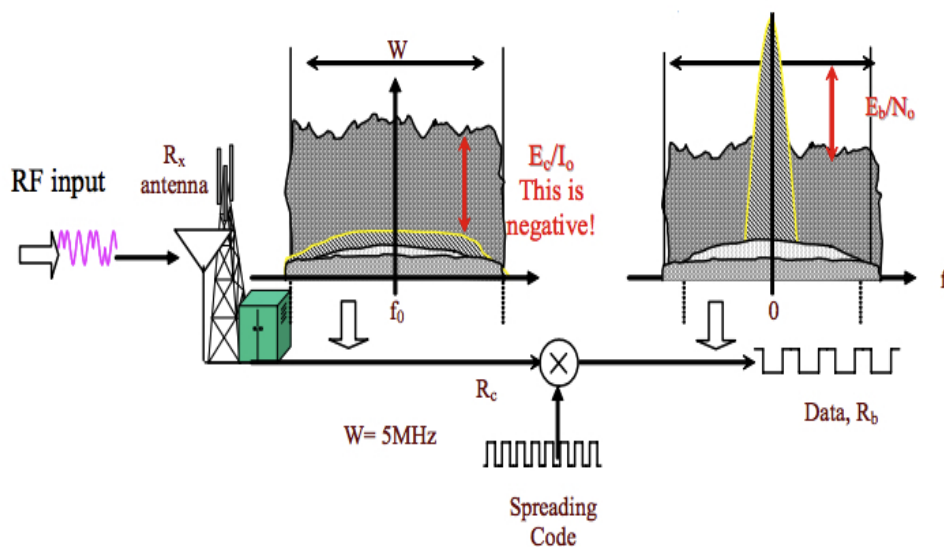


Figure 5.1: WCDMA decoding, [28].

One of the features of this device is that it can store values such as E_c/I_0 or RSCP level at the same time in every sector that is transmitted.

Therefore, we will represent all values for E_c/I_0 along the route to show that this value can be up to 30 dB. Figure 5.2 represents what we stated previously. It can be seen that the minimum range is set at 30dB for all the samples taken along the route.

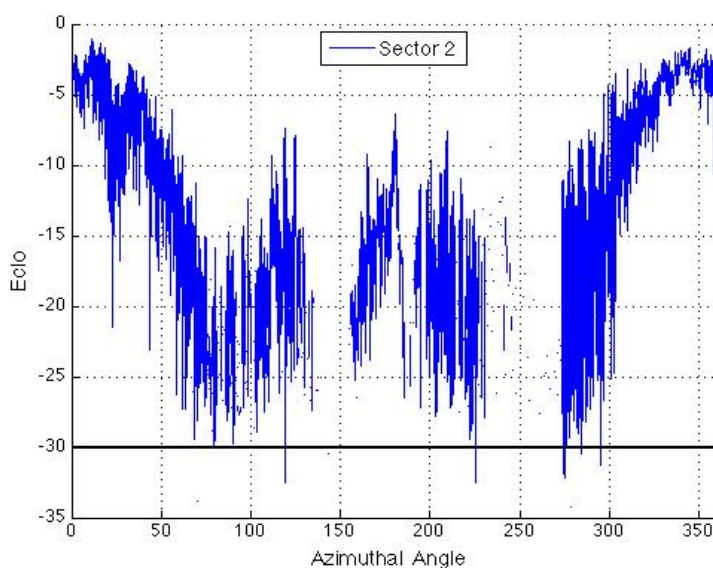


Figure 5.2: E_c/I_0 measured by Network scanner.

In conclusion, from the graphic, it shows that measured values are above -30 dB as previously represented. However, this does not give information for our real level between desired and interference signals. This only represents a parameter measured by the scanner where it can be shown the feature of 30 dB specified in the manufacturer scanner data sheet.

In contrast, we can also extract from the measurements the 8 highest signals in power for every sample along the route and calculate E_c/I_0 value as equation (5.1) defines it.

When analysing Figure 5.1, E_c/I_0 refers to the total level of the bandwidth with respect to the RSCP from the desired sector. Hence, the sum of the 8 strongest RSCP should not take into account the RSCP from its own sector.

$$E_c/I_0 = \frac{RSCP}{ISCP} \quad (5.1)$$

Where RSCP and ISCP are parameters defined as Appendix C mention.

This method is not as accurate as the realistic one because there may be more than 8 signals which would have influence in E_c/I_0 value. Although, the combination of this 8 signals represents almost the total percentage of power inside this specific bandwidth.

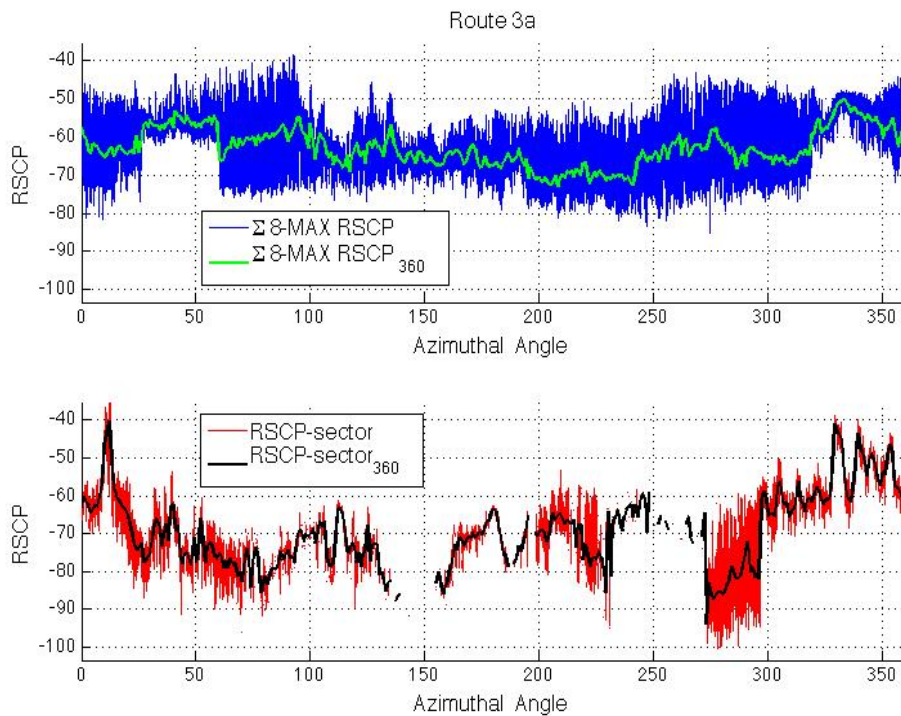


Figure 5.3: Comparison between 8 highest power sum and Single sector Received Power.

The result for this analysis is shown in Figure 5.3 where, the green and black lines represent the mean for each degree applied to 8 highest power signal and desired sector signal respectively.

By applying equation 5.1 to these two signals, we will obtain Figure 5.4. Where the graphic placed at the bottom of this figure shows the solution of the equation.

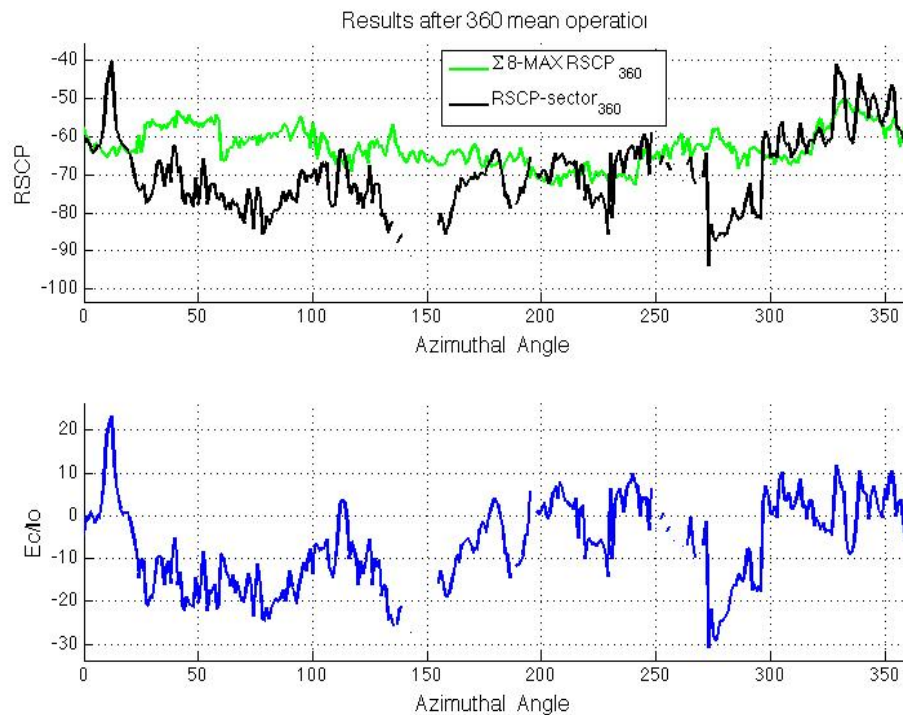


Figure 5.4: Comparison between 8 highest power sum and Single sector Received Power after mean value for each Azimuthal angle.

In conclusion, we can see how the desired signal is above the ISCP caused by other BSs; giving us the opportunity to conclude that our desired signal is not immerse in a high interference level. Therefore, our results from this data are not strongly affected by interference and we can rely on them.

Otherwise, it is possible to realize that the great difference in shapes between E_c/I_o defined by the manufacturer and the result from data measured by his device. A very probable reason for this issue can be the process implemented inside the network scanner. Besides, It can not be extracted the specific algorithm or procedure carried out inside it after the abstract definition given by RHODE & SCHWARZ [25].

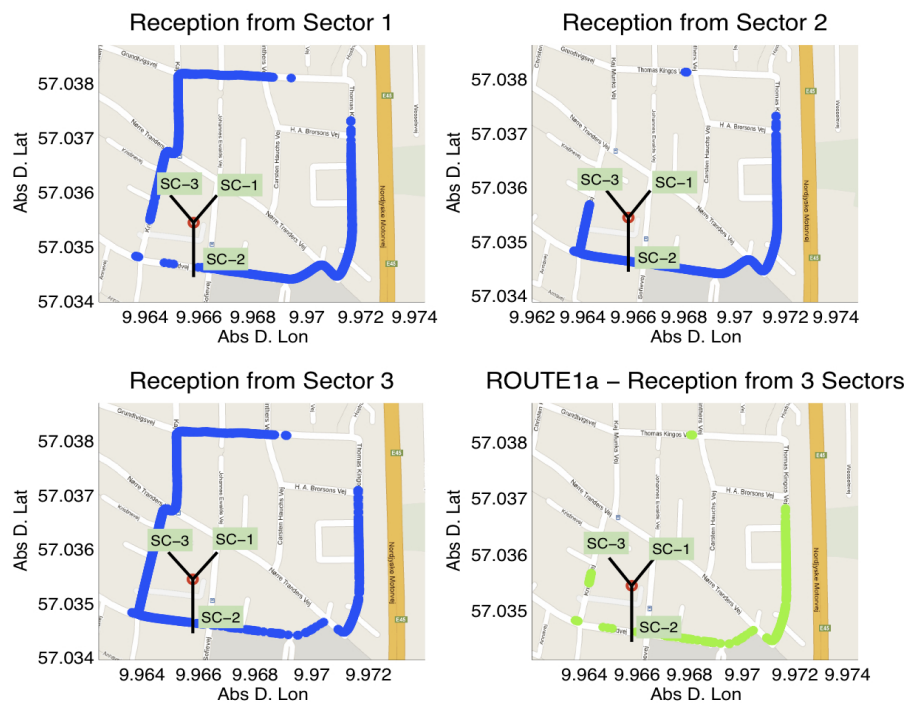


Figure 5.6: Information for routela.

The objective of this section is to show if we can find signal drop outs in the same places along the route. In order to carry out this task, we will plot them in divided routes in function of the bearing and, the distance where we can find drop outs.

Figure 5.7 shows a graphical representation where on the horizontal axis is plotted the bearing angle that is taken according to true North. On the vertical axis is plotted the distance where we receive signal power from one of the sectors from desired BS in terms of the bearing. This could be a clear way to check if drop outs are at the same places since the bearing and distance are the same for once and twice route.

The result of this plot shows that even if we would repeat these specific routes all over and over again, we were not able to measure the RSCP at such points. Thus, the only way to obtain information about these directions would be by planning an alternative route where a different response could be predicted.

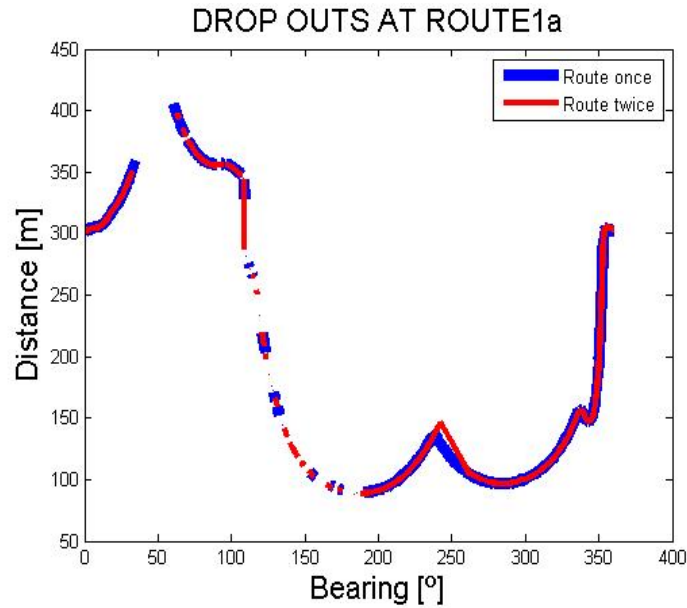


Figure 5.7: Signal drop outs for Route1a. The difference between routes at around 250° it is because both routes do not start and finish at same point and our software join them.

5.3 Procedure

In order to structure the analysis of measurements, we will carry out an algorithm to make the guidelines followed clearer. First of all, we will focus on route 3 (T-configuration) because we have collected samples from it in almost all directions in a radiation pattern, Figure 5.8. Then, we will procedure to analyse the rest of the potential routes.

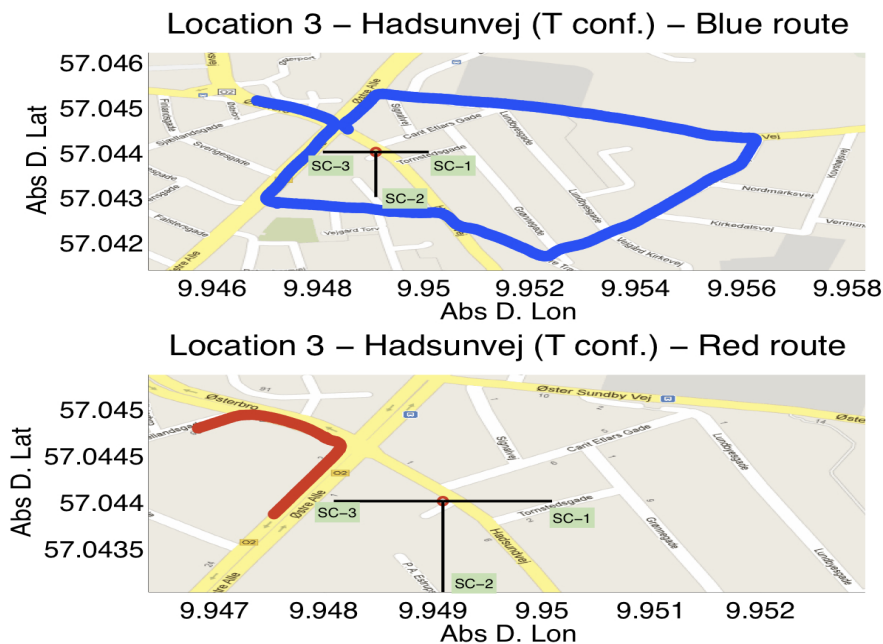


Figure 5.8: Interesting points at same Base Station for both routes.

Algorithm is shown in Figure 5.9. It consists of two different parts; the first part is to manipulate and condition data from measurements in order to adapt them to our purpose. And second part is related to appendix D where we extract the effective radiation pattern from measurements.

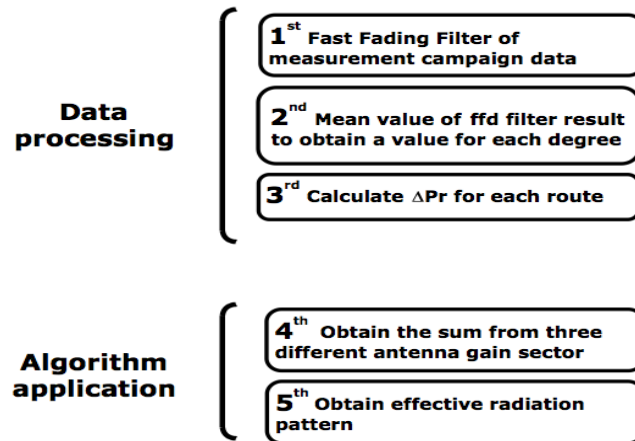


Figure 5.9: Algorithm divided into steps.

5.3.1 Data processing

Fast-fading filtering

First step to take is to reduce the small-scale variation in received power by the use of a fast-fading filter, we will apply an average every 10 samples. Figure 5.10 shows the result of applying this fast-fading filter.

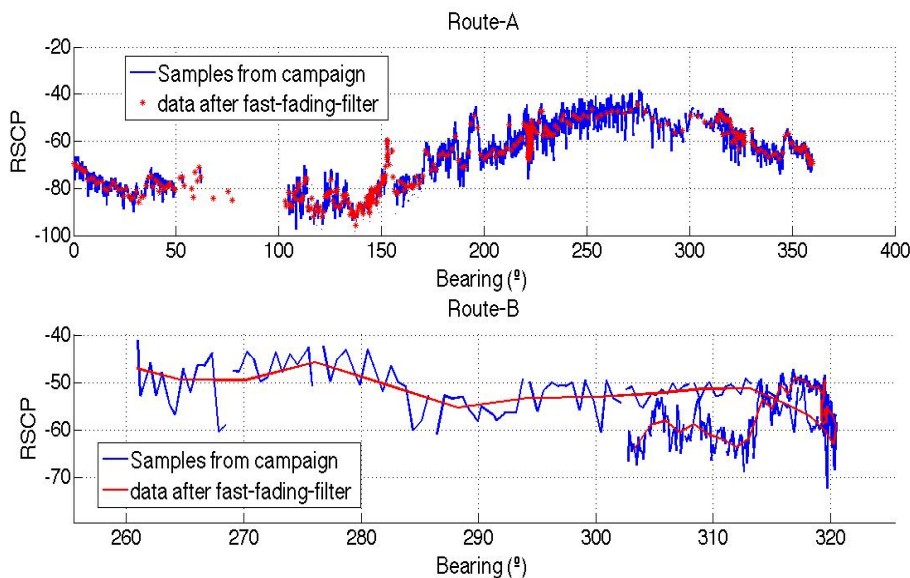


Figure 5.10: Received signal profile from one of the sectors for route 3a and 3b.

As it can be shown in this figure, there are some angles with two different values of power. The reason to explain the cause of this feature is that the route carried out around the BS has some positions with different distance but the same direction.

Azimuthal angular Mean

Basically, by taking this step, we obtain a value for each azimuthal angle point, since the fast fading filter is not characterised by a equispaced angular value for each RSCP point.

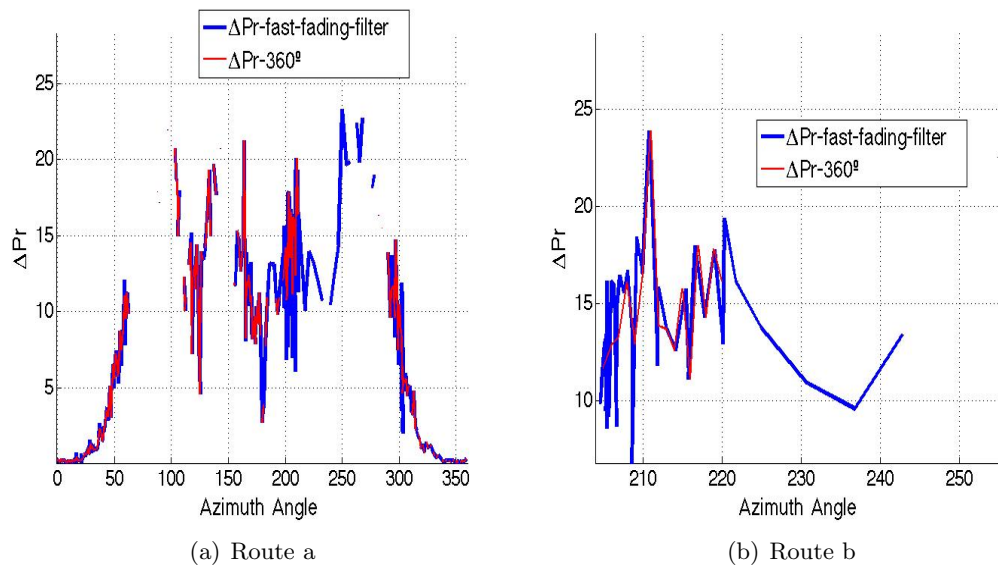


Figure 5.11: Red lines represent the mean value for each degree.

Figure 5.11 shows the result after applying a mean value for points which are inside condition expressed by equation (5.2).

$$x - 0.5 < x \leq x + 0.49 \tag{5.2}$$

Drop outs vary between red and blue lines because the blue line is represented by number of samples in x-axis. But the red line gives the x-axis graphic the azimuthal angular value between 0 and 360 degrees. It implies that the drop outs can be smaller or bigger because these two parameters are not represented into the same scale.

Variable ΔPr from real measurements

Appendix D shows how to obtain this variable from simulated parameters. It can also be calculated from a real Network once Received power is measured. In this case, this variable shows the performance in Figure 5.12.

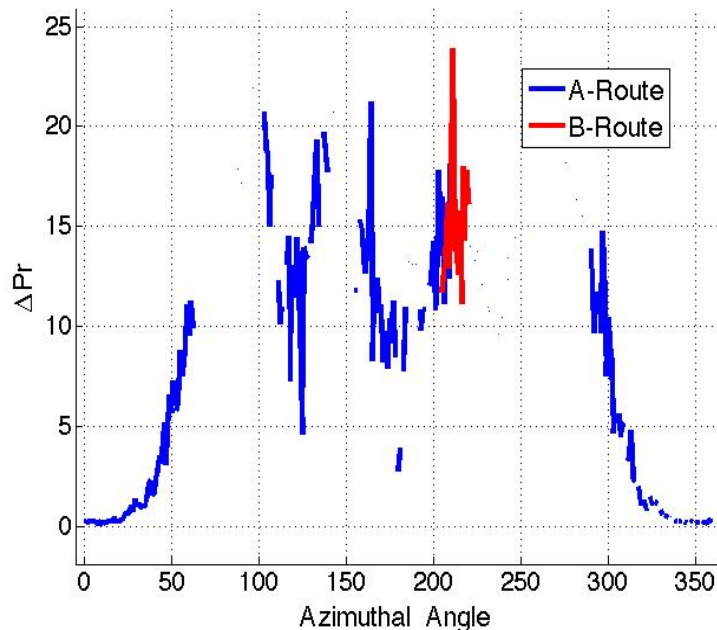


Figure 5.12: Performance of ΔPr for both routes.

This specific case is for a T-configuration BS as we have discussed previously at the beginning of this section, Figure 5.8. Although route B covers a small angle, it is enough to see that this algorithm obtains a similar mean value for both routes. Even if there are some samples in the same angular direction, it could be regarded as a problem.

5.3.2 Algorithm application

In this section we will apply the procedure designed in appendix D in order to extract an effective radiation pattern from measurements. After carrying out data processing treatment in the previous section, now our data is adapted to our purpose.

Sum from three antenna gain sectors

The last step to take before obtaining the effective radiation pattern is to build a new reference pattern. This reference consists of the sum of sector gains given by manufacturer, according to the antenna model and tilting depending on BS configuration.

Effective antenna pattern

Then, we will apply this new reference and combine it with ΔPr by means of equation (B.4). According to route 3, the effective pattern obtained is shown in Figure 5.13.

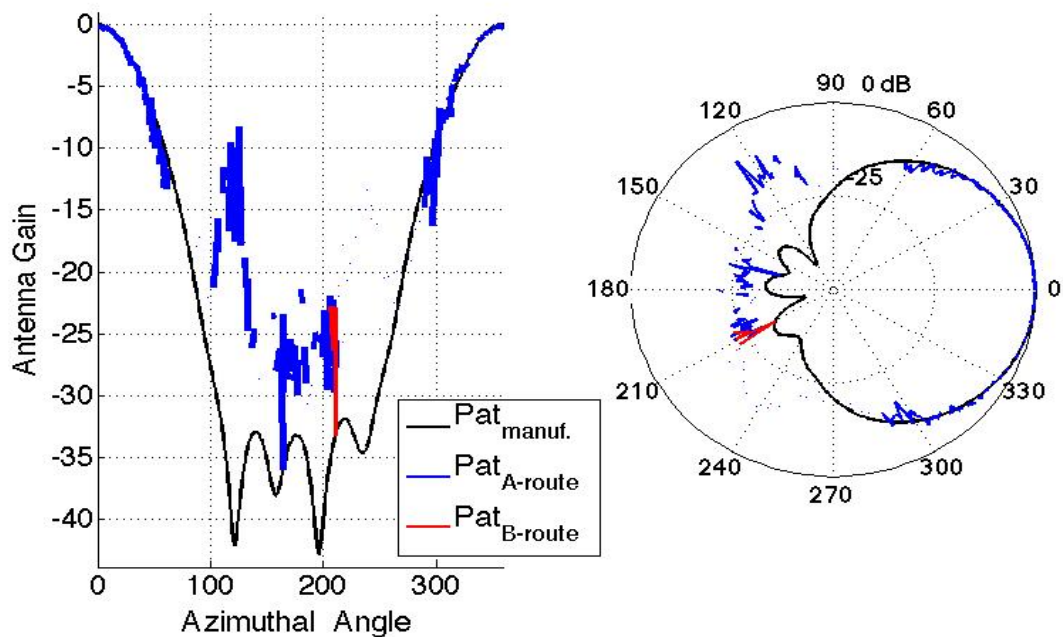


Figure 5.13: Effective radiation pattern from route 3.

From the graphic, it can be seen that the main lobe obtained matches perfectly with the pattern given by the manufacturer. The main appreciable difference from the manufacturer's is the back part of the pattern which is 7dB higher. This causes that Front-to-back ratio is lower. Moreover, we can also appreciate that two different routes done for route 3 are tracking each other.

Surprisingly where it was supposed to be null, there is not a null in that direction (117°). This may be because in a realistic environment the nulls are filled as it was shown in section 5.5 due to environmental interactions.

Once we have done for one route, we will analyse other potential routes that were done for other sites. Route 6 (near kastetvej) is shown in Figure 5.14. It is also other route in which we checked if it is possible to extract the same radiation pattern from both routes.

It can be appreciated from Figure 5.15 that unfortunately, we can only extract the back side of the radiation pattern. However, we can not focus the analysis on it because the main lobe should not be affected. In this case, the difference between the effective and manufacturer pattern is approximately 13dB which is a worse result than in route 3. Furthermore, both effective patterns have the same shape than the manufacturer's (see polar plot Figure 5.15).

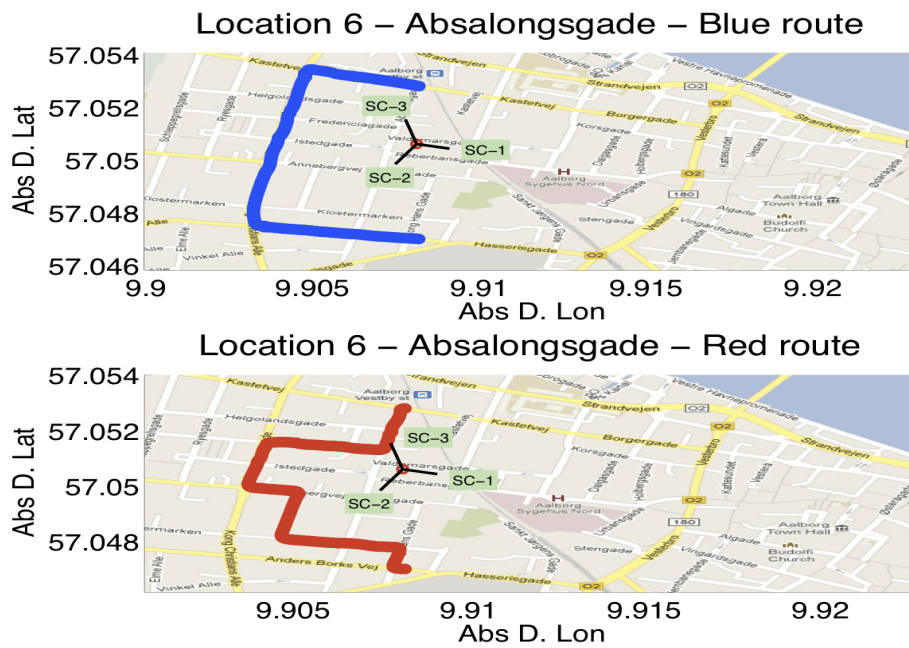


Figure 5.14: Route 6.

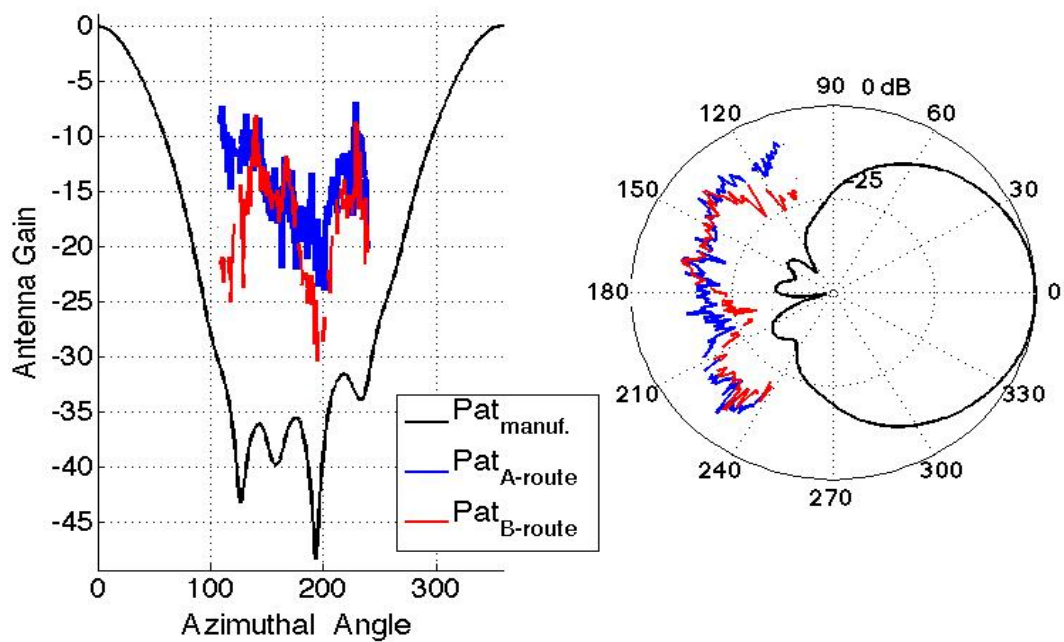


Figure 5.15: Effective radiation pattern from route 6.

From route 1 (Kritinevej) we only obtain the same radiation pattern for different routes. The same situation applies again in this case: the values for different gain in different directions are higher than the manufacturer's. It should be taken into account when the network planning needs to be done.

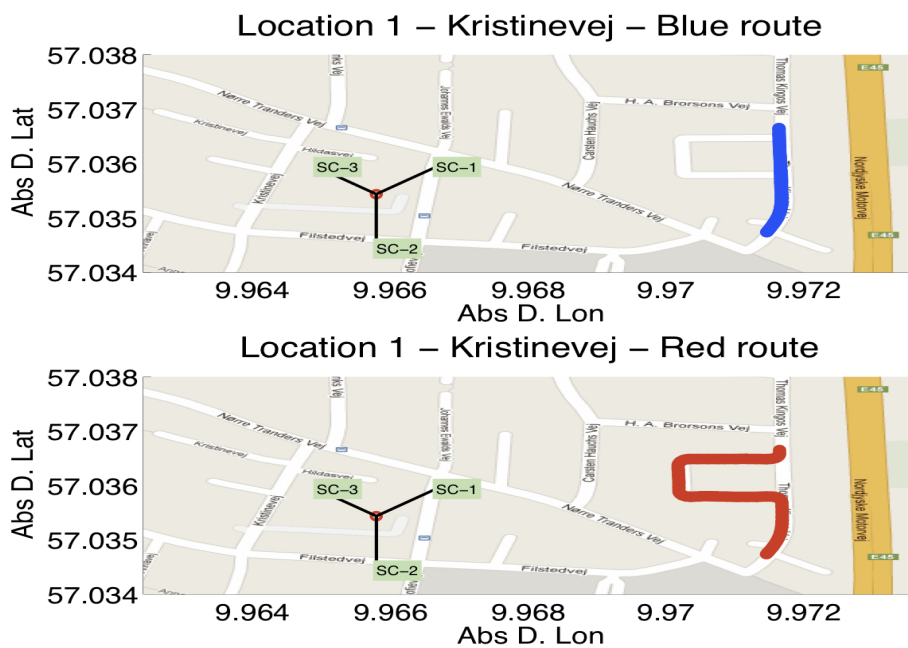


Figure 5.16: Route 1.

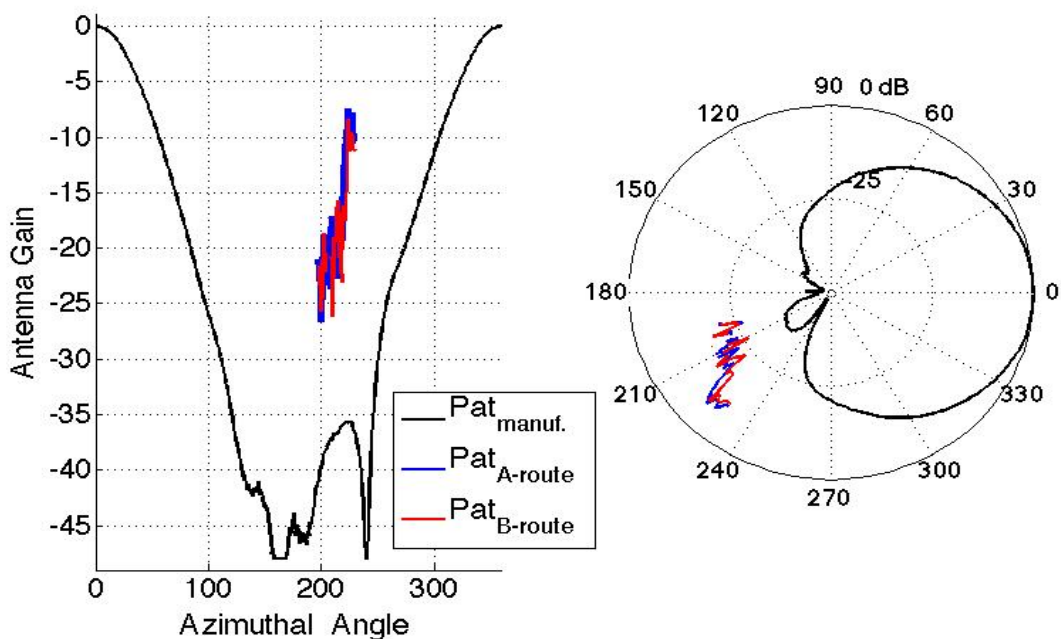


Figure 5.17: Effective radiation pattern from 1.

5.4 Real deployment analysis

As it was applied in the simulations, an analysis within a realistic deployment should be carried out. We will use the algorithm designed in one of the appendixes to calculate the

impact of distortions in terms of DBC, to see how the effective radiation pattern calculated for route 6 (absalongsgade) affects network parameters. This can only be considered as an approach because it is applied for a single BS and not within a whole network.

5.4.1 Effective pattern simulation

In order to introduce the extracted pattern for this BS into the software, we obtain the effective radiation pattern for one of the sectors as accurate as possible represented in Figure 5.18. We will assume that the antenna will be the same for the three sectors and they will suffer the same distortions since it is not possible to extract each sector separately due to lack of samples. The main lobe stays unaltered because we saw from some routes, that it preserves its shape; see Figure 5.13.

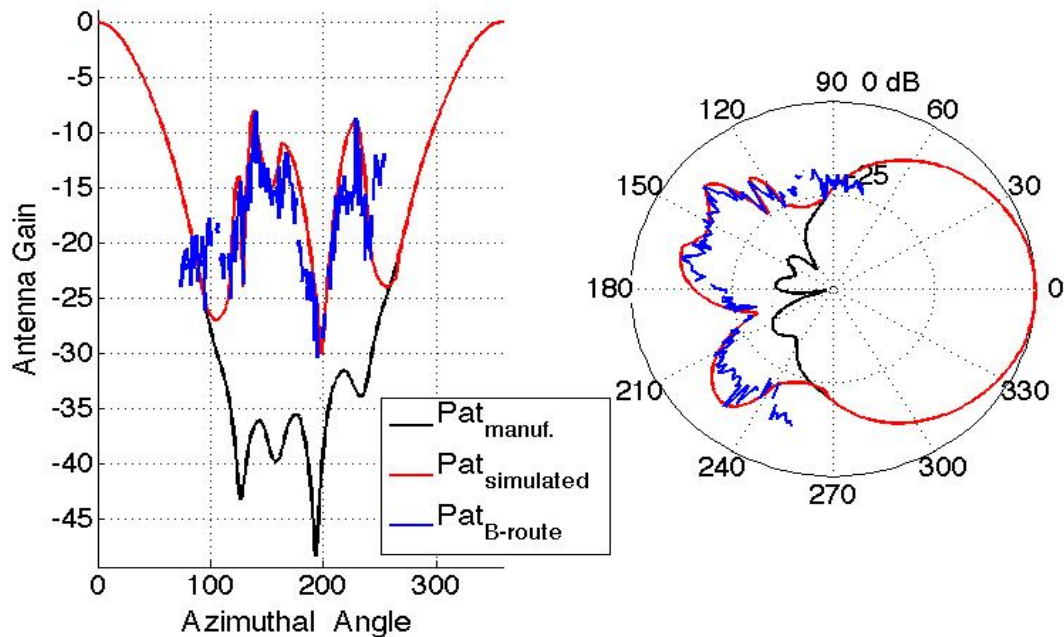


Figure 5.18: Simulated effective radiation pattern.

5.4.2 Impact on Network parameters

Considering the analysis done in Chapter III, we will conduct a similar study using this radiation pattern to find out how a network would be affected without taking these distortions into account.

5.4.2.1 Simulation results

First of all, it is necessary to represent the number of DBC affected within the area as Figure 5.19 shows. Thus, we will know which cells are affected and in which way. The green ones are the DBCs covered by both patterns (the effective and manufacturer's), the

blue ones are covered by the effective one but not by the manufacturer's and the red ones are covered by the manufacturer's but not by the effective.

In this case, the existence of the red ones is due to the effective estimation pattern we obtained previously. It is only above the manufacturer pattern gain in 1-2 degrees. Thus, these types of cells should not appear because this radiation pattern has never decreased its gain with respect to the manufacturers.

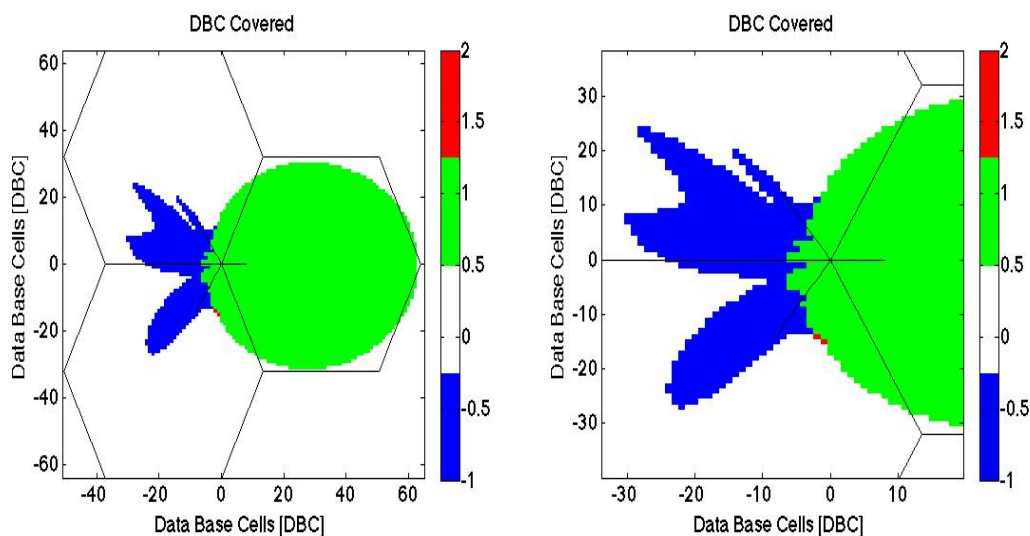


Figure 5.19: Variation of covered DBC compare with manufacturer pattern.

It is also of potential interest to know how many of them there are and which ratio from the total BS covered cell they represent. Equation (5.3) will help us to figure this result out.

$$DBC_{affected}[\%] = \frac{DBC_{affected}|_{oneselector}}{DBC_{covered}|_{oneselector}} = \frac{682}{8603} = 7.92\% \approx 8\% \quad (5.3)$$

Once we know the position and the approximated number of these cells, the next step that a network operator would take to simulate the values for basic parameters of their BSs. When trying to predict the possible coverage and throughput for this network cell, Figure 5.21 will be the result then.

As we can appreciate from this graphic, these kind of plots show an overview of the shape of these parameters but it is hard to reach a conclusion in terms of DBCs.

Cumulative probability density function of these specific cells, Figure 5.20, will tell us the percentage of DBCs affected by a fixed value. It is also useful to extract the number of cells between margins of parameter values.

Such results make possible that, an operator is be able to carry out their Network planning and dimensioning. In addition to it, the final step would be that operators could approach

coverage estimation as well as possible data rate within the covered area.

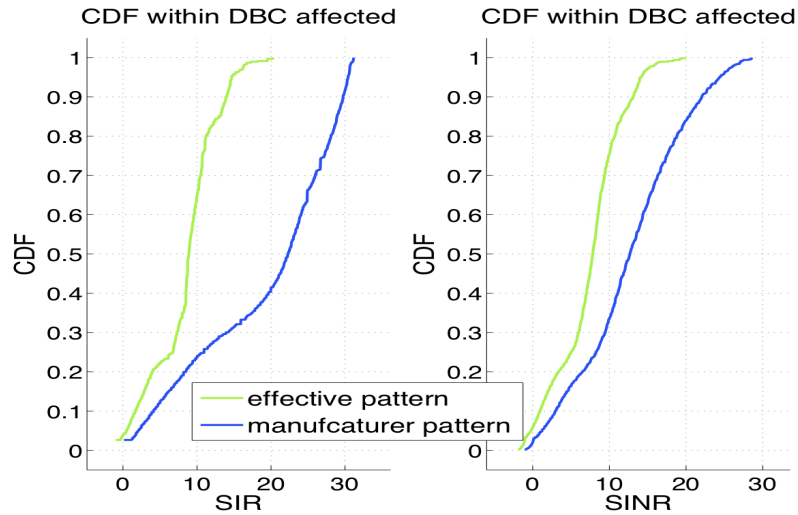


Figure 5.20: Absolute SIR and SINR values for affected DBC.

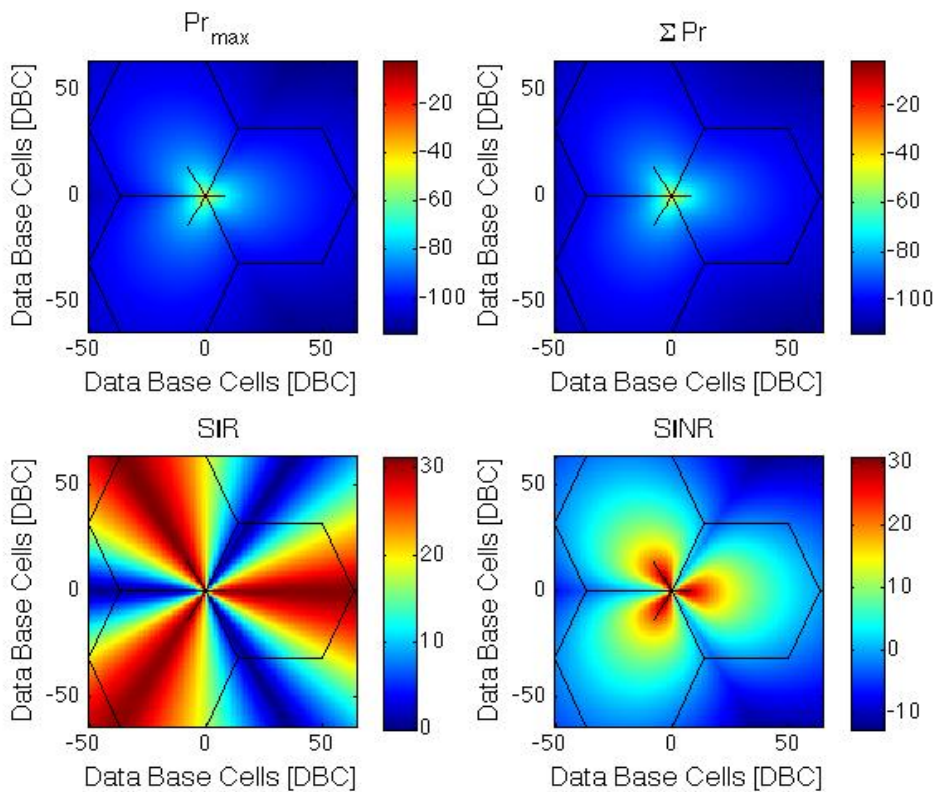


Figure 5.21: Absolute values of SIR and SINR within DBC affected for effective pattern.

However, it is hardly imaginable that an operator can predict their Network Planning with

results simulated by manufacturers radiation patterns. But, it is a reliable method to find out the error committed if this would be the way. Moreover, an accurate predictor of how an operator could be wrong with this preliminary assumptions.

Comparison analysis between radiation patterns

Figure 5.22 represents the increase of these basic parameters following the same procedure used in Chapter III defined in the appendices, see equation (A.10). These increments are the result after subtracting manufacturers pattern results from distorted pattern results. Therefore, a negative value shows that the results from distorted pattern are lower than the reference one.

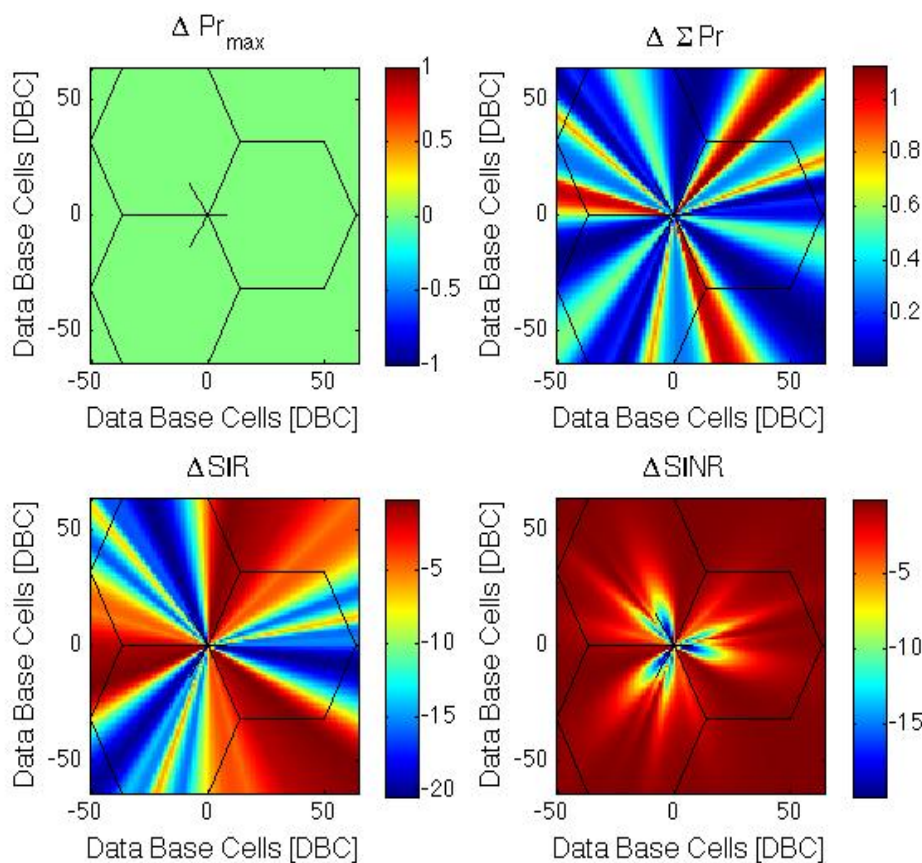


Figure 5.22: Relative result for most characteristic parameters between both patterns.

Comparing this figure with Figure 5.23, information about changes within DBC affected can be extracted. As a first approach, it can be appreciated from the graphics that SINR varies over 5dB in the desired area and over 10-15dB in the vicinities of the BS.

Furthermore, almost a linear variation between -20 to -5 dB in terms of SIR can be shown. This makes parameters such as SIR or SINR and decrease the quality of the communi-

ation. It could be even impossible to establish a communication link between BS and MS.

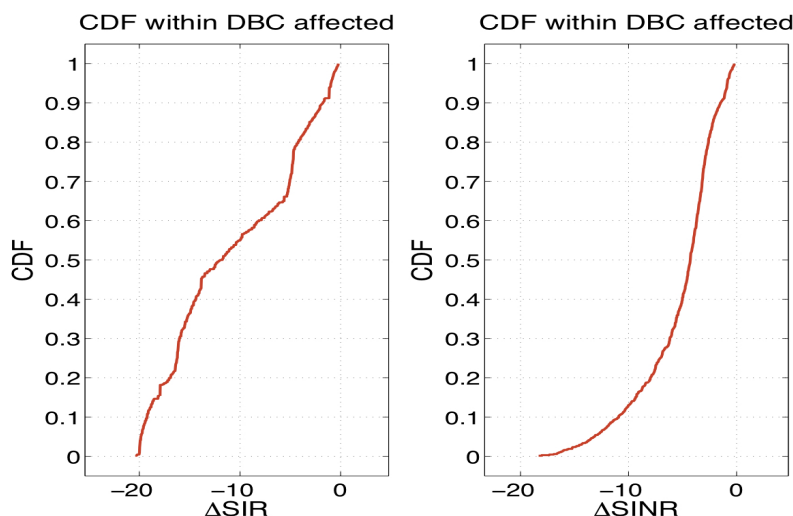


Figure 5.23: Increment value for SIR and SINR within affected DBC.

A Network operator usually works with a value of -10 dB for SIR parameter because a lower value could be very difficult to guarantee communication link between MS with BS. Otherwise, working with values from -10 to -5 to assure a high data rate within DBC could be difficult.

In order to be able to analyse the number of cells with critical values, we will also need to conduct a similar research in terms of color maps and CDF. For this research, Figure 5.20 represents results for this analytical method.

As it can be shown, the biggest increments in power are applied to DBC with the biggest absolute value. This behaviour leads to a decrease of SIR close to 0 dB or, even to negative values for SINR. Thus, we can not conclude that this BS has a certain number of DBC in which the communication breaks down. We can approach this fact in two different ways.

On the one hand, the main point of this section is that distortions at side and back lobe that reach a value from -15 to -5 dB for SIR. Using data from equation (5.3), this has a result of 340 DBC; where the operator has to manage with a enormous error in their parameters.

On the other hand, this simulation is only made for interferences introduced by the other two sectors of the same BS. However given the case that this interference level would include more interferences from other BS, this level probably increased to even higher values than the service threshold or, at least, decrease the network quality.

5.5 Explanation about difference between results from measurements and simulations

5.5.1 Antenna tilting

One of the main reasons that results from measurements and simulations have a great difference on side and backlobes, could be due to antenna tilting. The two patterns that we compare to evaluate if the effective pattern extracted from measurement campaign is similar to the one given by manufacturer specifying the tilt, are measured on different planes. While the manufacturer's pattern is measured in the plane where the antenna is mounted, the effective is measured on the measurement plane (or ground plane), what is to say, we can be measuring power with a different gain than the specified by the manufacturer for a certain tilt. Figure 5.24 illustrates previous explanation.

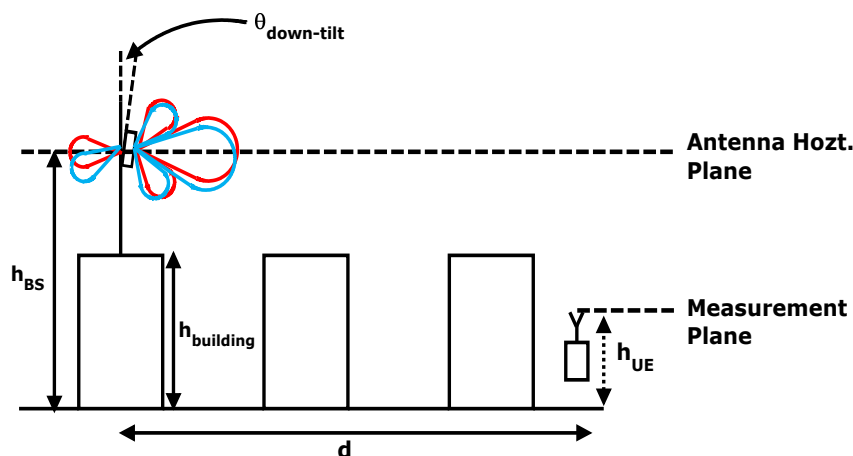


Figure 5.24: Plane where radiation pattern is measured.

Assuming that measurements were taken in a hilly terrain and the BS height is not too high, the gain received from the vertical plane can be supposed the same. One possible way in order to have an idea of the error committed, is to compare both patterns from manufacturer for different tilts. Figure 5.25 shows this comparison.

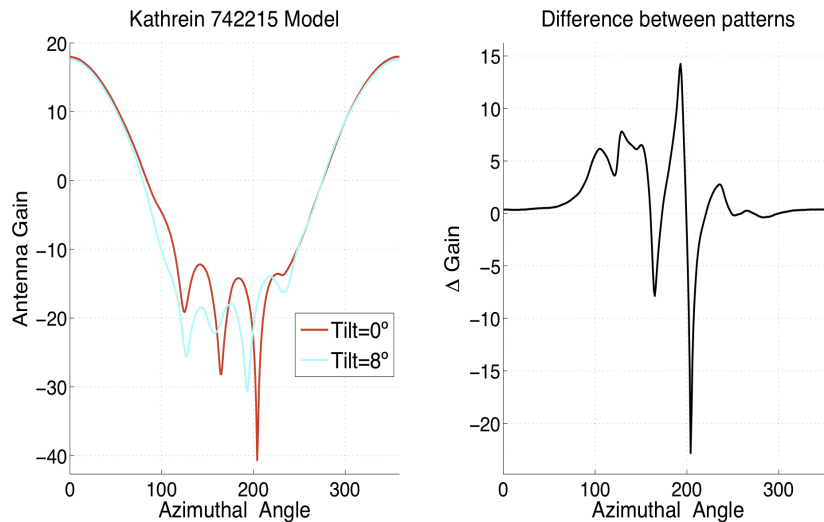


Figure 5.25: Comparison between manufacturer patterns with 0 and 8°.

Although there are high deviations between these patterns, excluding directions where the null from one pattern matches with the sidelobe from the other, it can be found a maximum deviation around 6 dB. As the BS height is not so big, we can use the manufacturer pattern with the specific tilt to carry out our comparison.

5.5.2 Non stationary value of Angular Spread along the area

By trying to find a reason due to the really high gain level in Figure 5.13, we used the results from a ray-tracing tool to search for the pathloss and angular spread values in every pixel along the area in route 3. Once the simulation was carried out, we realized that the angular spread had different values depending on the location. Figure 5.26 shows the angular spread values within the area for the desired sector which is pointed on the map.

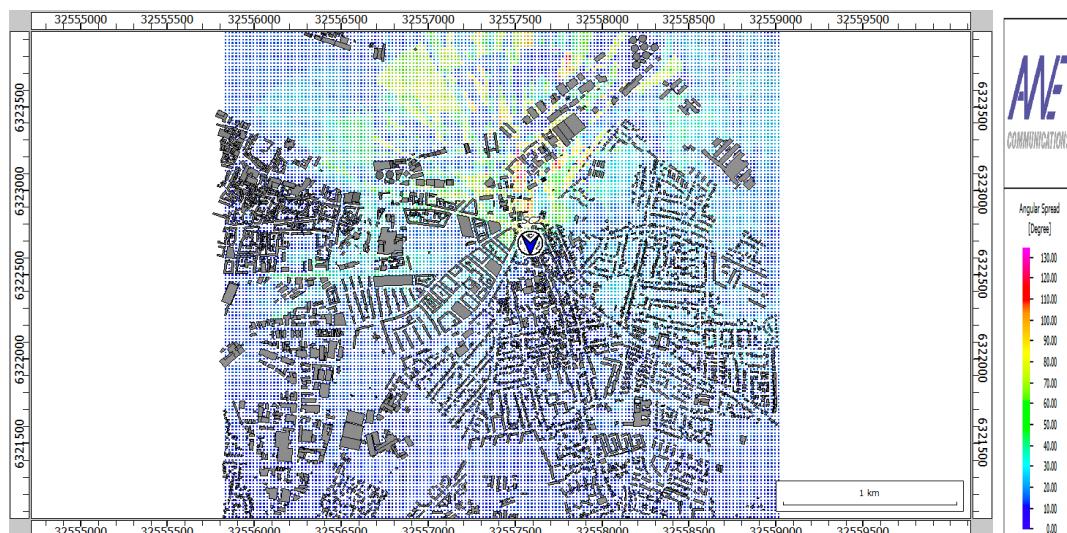


Figure 5.26: Angular spread results from ray-tracing tool.

We will follow a procedure in order to find the angular spread values of interest for our specific route. These values are shown in Figure 5.27, it can be seen that there are quite high values of angular spread in some directions.

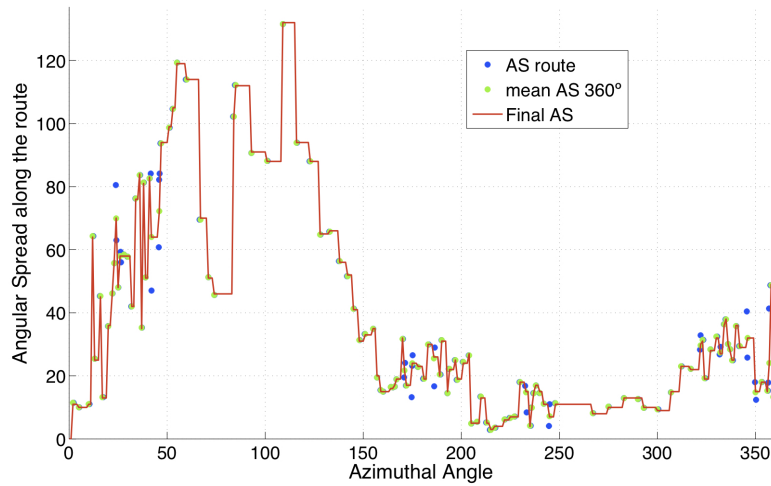


Figure 5.27: Angular spread values along route 3.

Once we have one value of angular spread for each degree, we will generate all the laplacian distributions for these values and normalize them with their respective area. Next step will be to rotate the radiation pattern in order to integrate it with each of these laplacian distributions. The result of this integration will be other effective pattern and it is shown in Figure 5.28 as well as effective pattern from measurements and manufacturer's.

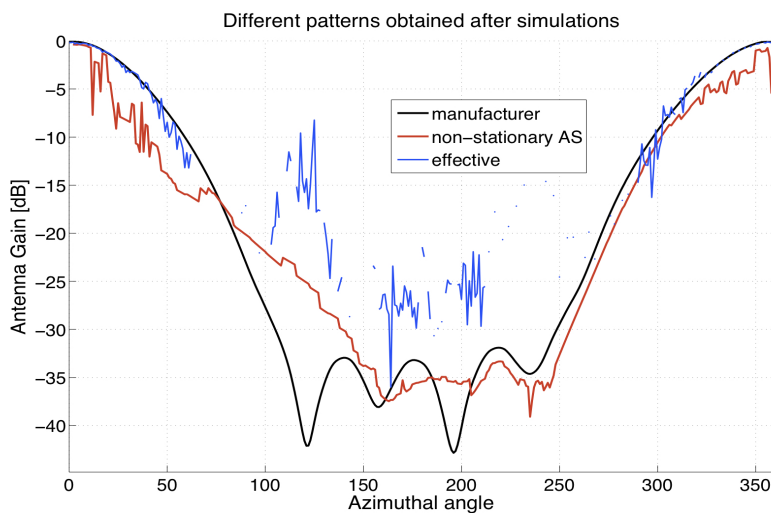


Figure 5.28: Comparison between patterns.

This result combined with mounting structure distortions and what it is explained in section 5.5.1 may justify the deviation between manufacturer pattern and the pattern extracted from the measurement campaign.

5.6 Summary

Basically, it can be seen from previous Figure 5.7 that for both routes signal drop outs appear almost in the same places. Besides, we can say that even repeating this routes we would not be able to measure power in these positions.

This happens because signal from this sector is lower compared to the Received power signal from other sectors. Received Power signal on this drop outs direction is bigger than 30 dB below the signal received from other BS surrounding it. Thus, it could not be possible to measure RSCP from this backlobe direction even if we repeat these routes more times.

While observing the behaviour of this algorithm throughout the different routes represented in the graphics, we could state that the result of the algorithm is very similar for the effective radiation pattern obtained. However, this algorithm is rough in the mainlobe direction pattern but not precise enough on back and side lobes. This is the reason why we do not have enough samples in these other directions.

When analysing the effective front-to-back ratio obtained from the effective pattern, we can conclude that it differs from the one measured for free space conditions for a value of 20 dB between 90 to 260 degrees. The fact that it has same shape as the original should be taken into account in future network planning in order to control of network and antennas parameters better.

In addition to it, the results exposed in the last section of this chapter showed an alteration in SIR in order of -10 dB for half of the DBC affected for this effective antenna pattern as well as a decreased value between 0 to -7 dB on SINR for a 80% of these cells.

To quantify the impact, we could say that this percentage represents a number of 340 DBC and 587 DBC respectively. Thus, this area in square kilometres represents 3.42 Km² and 5.87 km².

Chapter VI

Conclusions

After the results obtained from simulations and measurements, the following will be the overall conclusions about the project, firstly, with reference to the two sections: simulations and effective radiation pattern; and, finally, we will state the general conclusions.

6.1 Conclusions about simulations

Since angular spread has more impact on sidelobes and nulls than on mainlobe, network parameters are affected. As far as simulations are concerned, since these changes are not too big, they are not critical for the good network performance.

Considering the mounting structure and depending on it, distortions will be produced in a bigger or smaller scale. For instance, the structure with the biggest distortion has a great impact on network parameters. However, this kind of structure is not so common to find. Operators should take these distortions into account on the network design but they are difficult to estimate due to mounting structure and angular spread random behaviour.

6.2 Conclusions about effective radiation pattern

The pattern extracted from the measurement campaign tracks perfectly in shape in comparison with manufacturer's one. Considering the back side of the pattern, it has largely increased if compared with manufacturer's due non stationary angular spread and horizontal pattern measured with a specific tilting.

Regarding the front-to-back ratio, it is reduced in approximately 20 dB which is too aggressive compared to manufacturer's pattern. With respect to such a difference, network parameters are really affected, specially, in the vicinities of the BS. This can lead to poor coverage or data rate.

6.3 General conclusions

There is such a great difference when we compare the results obtained from simulations with the results from measurement campaign. The former do not match with the results

extracted from measurements.

Up to this point, we can conclude that simulations basically give us an overview of how distortions can interact with the radiation pattern. Nevertheless the real impact on the network is given by the effective pattern taken from measurements.

As last conclusion and regarding the objective of the project stated at the problem definition, any network operator has to take these distortions into consideration because it is seen from the real deployment analysis that network parameters are strongly affected by propagation and environment.

References

- [1] Andrea Goldsmith *"Wireless communications" 2005 by Cambridge University Press.*
- [2] Andreas F. Molish *"Wireless Communication" 2011 John Wiley and Sons Ltd.*
- [3] Ignacio Rodriguez Larrad *"Radio Link Modelling for Relay Deployment in Urban Macro-cells" Master Thesis 2010-2011, Aalborg university.*
- [4] Theodore S. Rappaport *"Wireless Communication Principles and Practice". 2nd Edition, Prentice Hall PTR Communications Engineering and Emerging Technologies Series.*
- [5] Harri Holma and Antti Toskala. *"WCDMA for UMTS" John Wiley and Sons Ltd.*
- [6] Juha Korhonen *"Introduction 3G mobile communication". 2003 ARTECH HOUSE, INC. 685 Canton Street Norwood, MA 02062.*
- [7] Zhi Ning Chen, Kwai-Man Luk. *"Antennas for base stations in Wireless Communication" 2009 by The McGraw-Hill Companies.*
- [8] Patrick C. F. Eggers *"Angular - Temporal analogies of short-term mobile radio propagation channel at the Base Station". Personal, Indoor and Mobile Radio Communications, 1996. PIMRC'96., Seventh IEEE International Symposium on , vol.2, no., pp.742-746 vol.2, 15-18 Oct 1996.*
- [9] Patrick C. F. Eggers *"Angular Dispersive Mobile Radio Environments sensed by highly Directive Base Station Antennas". Personal, Indoor and Mobile Radio Communications, 1995. PIMRC'95. 'Wireless: Merging onto the Information Superhighway'., Sixth IEEE International Symposium on , vol.2, no., pp.522-526 vol.2, 27-29 Sep 1995.*
- [10] Patrick C.F. Eggers. *"Angular Propagation Descriptions Relevant for Base Station Adaptive Antenna Operations". Wireless Personal Communications Volume 11, Number 3 (1999), 337-338.*
- [11] Andreas F Molish, Josef Fuhl, and Ernst Bonek *"Pattern distortion of mobile radio base station antennas by antenna masts and roofs". Microwave Conference, 1995. 25th European , vol.1, no., pp.71-76, 4-4 Sept. 1995.*
- [12] K.I. Pedersen, P.E. Mogensen and B.H. Fleury. *"Power azimuth spectrum in outdoor environments". Electronics Letters , vol.33, no.18, pp.1583-1584, 28 Aug 1997.*

- [13] Vaughn P. Cable "Error Margin for Antenna Gain Measurements Anatomy of an Error Budget". Antennas and Propagation Society International Symposium, 2002. IEEE , vol.1, no., pp. 262- 265 vol.1, 2002.
- [14] Kanagalu R. Manoj "Coverage estimation for mobile cellular networks form signal strength measurements". THE UNIVERSITY OF TEXAS AT DALLAS, April 1999.
- [15] James Demetriou and Rebecca MacKenzie "Propagation Basics". September 30, 1998.
- [16] Fredrik Gunnarsson, Martin N Johansson, Anders Furuskr, Magnus Lundevall, Arne Simonsson, Claes Tidestav, Mats Blomgren. "Downtilted Base Station Antennas A Simulation Model Proposal and Impact on HSPA and LTE Performance". Vehicular Technology Conference, 2008. VTC 2008-Fall. IEEE 68th , vol., no., pp.1-5, 21-24 Sept. 2008.
- [17] Sanjaya Gurung Nilab Pradhan. "Antenna system in cellular mobile communication". Department of Electrical & Electronics Engineering School of Engineering. KATHMANDU UNIVERSITY
- [18] Shveta Sharma and Prof. R S Uppal. "RF Coverage estimation of cellular mobile system" 1CMTS, BSNL, Sec49C, Chandigarh, India. Department of ECE, BBSBEC, Fatehgarh Sahib, Punjab, India
- [19] Osman N. C. Yilmaz, Sepo Hmlinen, Jyri Hmlinen "System Level Analysis of Vertical Sectorization for 3GPP LTE". Wireless Communication Systems, 2009. ISWCS 2009. 6th International Symposium on , vol., no., pp.453-457, 7-10 Sept. 2009
- [20] Dr. Steven R. Best "Antenna properties and their impact on wireless system performance". Cushcraft Corporation 48 Perimeter Road Manchester, NH 03013.
- [21] 3GPP TR25.814, Technical Specification Group Radio Access Network "Physical layer aspects for evolved Universal Terrestrial Radio Access (UTRA)"
- [22] 3GPP TS 25.211 (2010-09), 2010. Physical channels and mapping of transport channels onto physical channels (FDD).
- [23] Electronic Communications Committee (ECC) within the European Conference of Postal and Telecommunications Administrations (CEPT). UMTS Coverage Measurements Nice, May 2007.
- [24] Huber-suhner antenna manufacturer. "<http://www.hubersuhner.com/Products/2652724>". Accessed on 12th of April 2012.
- [25] RHODE & SCHWARZ radio network scanner TSMW. "www.rohde-schwarz.com". Accessed on 29th of March 2012.
- [26] "<http://www.raymaps.com/index.php/antenna-radiation-pattern-and-antenna-tilt/>". Accessed on 22nd of April 2012.

- [27] Mississippi State University "<http://www.ece.msstate.edu/donohoe/ece4990notes2.pdf>". Accessed on 1st of May 2012.
- [28] "<http://www.banrepcultural.org/blaavirtual/tesis/colfuturo/cosme/cosme1z1.pdf>". Accessed on 29th May 2012

Appendix A

Antenna pattern processing

This section will be used to define an algorithm which will allow us to represent the antenna footprint in terms of power or difference power in each DBC (Data Base Cell), defining a survey area in which the antenna footprint is within it. This algorithm will be designed to compare the original antenna pattern (manufacturer) with one which has been modified because some source of distortion.

There will be three basic steps to carry out this algorithm. These steps will be in order: discretize the survey area in DBC in order to obtain the BS footprint, see the difference between antenna manufacturer footprint and antenna distorted footprint, and finally, do an evaluation of the results.

A.1 Discretize

In the beginning, we use cartesian axes x and y to define our research area in which the antenna footprint will be fitted in. These expressions are measured in DBC of 0.1 Km side (100m x 100m).[2]

$$-20 \leq x \leq 210 \tag{A.1}$$

$$-100 \leq y \leq 100 \tag{A.2}$$

In order to control the angular domain, by means of equation (A.3) and equation (A.4), it is possible to get the change from cartesian to angular domain. The magnitude of d is calculated by x and y values expressed in kilometres, this value will give us the received power (Pr) (Figure A.1) for each DBC through the propagation model COST231-HATA, equation A.5.

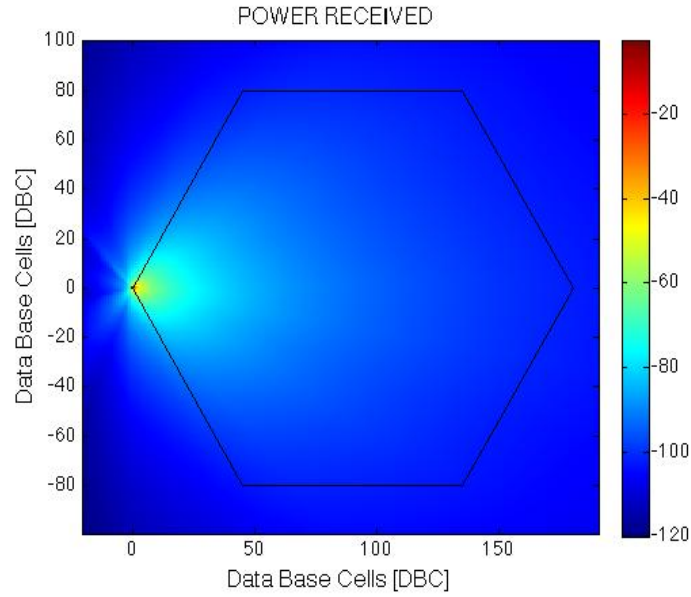


Figure A.1: Received signal power level.

$$\theta_0 = \arctan\left(\frac{y}{x}\right) \begin{cases} \theta = \theta_0 & \text{if } x > 0 \text{ and } y > 0 \\ \theta = \theta_0 + 180^\circ & \text{if } x < 0 \text{ and } y > 0 \\ \theta = \theta_0 + 180^\circ & \text{if } x < 0 \text{ and } y < 0 \\ \theta = \theta_0 + 360^\circ & \text{if } x > 0 \text{ and } y < 0 \end{cases} \quad (\text{A.3})$$

$$d = \sqrt{\left(\frac{y}{0.1}\right)^2 + \left(\frac{x}{0.1}\right)^2} \quad (\text{A.4})$$

$$\begin{aligned} P_r &= P_t + G_{tx}(\text{index}) + 46.3 - 33.9 \log_{10}(f_c) + 13.82 \log_{10}(H_b) + A_{HM} \\ &- [44.9 - 6.55 \log_{10}(H_b)] \log_{10}(d) \end{aligned} \quad (\text{A.5})$$

$G_{tx}(\text{index})$ will be discretized because it is not possible to obtain infinite samples of the antenna radiation pattern in function of the angle. Hence, the algorithm is designed to take 1440 samples of the radiation pattern (4 samples per degree) instead of 360 (1 sample per degree) due to the side and back lobes variation need to be more precise, equation (A.6).

Figure A.2 shows the difference in terms of error between neighbour samples of the antenna radiation pattern.

$$index = round(\theta) * 4 \quad (A.6)$$

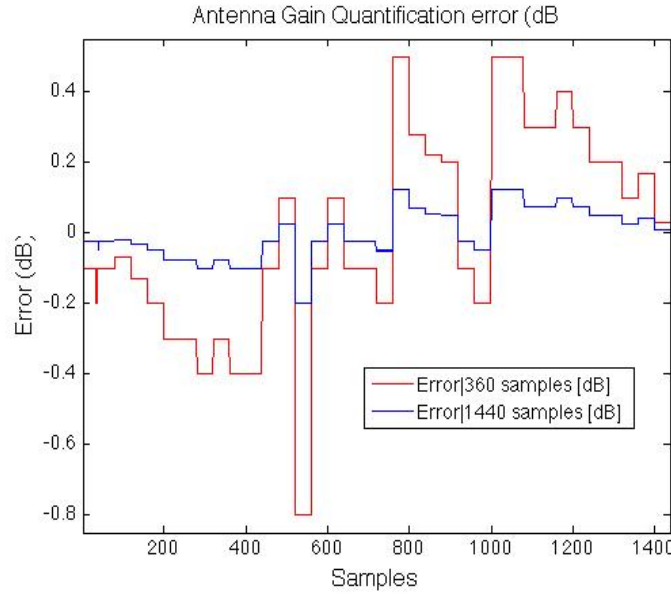


Figure A.2: Comparison between discretizing antenna pattern with 1440 samples and 360 in terms of error between neighbour samples.

A.2 Difference

The aim of the algorithm in this second step will be to compare the differences between manufacturer antenna pattern and the same pattern introducing some source of distortion to make it more similar to a realistic one. Thus, a threshold will be used in each DBC to quantify whether it is covered or not, equation (A.7) and (A.8). The chosen threshold will be the minimum sensibility power range to keep communication between UE and BS available and its value is -102dBm[21]. Afterwards, we will do a subtraction between power distorted pattern and the reference (equation (A.9)). The meaning of the subtraction result is shown in Table A.1.

$$Coverage(x, y)|_{reference} = \begin{cases} 3 & \text{if } P_r(x, y) < threshold \\ 1 & \text{others} \end{cases} \quad (A.7)$$

$$Coverage(x, y)|_{distorted} = \begin{cases} 3 & \text{if } P_r(x, y) < threshold \\ 2 & \text{others} \end{cases} \quad (A.8)$$

$$\Delta C(x, y) = Coverage(x, y)|_{distorted} - Coverage(x, y)|_{reference} \in [2, 1, 0, -1] \quad (A.9)$$

Value(ΔC)	Description	Colour code
2	DBC covered by reference but not by distorted	red
1	DBC covered by both footprints	green
0	DBC not covered by any of them	white
-1	DBC covered by distorted but not by reference	blue

Table A.1: Summary of the general parameters in the simulation and colour.

A.3 Evaluation

Once the first two steps are done, it is needed to evaluate the results. It is possible to translate data from Table A.1 into increment of power (ΔP_r) since we know the received power for each pattern and position in DBC, equation (A.10).

In order to appreciate or analyse the difference between both patterns, a cumulative distribution function (CDF) of power increment (ΔP_r) can be applied.

$$\Delta P_r[dB] = P_r(x, y)|_{distorted} - P_r(x, y)|_{reference} \quad (A.10)$$

Where:

$P_r(x, y)|_{distorted}$: Received power at DBC(x,y) with distorted pattern [dBm].

$P_r(x, y)|_{reference}$: Received power at DBC(x,y) with pattern without distortions [dBm].

Example

Figure A.3 shows an example of this algorithm, it is used to compare the manufacturer radiation pattern and a distorted one with angular spread. In this figure is represented the logical values $\Delta C(x, y)$ in which the antenna pattern is affected by angular spread in order to see the different DBCs which change the 'status' with the distortion applied. Figure A.4 is a zoom to appreciate clearer the results. Relation between colours is shown in Table A.1.

Figure A.5 represents the result for the CDF of this ΔP_r taking into account different values of angular spread.

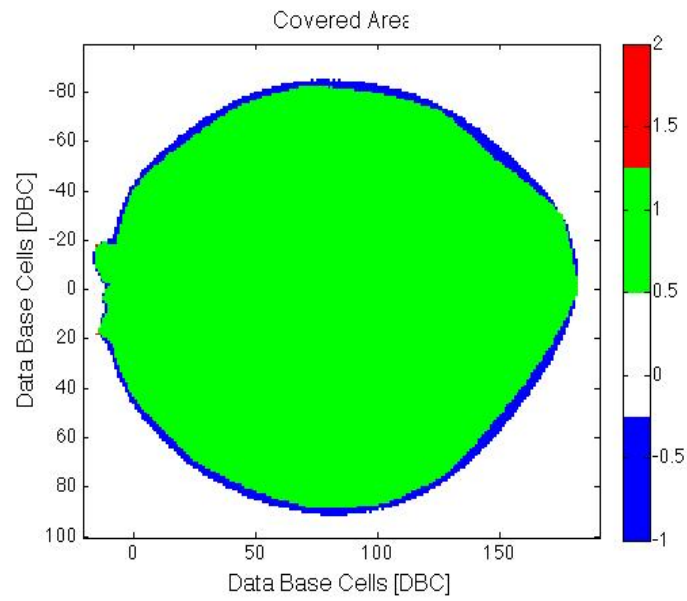


Figure A.3: Example of using the algorithm with angular spread.

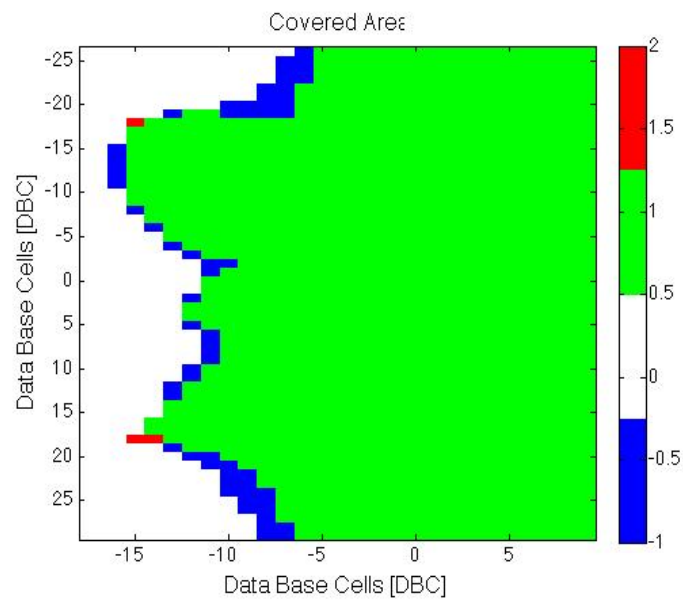


Figure A.4: Zoom of Figure A.3 for a better view of the difference between patterns.

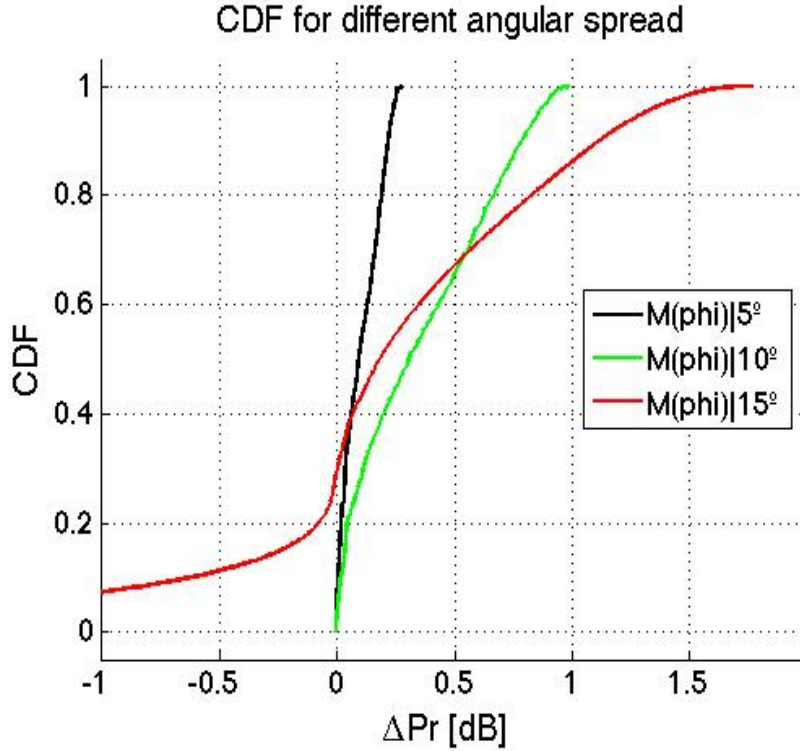


Figure A.5: CDF of increment of power (ΔP_r).

A.4 Network parameters performance

Until now, we are able to evaluate and analyse distortions in one sector. However, in mobile communications we do not have only one isolated sector but we have a complete communication network. Thus, the point to do this algorithm more realistic would be calculated the SINR to see the impact of the other two sectors inside a base station deployment.

Interference

This section gives an idea about how important is the Power received in a fixed point compared to the other sectors. We will use different parameters to measure and define its relevance. Previously, it is necessary to define the interference signal level. It will be defined as the sum of the different received power in a point of our footprint area due to a different sector from the one of interest. Thus, this definition is represented in the equation (A.11).

$$I_{Sx-Sn}(x, y)[dBm] = 10 * \log_{10} \left(\sum_{Sn \neq X} 10^{\left(\frac{P_{rx, Sn}(x, y)[mW]}{10} \right)} \right) \quad (A.11)$$

Where:

$I_{Sx-Sn}(x, y)$: interference level at DBC(x,y) [dBm].

$P_{rx,Sn}(x, y)$: received power from other two sectors of the same BS within the located sector. [mW].

SIR

The first parameter is called Signal to Interference Ratio (SIR), and follows the expression according to equation (A.12). Hence, SIR represents the level between the Signal level of interest and the others. Therefore, when this ratio is positive shows the magnitude that the received signal level is above the interference and just the opposite for negative value.

$$SIR(x, y)[dB] = P_{rx}(x, y)[dBm] - I_{Sx-Sn}(x, y)[dBm] \quad (A.12)$$

Where:

$I_{Sx-Sn}(x, y)$ is shown in equation (A.11).

$P_{rx}(x, y)$ is the received signal power from the located sector [dBm].

Figure A.6 shows the result when we obtain the SIR into our predefined area. It is more representative a result that show the behaviour of the SIR into the footprint. Hence, the CDF of this parameter can give much information of the footprint, see Figure A.8.

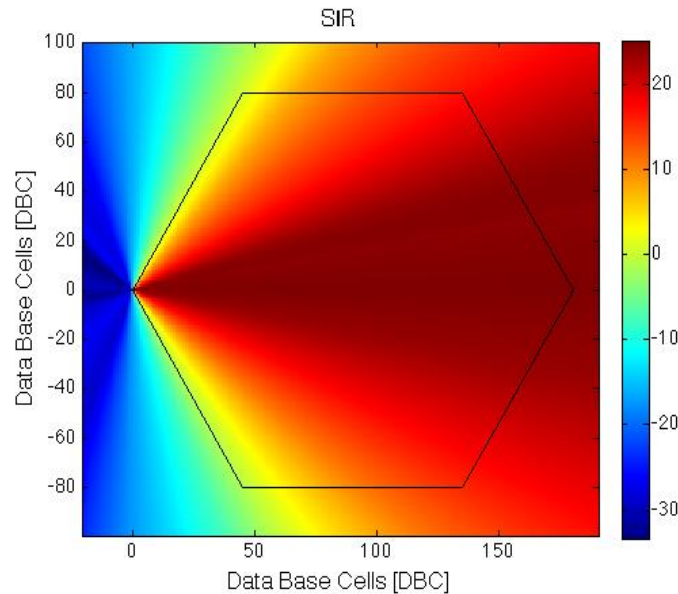


Figure A.6: SIR level into the footprint.

SINR

Besides SIR, it exists another parameter which relates signal ratio to noise. Noise parameter can be modelled by equation (A.13) and it is a constant background noise to do the simulation more realistic. Table A.2 shows the usual values for this parameters specified for UMTS technology.

$$N[dBm] = NPSD + 10\log_{10}(BW[Hz]) + NF \quad (A.13)$$

GENERAL	
Parameters	Value
NPSD	-174dBm/Hz
NF	5 dB
BW	5 MHz

Table A.2: Summary of the general parameters defined by [21]

Signal to Interference plus Noise ratio (SINR) takes this constant noise into account added to the interference level, see equation (A.14). Thus, this parameter represents how much strength is the received power above the sum of the different noises.

$$SINR(x, y)[dB] = P_{rx}(x, y)[dBm] - 10 * \log_{10} \left(\sum_{S_n \neq X} P_{rx, S_n}(x, y)[mW] + 10^{\left(\frac{N[dBm]}{10}\right)} \right) \quad (A.14)$$

Where:

$P_{rx}(x, y)$: seen in equation (A.12).

$P_{rx, S_n}(x, y)$: seen in equation (A.11).

N : noise component added to the survey (equation (A.13)).

Following the same procedure for the SIR, we are able to calculate the SINR in our predefined area and estimate its performance within the footprint. Figure A.7 shows the same graphics but for SINR ratio. As it is done in previous section, Figure A.8 shows CDF of this parameter in which it is seen relation between values.

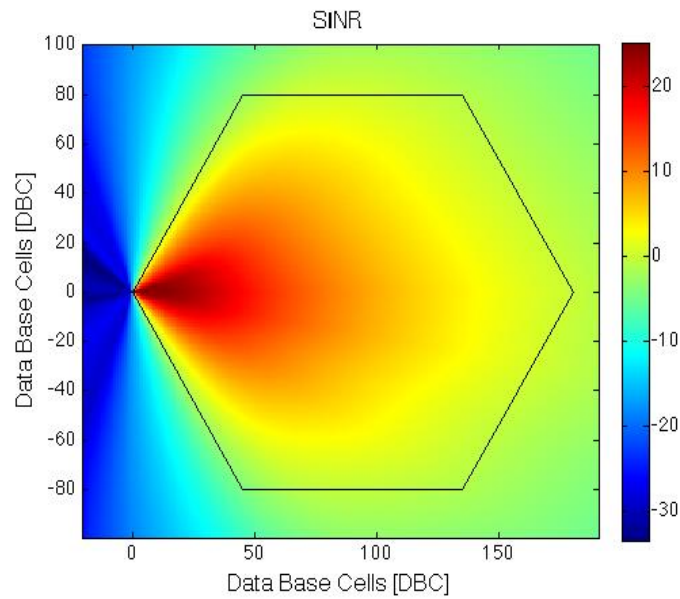


Figure A.7: SINR level into the footprint.

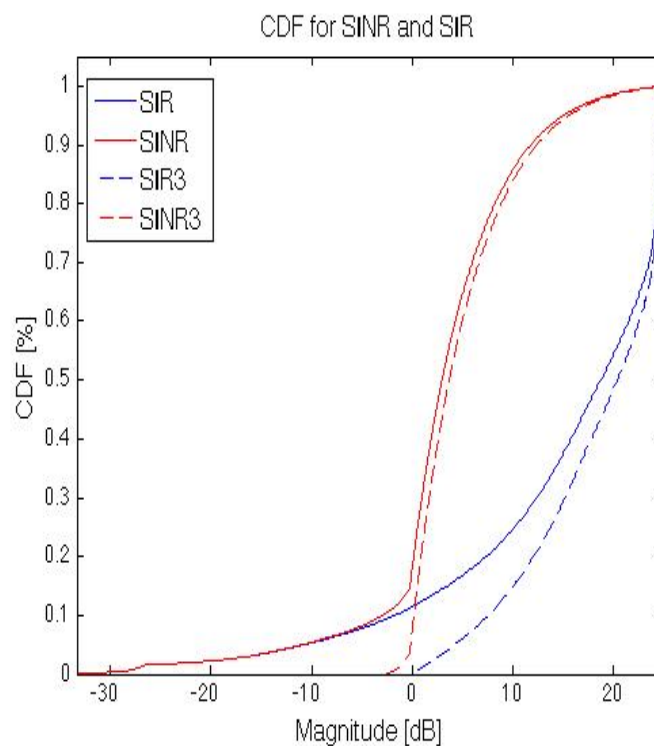


Figure A.8: CDF of the SINR value into the footprint.

Once simulations have been done with one single sector, two more sectors can be added to the simulation in order to make simulations more realistic and simulate a real BS deployment as it was mentioned before. Figures A.9 A.10 and A.11 show the performance of parameters calculated previously for one single sector. Thus, it is easier to appreciate the BS performance in terms of network planning. The same antenna was used for all sectors

and the same configuration.

In Figure A.8, it is also represented the statistical SINR and SIR for this three-sector BS behaviour by means of CDF in which it is observed that in three sectors there are less negative values in comparison between one single sector. This fact is due to overlap between sectors.

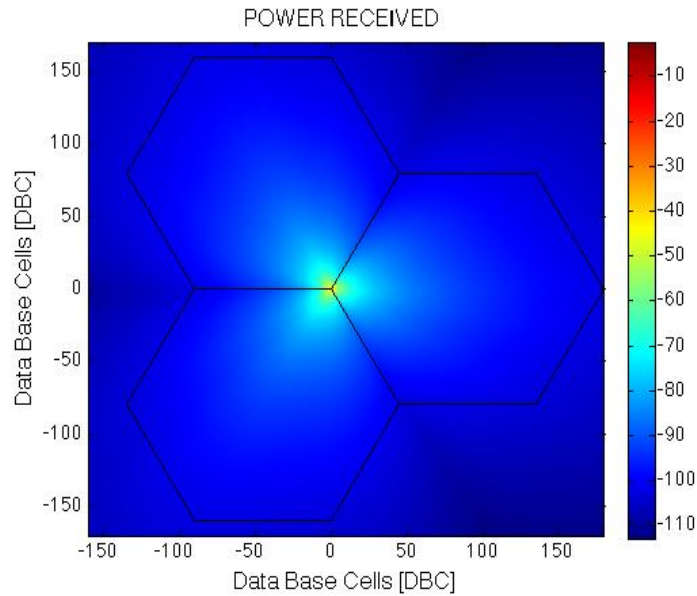


Figure A.9: Received power level into the footprint for a three-sector BS.

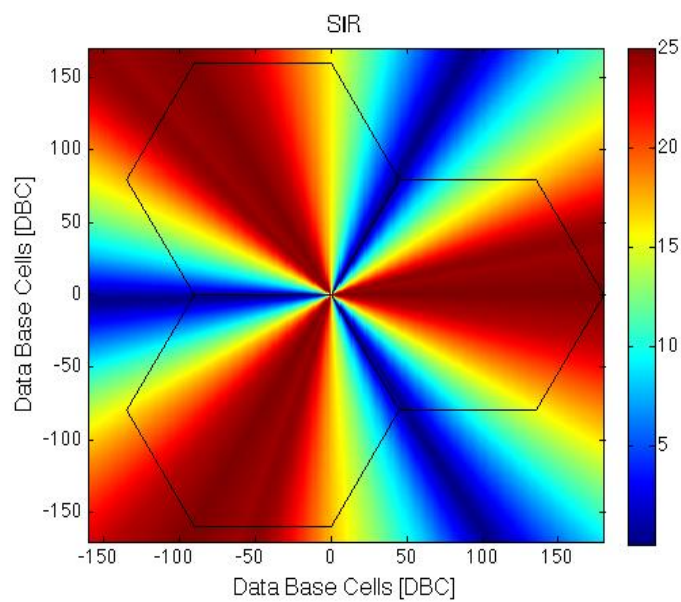


Figure A.10: SIR level for a three-sector BS.

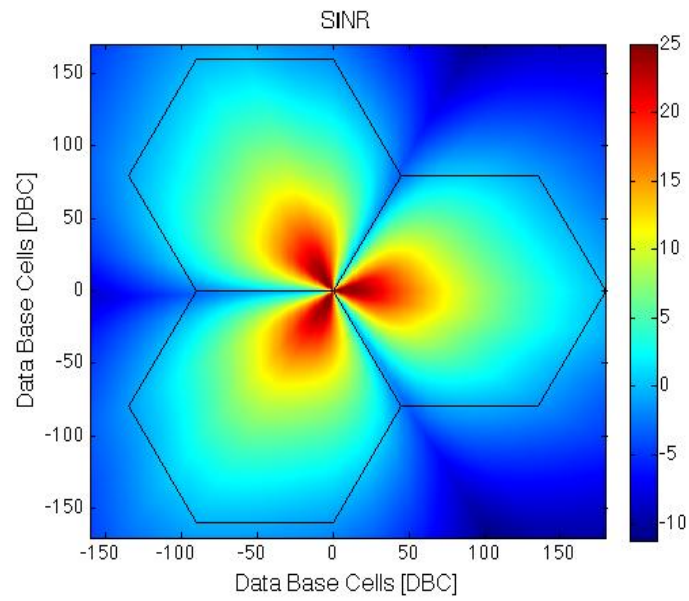


Figure A.11: SINR level for a three-sector BS.

Appendix B

Effective pattern algorithm

As it was stated at the project motivation, a measurement campaign will be carried out in order to verify the viability of an effective BS antenna pattern obtained by real measurements. Due to city deployment and Aalborg downtown geometry, taking measurements will be a tedious task. Thus, before starting the measurement campaign a process will be defined to deal with data from measurements.

Measurement devices, BS deployments, RF propagation,... will also be a handicap for our purpose since their performance within a cellular network is rather unknown. Hence, along this appendix we will establish guidelines which let us solve these kind of problems.

B.1 Objectives

The purpose of this appendix as it was already mentioned before, is to manage a procedure to remove range, shadowing and environment dependence from measurement data. We will prove by means of MATLAB simulations that we can achieve the goal of the appendix.

B.2 Methodology

In order to prove that we can isolate effects mentioned above, a reference radiation pattern will be defined choosing between three models; one will be an omnidirectional antenna (Pat_{omni}), another one will be the sum of gain from each sector in a three-sector BS (Pat_{sum}) and last one will be the maximum gain (Pat_{max}) from each sector (see Figure B.1).

$$G_x(\phi)|_{ref} = \begin{cases} Pat_{sum} & \text{if } G_x(\phi)|_{ref} = \sum(G(\phi)|_{sect1} + G(\phi)|_{sect2} + G(\phi)|_{sect3}) \\ Pat_{max} & \text{if } G_x(\phi)|_{ref} = \max(G_{sect1}(\phi), G_{sect2}(\phi), G_{sect3}(\phi)) \\ Pat_{omni} & \text{if } G_x(\phi)|_{ref} = cte. \end{cases}$$

$$G_{sum-manufac-ref}(\phi)|_{ref} = G_x(\phi)|_{ref} \tag{B.1}$$

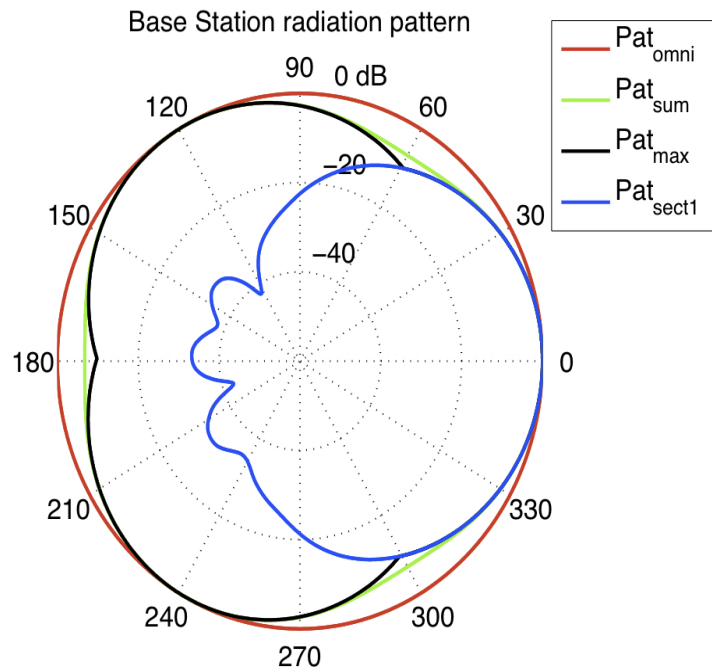


Figure B.1: Different reference antenna radiation pattern.

As a first step several routes around a BS site will be simulated to check range dependence, then a log-normal noise will be introduced as a shadowing fading model and last test will be to introduce two noises with different correlation factor.

B.2.1 Routes

Figure B.2 shows routes defined around a BS site; which are a square route, a triangular route and a random route as if it was a real route among city streets. In order to check that we can isolate range dependence we will calculate power received by means of COST-231-HATA for urban environment (equation (B.2)) from every defined route for one sector and for reference patterns. Then, we will compare both radiation patterns doing a subtraction between them (equation (B.3)), this is a way of removing range dependence from the analysis.

It is possible to translate the difference in power (ΔP_r) into difference in gain ($\Delta G(\phi)$) because all common terms are compensated in the propagation model equation except for gain terms (equation (B.3)).

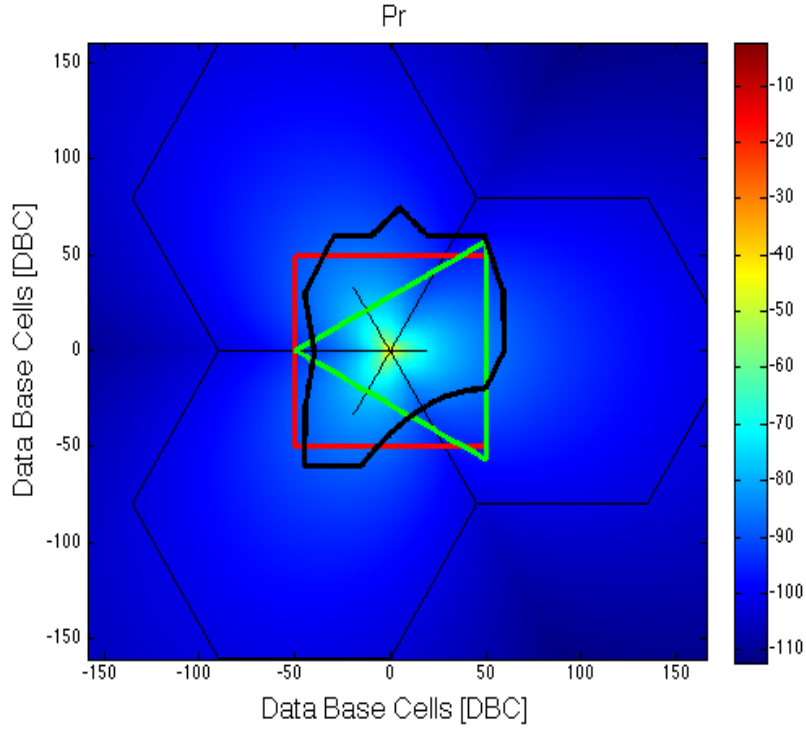


Figure B.2: Different routes around BS site.

$$\begin{aligned}
 P_r &= P_t + G_t - 46.3 - 33.9 * \log_{10}(fc) + 13.82 * \log_{10}(Hb) + A_{Hm} - \\
 &- [44.9 - 6.55 * \log_{10}(Hb)] * \log_{10}(d)
 \end{aligned} \tag{B.2}$$

$$\begin{aligned}
 \Delta P_r(\phi) &= P_r(\phi, R)|_{ref} - P_r(\phi, R)|_{sect} \\
 \Delta P_r(\phi) &= \Delta G(\phi) = G_{ref}(\phi) - G_{sect}(\phi)
 \end{aligned} \tag{B.3}$$

Where:

$\Delta P_r(\phi)$: error in received power [dB]

$P_r(\phi, R)|_{ref}$: received power from reference pattern [dBm].

$P_r(\phi, R)|_{sect}$: received power from one single sector [dBm].

$\Delta G(\phi)$: error gain between antenna pattern and effective antenna pattern [dB]

$G_{ref}(\phi)$: antenna gain from reference pattern [dB].

$G_{sect}(\phi)$: antenna gain from one single sector [dB].

Figure B.3 shows received power for all reference patterns and one single sector in square route. As it was said before, we are searching for a reference to compensate range variation due to routes and environment, in principle, it does not matter which pattern to choose since all of them will compensate range and shadowing.

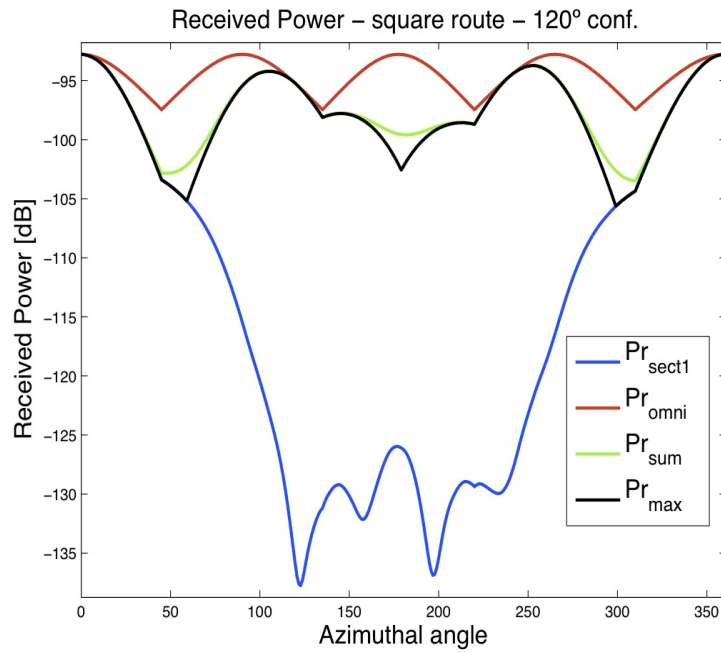


Figure B.3: Different Received Power for each method.

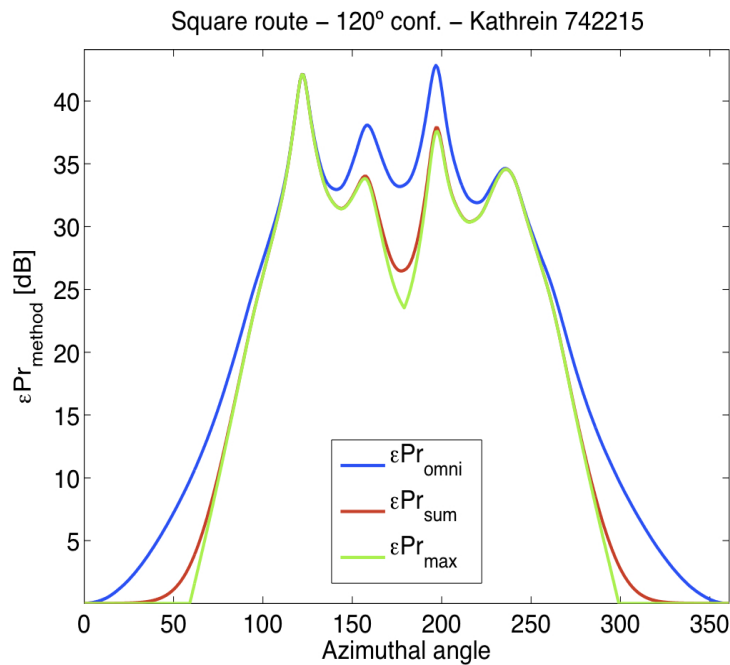


Figure B.4: ΔP_r obtained for each different method.

Figure B.5 represents different error powers ($\Delta P_r(\phi)$) for three different routes explained above. It means that our comparison between patterns has no dependence with the chosen

route. Hence, we will choose as reference pattern the sum of received powers provided by BS three sectors (P_{r_sum}) because we need a reference taken from measurements and taken in the same route as power received from one single sector.

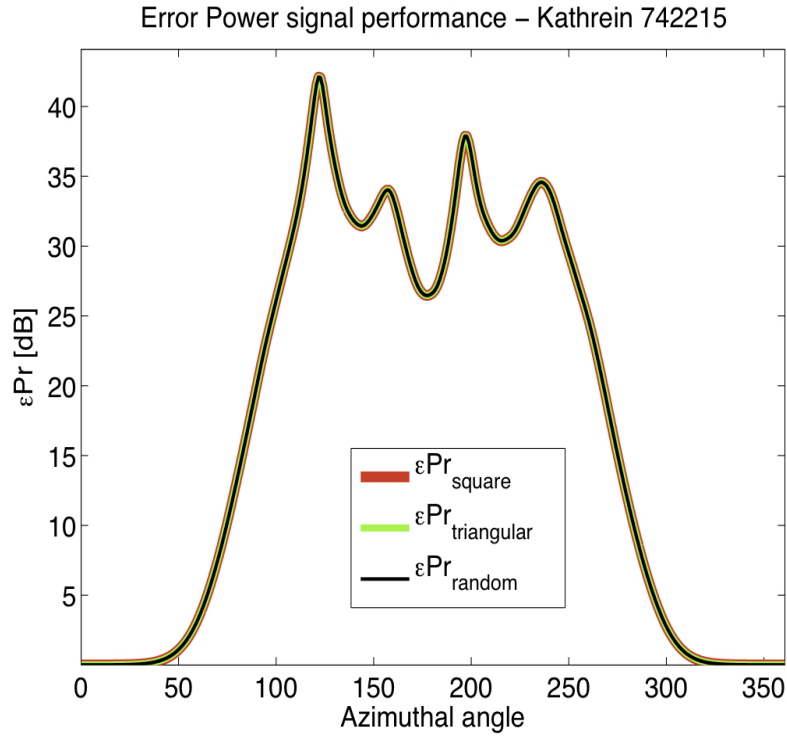


Figure B.5: ΔP_r for each route calculated by P_r sector sum method.

Once comparison between pattern is done, we can combine the result from the subtraction in equation (B.3) and our chosen reference pattern to obtain the effective radiation pattern from measurements of one of the sectors (equation (B.4)) and compare it to manufacturer one (Figure B.6).

$$G_{eff}(\phi) = G_{sum-manufac-ref}(\phi) - \Delta G(\phi) = G_{sum-manufac-ref}(\phi) - [G_{ref}(\phi) - G_{sect}(\phi)] \quad (B.4)$$

Where:

$G_{eff}(\phi)$: Effective radiation pattern obtained by measurements [dB].

$G_{sum-manufac-ref}(\phi)$: Pattern calculated from manufacturer's data as sum of gain from the three sectors BS [dB].

$\Delta G(\phi)$: error gain calculated from measurements data using B.3 [dB].

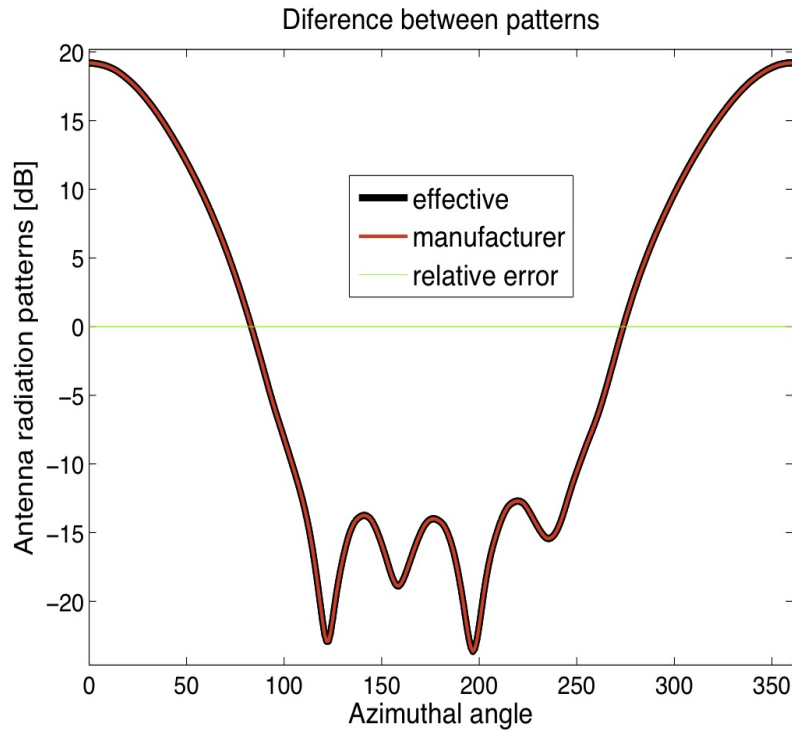


Figure B.6: Error between antenna pattern and effective antenna pattern, ΔG .

B.2.2 Log-normal fading

One of the most important parameters that can affect the measurements is shadowing. In this small section we will add to the research this parameter which will be modelled as a log-normal distribution in terms of equation (2.7).

We will translate parameters from (Chapter II) to generate what it is named as "shadowing" and it will be added to (B.5) in order to include this impact to the received power equation. It can be seen from Figure B.7 that "shadowing" affects randomly through all directions.

$$P_r(\phi, R) = P_r(\phi, R) - \text{"Shadowing"}(\phi) \quad (\text{B.5})$$

Following the same procedure as equation (B.3) and doing the same combination to compare the measured pattern with the manufacturer pattern, we can observe that there is no dependence either with environment impact.

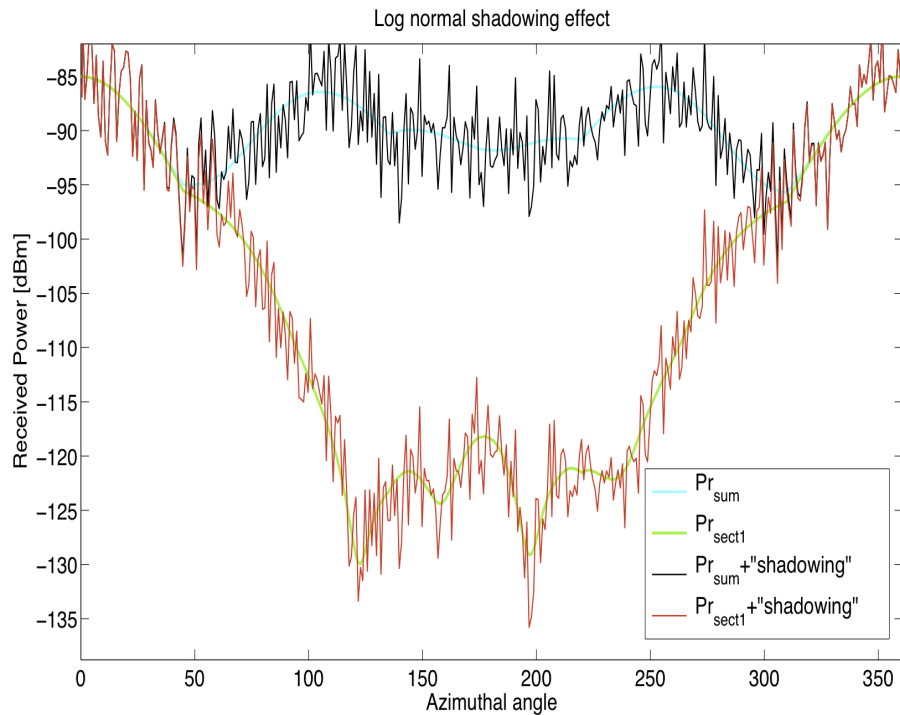


Figure B.7: Received power including shadowing effect.

B.2.3 Uncorrelated noise

To make a more realistic analysis we will add different correlated noises. Previously, we only treated in a deterministic environment but noises which come from different kind of sources like tolerance of transmission antenna gain, tolerance of reception antenna gain or measurement equipment error (B.9) will bring random behaviour to the analysis.

Table B.1 shows tolerances values for elements described above according to [13] and Appendix E.

GAIN DEVIATION	
Device	Tolerance
Transmitter Antenna	± 0.5 dB
User Equipment	± 1 dB
Receiver Antenna	± 0.5 dB

Table B.1: Gain tolerances obtained by [13] and UE datasheet (Appendix E).

Assumption:

As manufacturer's specifications do not mention about tolerance treatment, we will assume that all tolerances follow a Normal distribution and they are given by 3σ , that is to say, an accuracy of 99.6% as Figure B.8 explains.

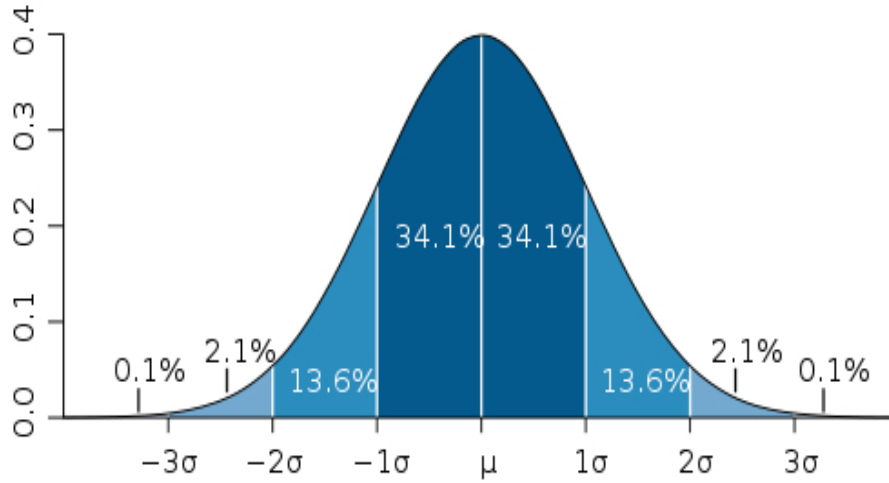


Figure B.8: Normal distribution function with $\mu = 0$ and $\sigma = 3$.

As we assume that tolerances follow a normal distribution process, in order to combine these different previous tolerances, we will apply one of the normal distribution properties for the sum of them (B.6).

$$\mathcal{N}(\mu_x, \sigma_x^2) + \mathcal{N}(\mu_y, \sigma_y^2) = \mathcal{N}(\mu_x + \mu_y, \sigma_x^2 + \sigma_y^2) \quad (\text{B.6})$$

Thus, we will treat tolerances according to (B.7) and (B.8). We will calculate two variances, one for the reference pattern which will be for the sum of received power from each BS sectors (σ_{sum}^2) and the other for the received power from one single sector (σ_{sect}^2).

We will assume for σ_{sum}^2 that, taking measurement in a certain point, we will received power from each sector in an independent way. Hence, in (B.7) tolerances from three sectors are combined.

$$\sigma_{sum} = \sqrt[2]{\frac{2}{9}} = 0.5[dB] \quad (\text{B.7})$$

$$\sigma_{sect} = \sqrt[2]{\frac{1.5}{9}} = 0.4[dB] \quad (\text{B.8})$$

Where:

σ_{sum} : standard deviation obtained for three sector sum Power, Pr_{sum} .

σ_{sect} : standard deviation obtained for a single sector Power, Pr_{sect} .

By using these values we can define the final gaussian distribution which will define our

procedure to obtain different correlated noises.

As it was already explained before, the purpose of calculating normal distribution parameters is to generate random correlated noise. Thus, the process will start with two random variables from (B.9) and then combine these two variables according to (B.10) to correlate them.

$$\begin{aligned} X_1 &= \mathcal{N}_{sum}(0, \sigma_{sum}^2) \\ X_2 &= \mathcal{N}_{sect}(0, \sigma_{sect}^2) \end{aligned} \quad (\text{B.9})$$

Where X_1 and X_2 are random variables created by the specific gaussian distribution functions, (B.7) and (B.8).

$$\begin{aligned} NOISE_1 &= X_1 \\ NOISE_2 &= \rho X_1 + \sqrt{1 - \rho^2} X_2 \end{aligned} \quad (\text{B.10})$$

Where $NOISE_1$ and $NOISE_2$ are random variables with a specific correlation factor (ρ) between them.

Figure B.9 shows one example for these correlated noises but only for a correlation factor value of 0.9. We will generate different noises with different correlation factor which would be interesting to evaluate the impact of the noise in our design.

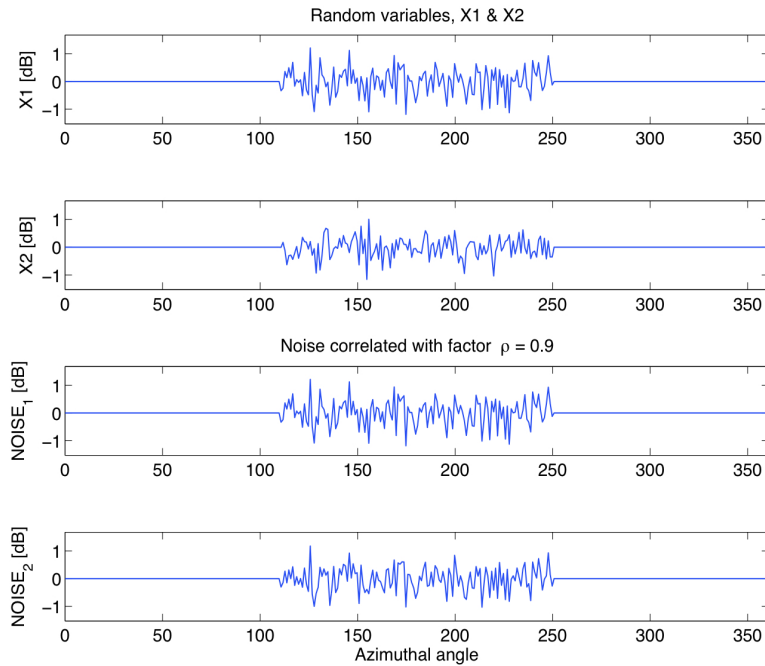


Figure B.9: Signals created to model our correlated noise.

B.3 Results

Applying equations seen in previous section, we are ready to estimate process reliability in this appendix. Figure B.10 shows the comparison between received power from one single sector and the reference adding correlated noise with $\rho = 0.9$ calculated in previous section for square route around BS. As it was said before we will include the effect of these noises at the side/back lobe direction since main lobe is fairly robust to distortions.

This is a way of giving a random behaviour to the analysis that affects directions indistinctly. We will base on equation (B.11) to include this random noise.

$$\begin{aligned} P_r(\phi, R) &= P_r(\phi, R) - \text{''Shadowing''}(\phi) - NOISE_1 \\ P_r(\phi, R) &= P_r(\phi, R) - \text{''Shadowing''}(\phi) - NOISE_2 \end{aligned} \quad (\text{B.11})$$

Table B.2 shows different noise parameters in order to find out how much tolerance our procedure can bear in function of correlation factor and how they are arranged in Figure B.12, which represents the difference between effective pattern and manufacturer's one depending on correlation factor.

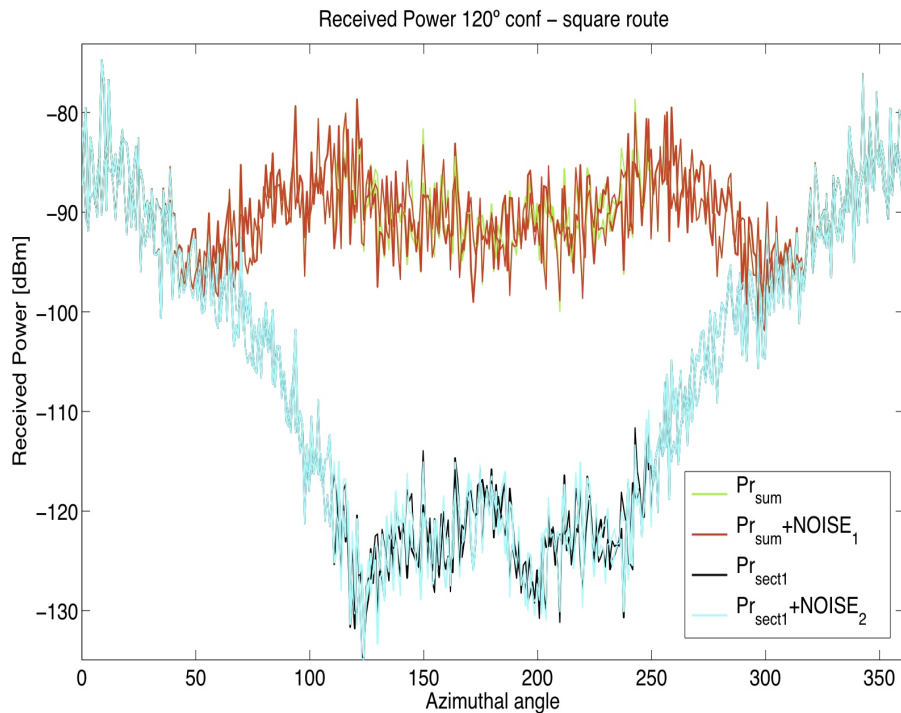


Figure B.10: Received power including shadowing effect and both different noise signal, equations (B.11).

Position in Figure B.12	Correlation factor, ρ
(1,1)	0.9
(2,1)	0.7
(3,1)	0.4
(4,1)	0.2

Table B.2: Correlation factor values.

In order to evaluate if it is possible to extract an effective radiation pattern we will follow the same procedure as before but in this section we will obtain the relation between the measured pattern and manufacturer one. This comparison is shown in Figure B.11 and represents how different these patterns are.

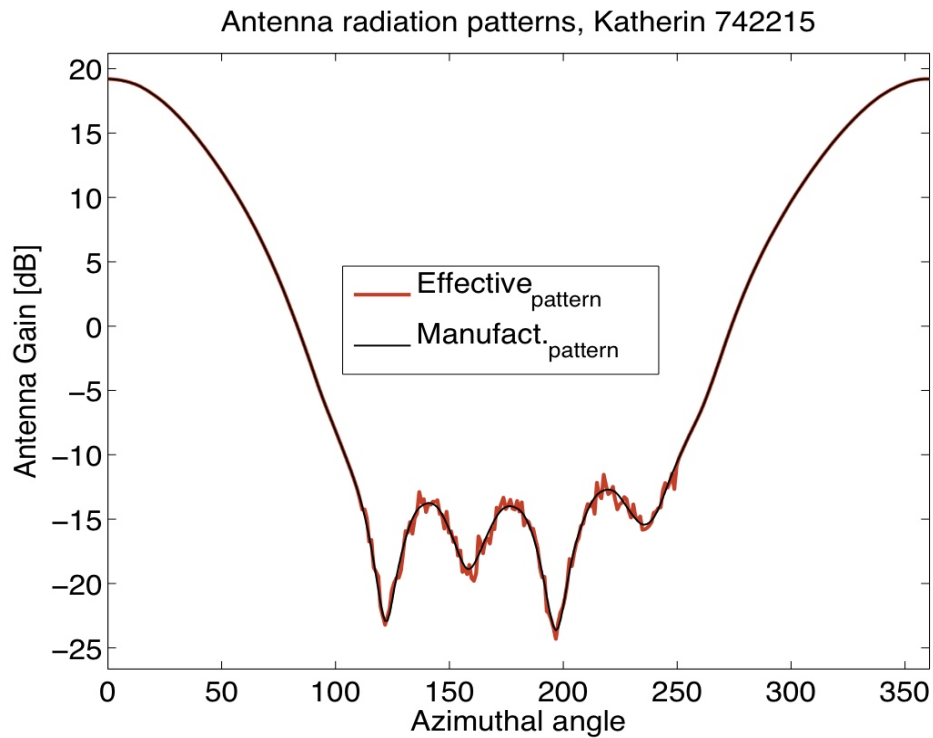


Figure B.11: Comparison between $G_{eff}(\phi)$ and $G_{manufacturer}(\phi)$ when $\rho = 0.9$.

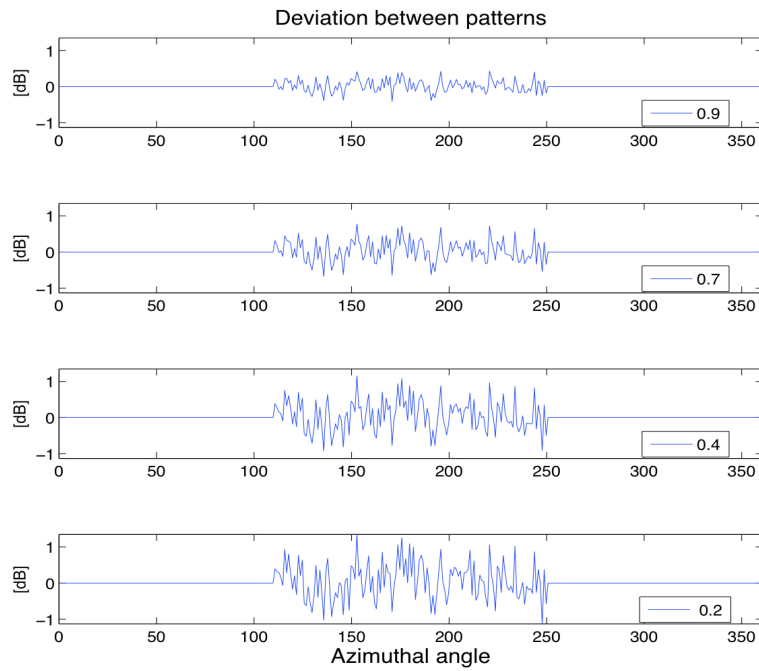


Figure B.12: Comparison between $G_{eff}(\phi)$ and $G_{manufacturer}(\phi)$ for different values of ρ .

Eventually and with the purpose of doing a more accurate analysis, it would be interesting how uncorrelated noises affect network parameters like P_r , SIR, SINR or the number DBCs according to Appendix A process are affected when a change in radiation pattern is introduced. Figure B.14 represents a evaluation for these parameters in order to compare the differences between patterns.

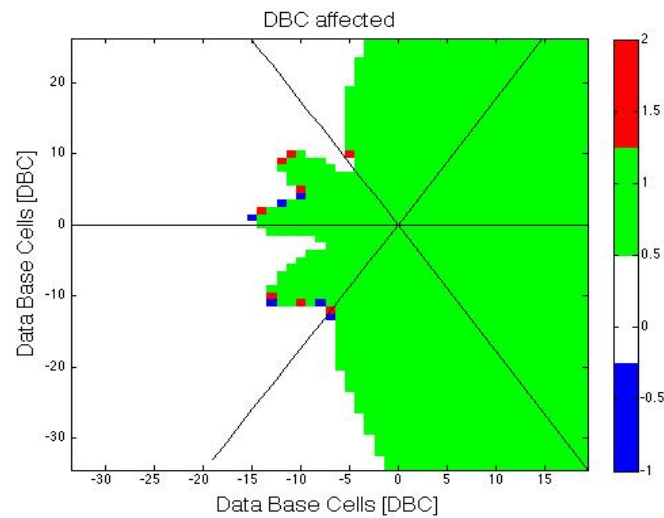


Figure B.13: DBC affected within network performance due to $\rho = 0.2$.

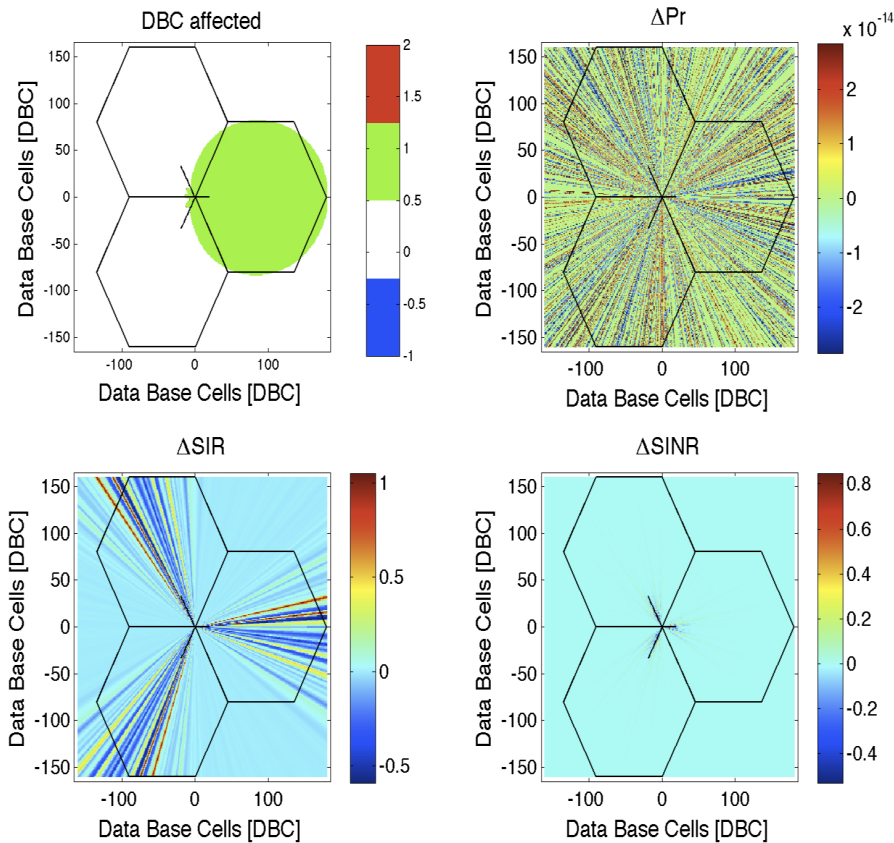


Figure B.14: Network parameters analysis when $\rho = 0.2$.

B.4 Conclusions

First of all, we have designed a procedure to extract an effective antenna radiation pattern from measurement data. It is a tedious task because of city building deployment and geometry streets.

We have found a way of isolating distance dependence and environment impact, what it means that, it does not matter which route we make or where the BS is placed.

Since environment does not have a deterministic response, another of our proposals is to estimate the margin we can tolerate in order to get the effective antenna pattern when the noise has a certain correlation value. Hence, in our experiment we can conclude that for a lower correlation factor of 0.2 the effective pattern can vary between ± 1 dB what is not very critical due to results section prove that this variation just affect few cells and do not modify more than 1 dB critical parameters like SIR or SINR.

Appendix C

Measured Signal

One of the main sections of the project consists of run a measurement campaign into a real network to explore the signal affected by real interference along different routes.

It would be difficult to measured the signal within the back and side lobes direction of the antenna pattern. Thus, it is necessary to understand what and how it is really measured.

C.1 UMTS Basics

The Universal Mobile Telecommunication System (UMTS) is based on a technology that spreads the RF energy over a wide band, resulting in higher occupied bandwidth. [23]

This process carried out in UMTS allows multiple BS to transmit at the same time allocated in the same frequency, besides, still keeping the possibility of separate the different transmissions in the receiver side (CDMA).

To allow the separation, the user data is first "modulated" onto a binary code (key) before it is transmitted. WCDMA applies a two-layered code structure consisting of a orthogonal spreading code and Pseudo-random Scrambling Codes (SC). [23]

Finally, a correlation between the signal and the known code is done at the receiver. This method is highly confidence even if some bits are destroyed due to interfering emissions from other UMTS stations on the same frequency. Physically, receiver "collect" the RF energy spread on a wide bandwidth and reduce it to a narrow band by the correlation process. [23]

C.2 WCDMA FDD parameters

In WCDMA cellular systems, exists a broadcast downlink channel common for each cell, CPICH (Common Pilot CHannel), transmitted by the BS with a pre-defined bit sequence.

It also has a constant power usually fixed between 5% and 15% of the total power transmitted. [22]

CPICH is divided in P-CPICH and S-CPICH, Primary and Secondary CPICH respectively. The first one is used by the UE to complete the identification of the Primary scrambling code, while the Secondary can be used by other BS. [22]

In addition, CPICH channel can be used to carry out measurements once, the scrambling code is known. In this case, signal quality is defined by measuring parameters such as RSCP and E_c/I_o . Otherwise, it exists other parameters in relation like RSSI, SIR, ISCP.

We will provide a deeper explanation of these parameters to analyse them from Measurement Campaign.

C.2.1 RSCP

The Received Signal Code Power represents the received power on one code measured on the pilot bits of the primary CPICH. Thus, it is calculated after the descrambling process of the signal.

In the TSMW scanner, RSCP is defined as the sum of the received power of all peaks on one code, measured on the pilot bits of the P-CPICH.

C.2.2 ISCP

The interference Signal Code Power represents the interference on the received signal measured on the pilot bits of the primary CPICH, also after correlation as RSCP. This parameter makes reference to the interference on the received signal measured on the pilot bits.

In the TSMW, ISCP is taking the orthogonal and the non orthogonal parts of the interference into account. However, it is taken as the sum of the eight highest RSCPs along the route instead of the parameter measured from the scanner.

C.2.3 SIR

The Signal to Interference Ratio can be defined by both previous parameters as equation (C.1) shows. It is the linear ratio between RSCP and ISCP multiplied by the Spreading Factor. When measurements are taken in CPICH, $SF=256$. [22]

$$SIR = \frac{RSCP}{ISCP} * SF \quad (C.1)$$

C.3 TELENOR

Real measurements are from the UMTS network that Telenor has extended in the city of Aalborg. His signal operates on UMTS2100 Hz, band I, with a radio channel of 5 MHz bandwidth. The frequency separation between transmission and reception is 190 MHz.

PARAMETER	DOWNLINK
UARFCN	10813
f_c	2162.6 MHz
f_l	2160.1 MHz
f_h	2165.1 MHz

Table C.1: Telenor UMTS parameter specifications, UMTS2100 band I.

Appendix D

Measurements Campaign Routes

This appendix summaries data extracted from the Measurement Campaign including plots of BSs covered with the different routes performed.

As well as, it gives a basic explanation from the most relevant properties to take into account along the project like antenna height, antenna models and their respective tilting, mounting structure aperture angle (see Figure 3.11),....

Otherwise, we represent real pictures where antenna deployments are placed. We will have an idea about the different antenna mounting structure used by the operator.

D.1 Route 1 Data

- Antenna height of 12 meters.
- Antenna models and configuration:
 - Sector 1: Model= Kathrein 206516, Tilt= 2°, Bearing= 60°.
 - Sector 2: Model= Kathrein 206516, Tilt= 2°, Bearing= 180°.
 - Sector 3: Model= Kathrein 206516, Tilt= 2°, Bearing= 300°.
- Mounting structure aperture angle ($\alpha \approx 53^\circ$), distortion $1 \rightarrow 50^\circ < \alpha \leq 90^\circ$
- Urban Environment with Homogeneous building density (3-4 floors, around 15 meters of height). Actually, we adapt Cost-231 Propagation model selecting $C = 0dB$ because of the almost suburban environment behaviour.

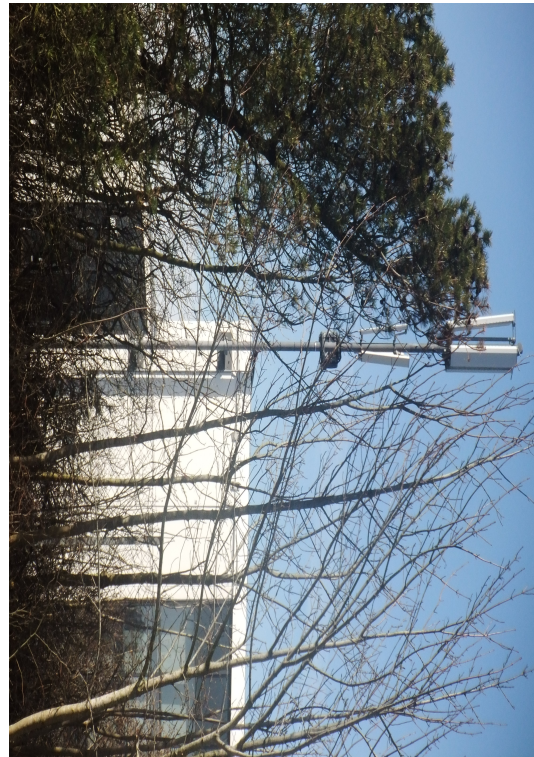


Figure D.1: Diferent routes and deployment specification for route 1.

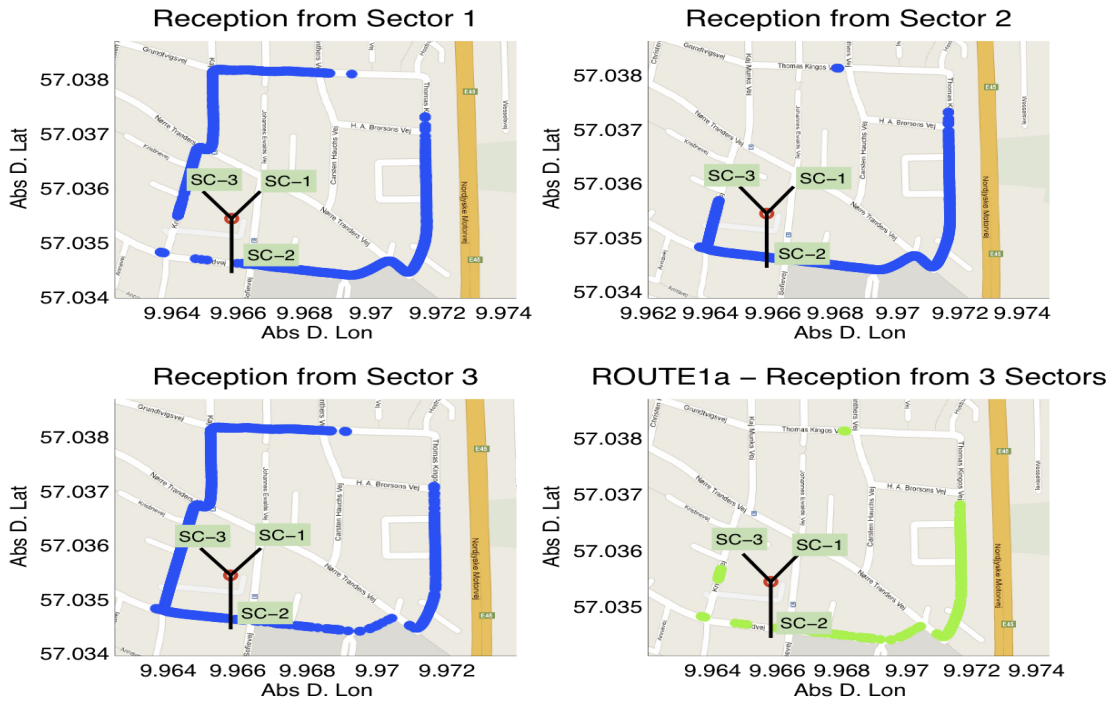


Figure D.2: Received power points along the route 1-A.

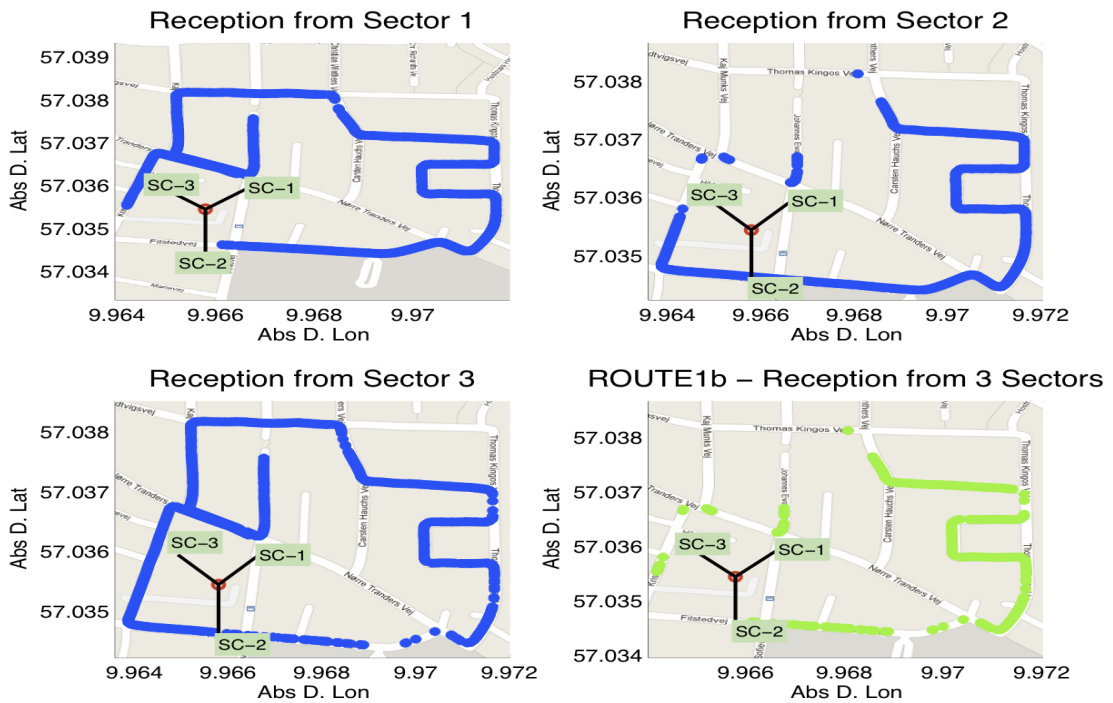


Figure D.3: Received power points along the route 1-B.

D.2 Route 2 Data

- Antenna height of 30 meters.
- Antenna models and configuration:
 - Sector 1: Model= Kathrein 742215, Tilt= 6° , Bearing= 60° .
 - Sector 2: Model= Kathrein 742215, Tilt= 6° , Bearing= 180° .
 - Sector 3: Model= Kathrein 742215, Tilt= 8° , Bearing= 300° .
- Mounting structure aperture angle impossible to determine, unknown mast dimensions.
- Urban Environment with Homogeneous building density (3-4 floors, around 15 meters of height). Actually, we adapt Cost-231 Propagation model selecting $C = 0dB$ because of the almost suburban environment behaviour.

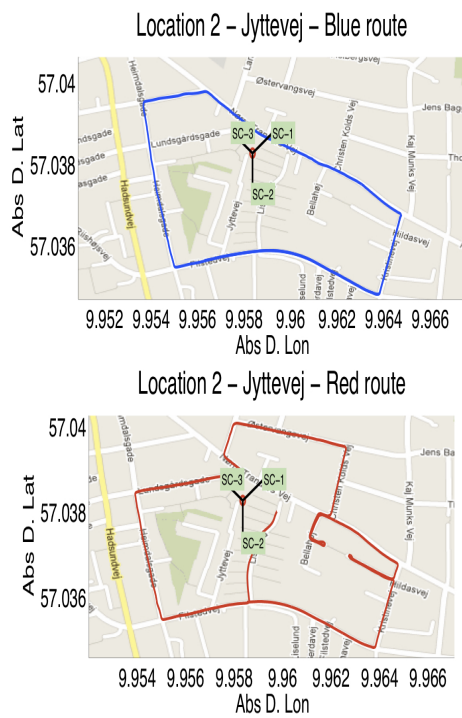


Figure D.4: Diferent routes and deployment specification for route 2.

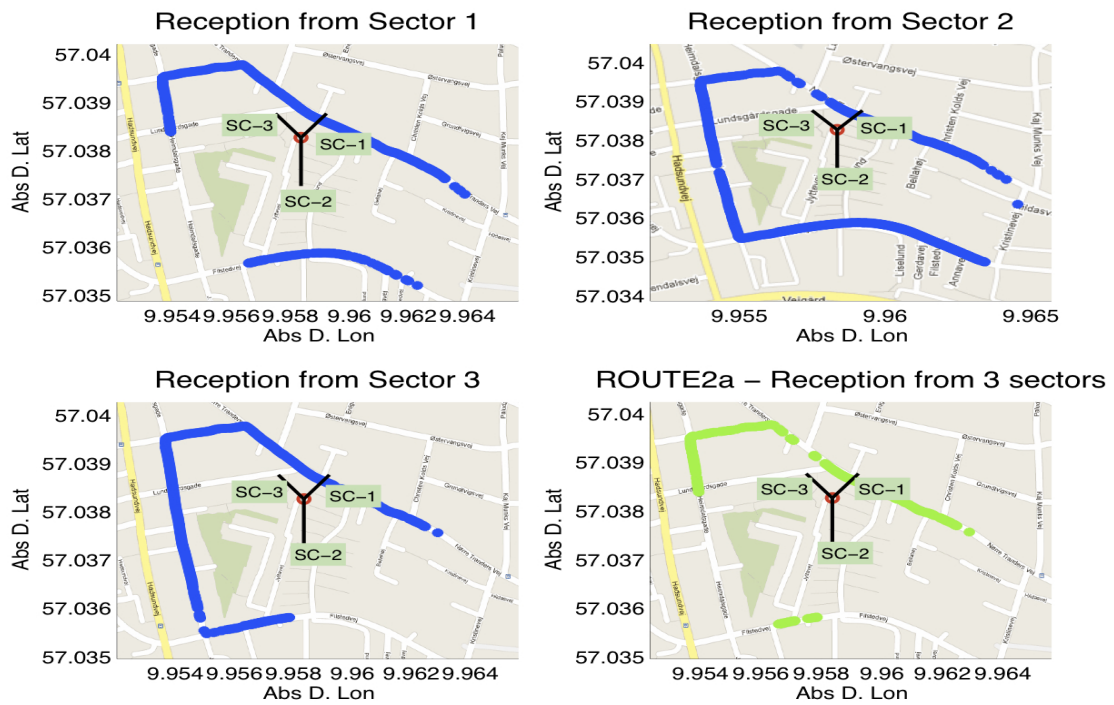


Figure D.5: Received power points along the route 2-A.

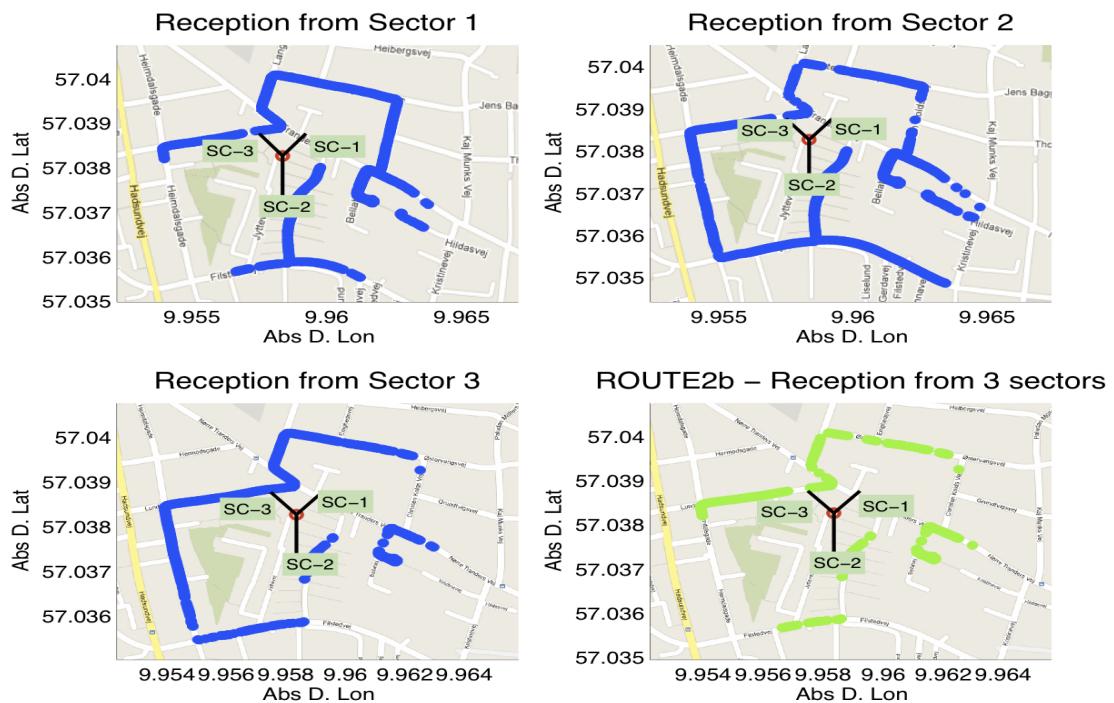


Figure D.6: Received power points along the route 2-B.

D.3 Route 3 Data

- Antenna height of 19 meters.
- Antenna models and configuration:
 - Sector 1: Model= Kathrein 742215, Tilt= 4° , Bearing= 90° .
 - Sector 2: Model= Kathrein 742215, Tilt= 6° , Bearing= 180° .
 - Sector 3: Model= Kathrein 742215, Tilt= 8° , Bearing= 270° .
- Mounting structure aperture angle impossible to determine. It is a chimney structure what makes impossible to see the mast and we did not find any manufacturer specifying their dimensions.
- Urban Environment with Homogeneous building density (3-4 floors, around 15 meters of height). Actually, we adapt Cost-231 Propagation model selecting $C = 0dB$ because of the almost suburban environment behaviour.

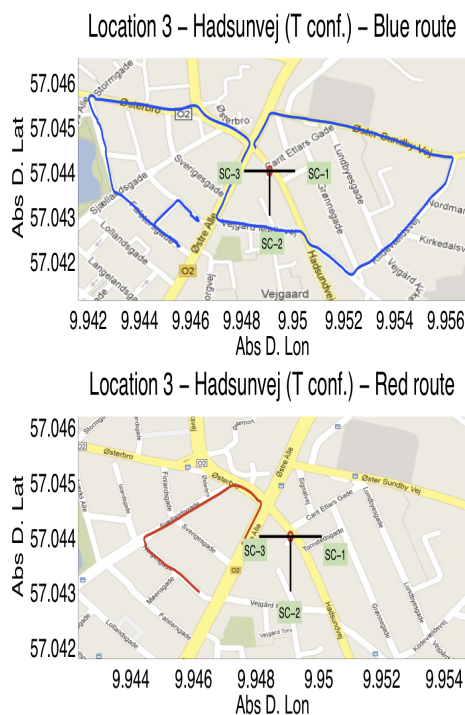


Figure D.7: Diferent routes and deployment specification for route 3.

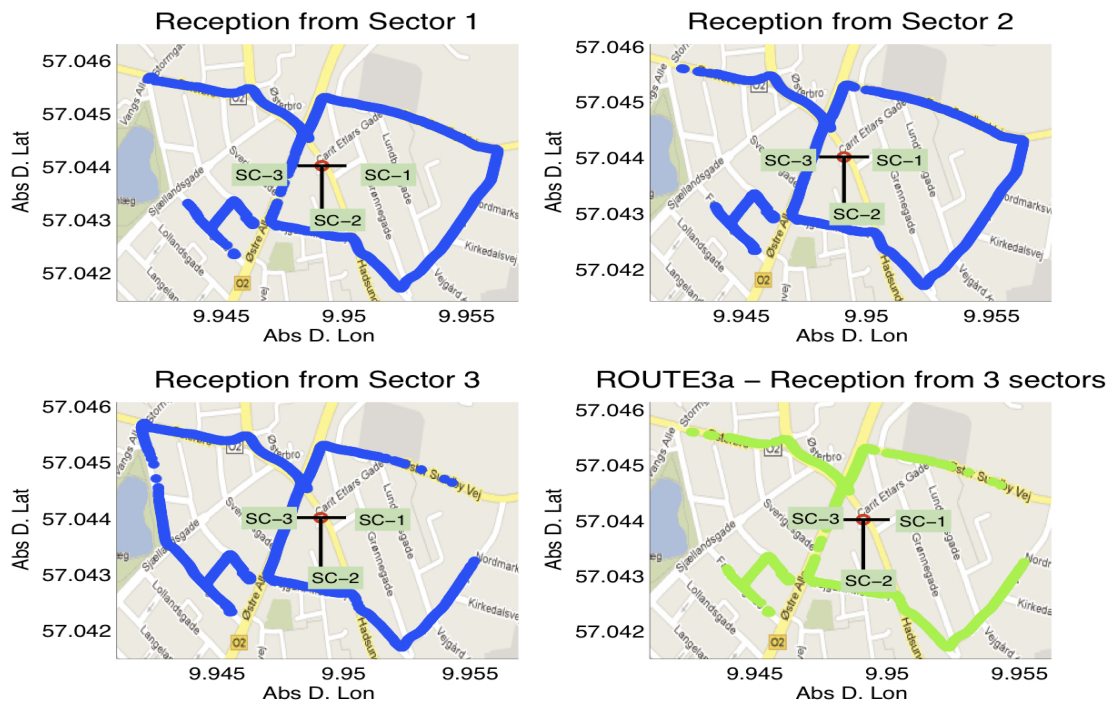


Figure D.8: Received power points along the route 3-A.

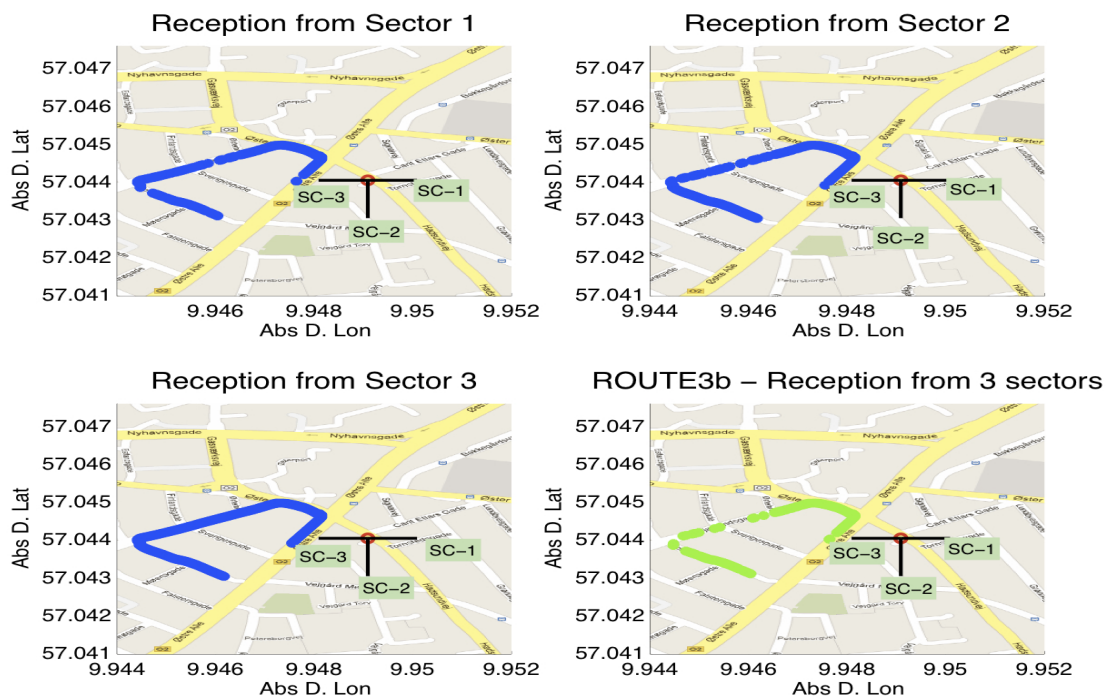


Figure D.9: Received power points along the route 3-B.

D.4 Route 4 Data

- Antenna height of 17 meters.
- Antenna models and configuration:
 - Sector 1: Model= Kathrein 742215, Tilt= 2° , Bearing= 30° .
 - Sector 2: Model= Kathrein 742215, Tilt= 2° , Bearing= 150° .
 - Sector 3: Model= Kathrein 742215, Tilt= 2° , Bearing= 270° .
- Mounting structure aperture angle impossible to determine. It is a chimney structure what makes impossible to see the mast and we did not find any manufacturer specifying their dimensions.
- Urban Environment with Homogeneous building density (3-4 floors, around 15 meters of height). Actually, we adapt Cost-231 Propagation model selecting $C = 0dB$ because of the almost suburban environment behaviour.

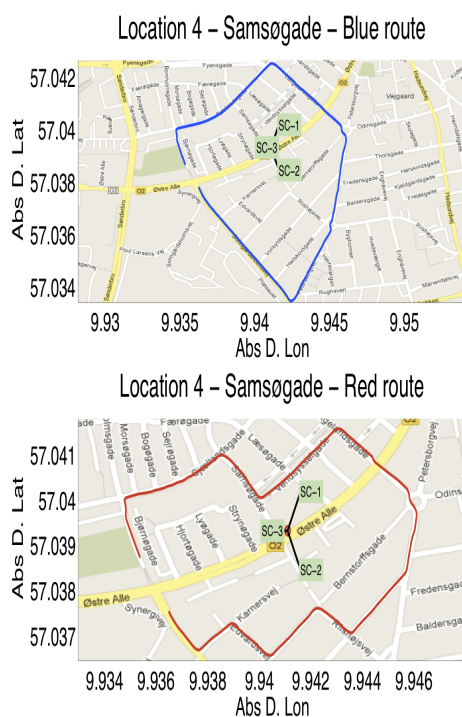


Figure D.10: Diferent routes and deployment specification for route 4.



Figure D.11: Received power points along the route 4-A.

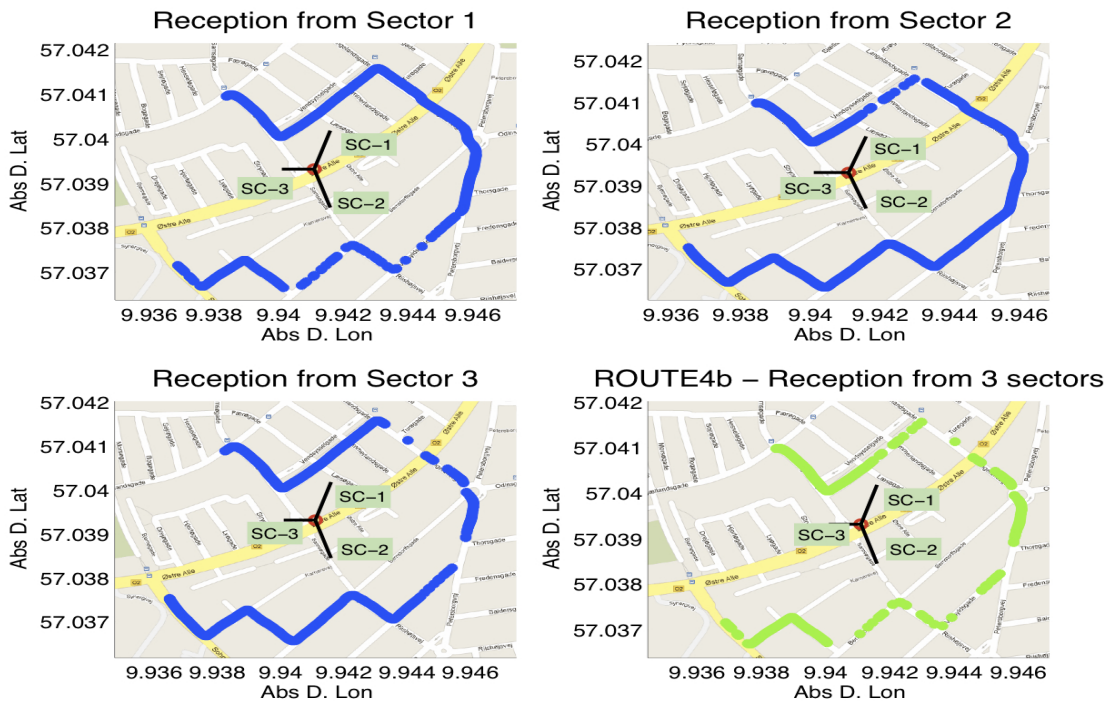


Figure D.12: Received power points along the route 4-B.

D.5 Route 5 Data

- Antenna height of 34 meters.
- Antenna models and configuration:
 - Sector 1: Model= Kathrein 206516, Tilt= 9° , Bearing= 40° .
 - Sector 2: Model= Kathrein 206516, Tilt= 8° , Bearing= 180° .
 - Sector 3: Model= Kathrein 206516, Tilt= 6° , Bearing= 280° .
- Mounting structure aperture angle impossible to know. Antennas are mounted in a metallic structure but not with the manufacturer predefined mounting structure, Appendix F.
- Urban Environment with Homogeneous building density (3-4 floors, around 15 meters of height). Actually, we adapt Cost-231 Propagation model selecting $C = 0dB$ because of the almost suburban environment behaviour.

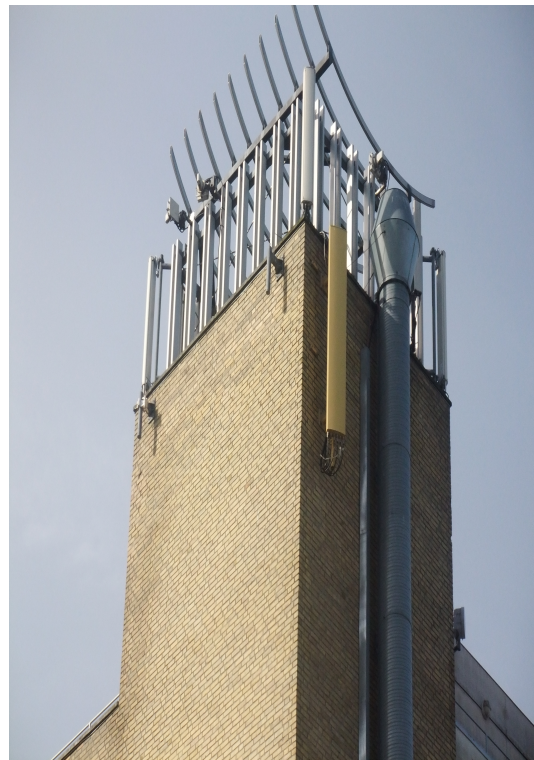
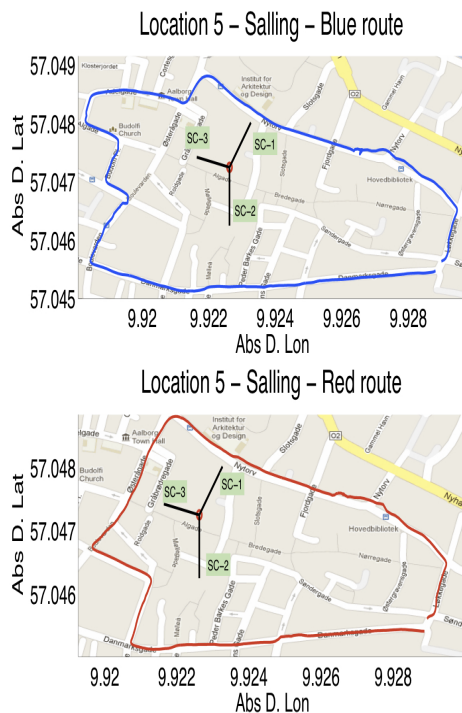


Figure D.13: Diferent routes and deployment specification for route 5.

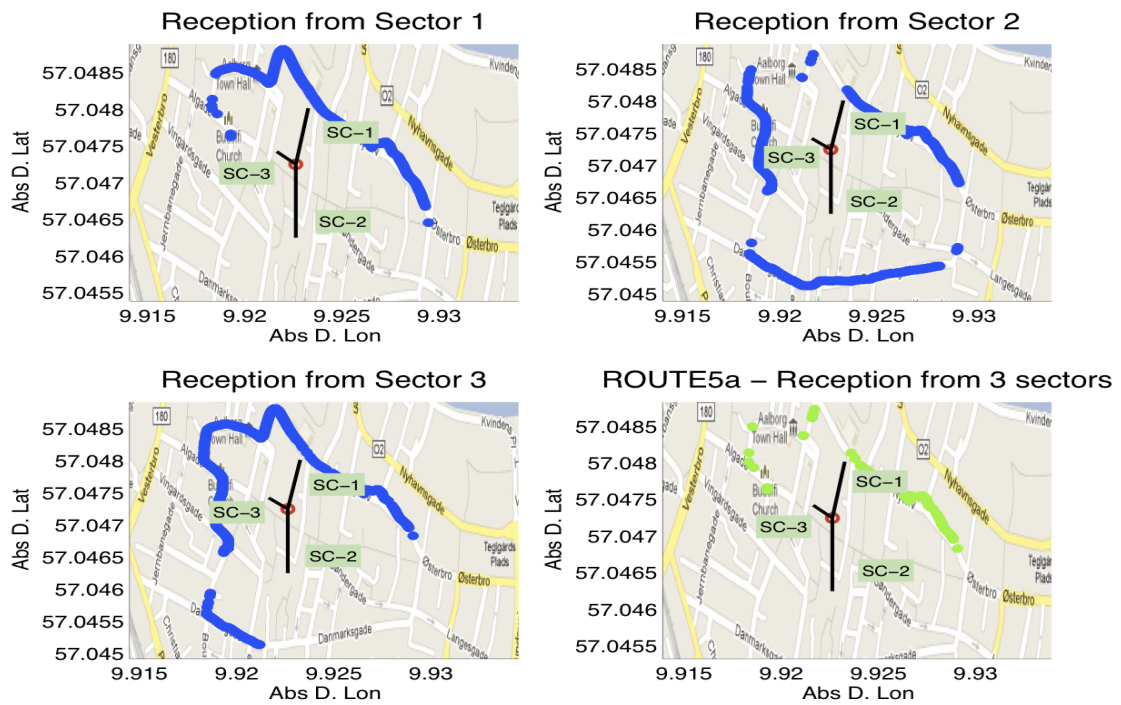


Figure D.14: Received power points along the route 5-A.

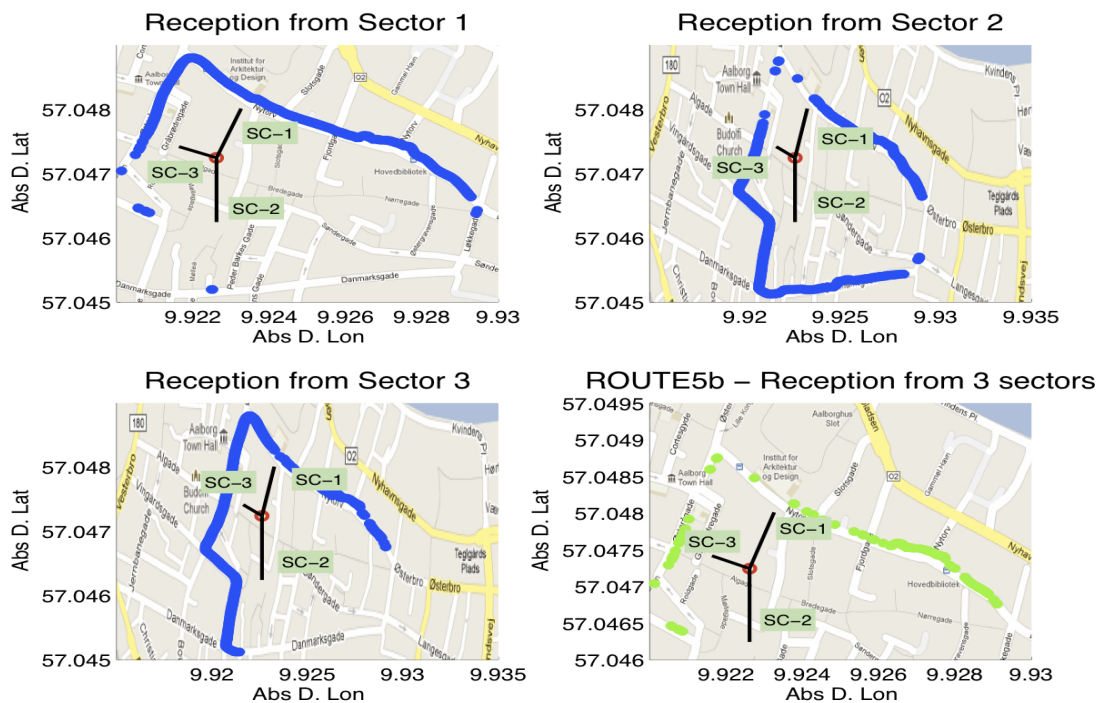


Figure D.15: Received power points along the route 5-B.

D.6 Route 6 Data

- Antenna height of 23 meters.
- Antenna models and configuration:
 - Sector 1: Model= Kathrein 742215, Tilt= 8° , Bearing= 100° .
 - Sector 2: Model= Kathrein 742215, Tilt= 6° , Bearing= 220° .
 - Sector 3: Model= Kathrein 742215, Tilt= 8° , Bearing= 340° .
- Mounting structure aperture angle impossible to determine. It is a chimney structure what makes impossible to see the mast and we did not find any manufacturer specifying their dimensions.
- Urban Environment with Homogeneous building density (3-4 floors, around 15 meters of height). Actually, we adapt Cost-231 Propagation model selecting $C = 0dB$ because of the almost suburban environment behaviour.



Figure D.16: Diferent routes and deployment specification for route 6.

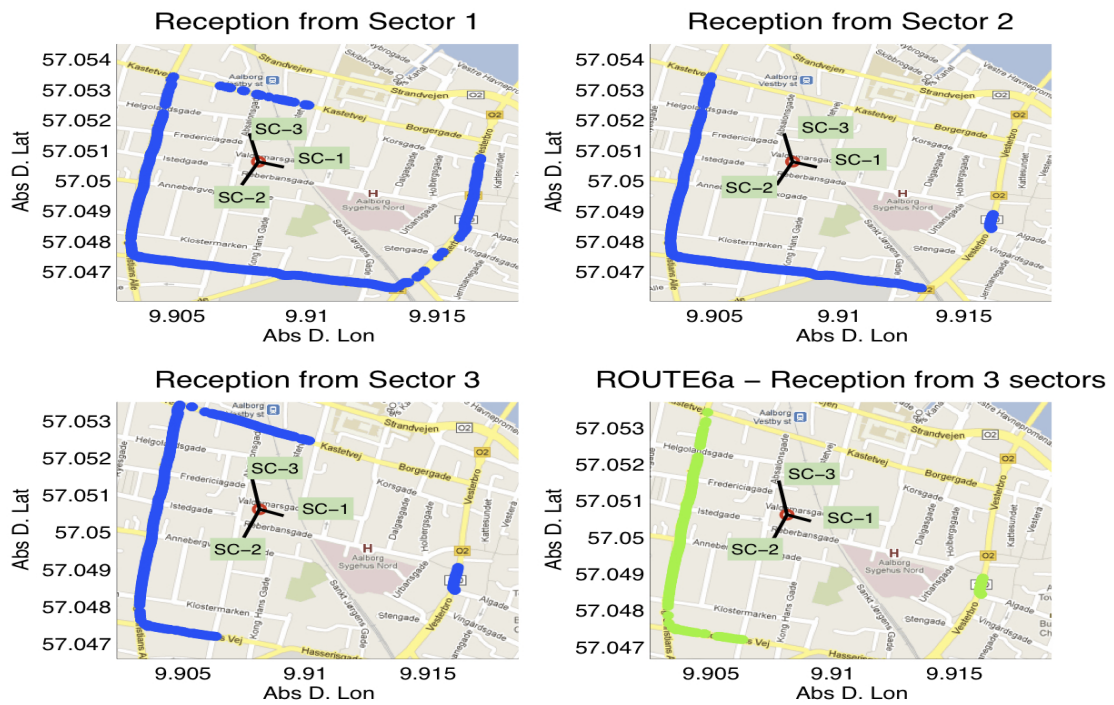


Figure D.17: Received power points along the route 6-A.

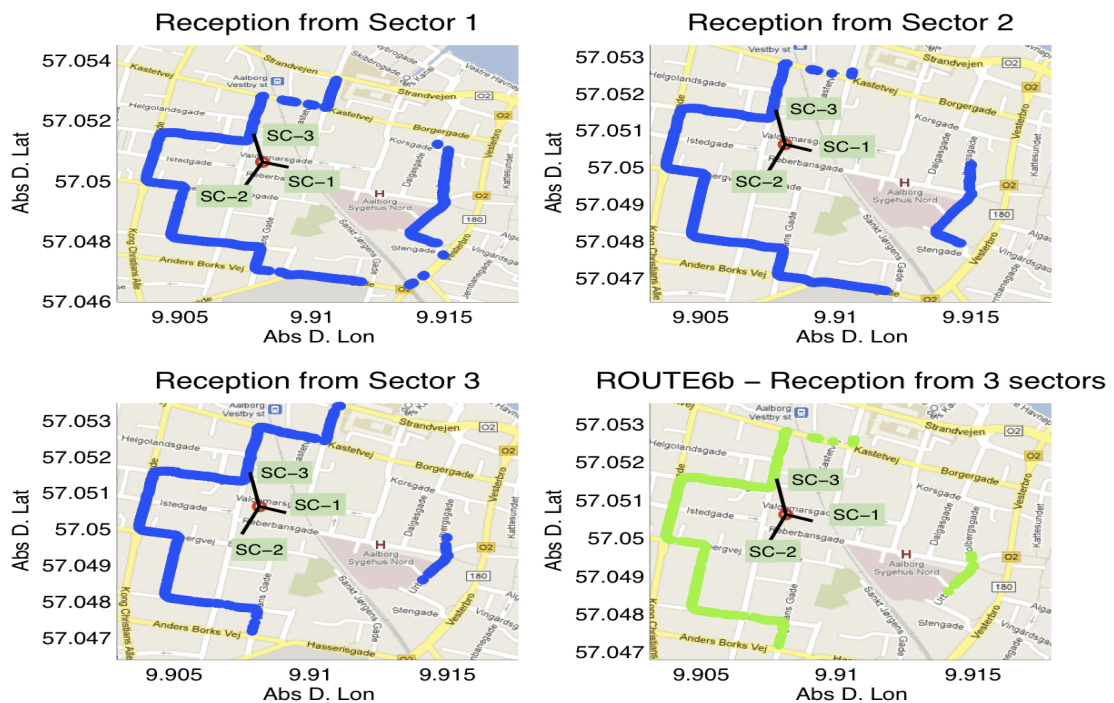


Figure D.18: Received power points along the route 6-B.

Appendix E

Equipment Information

In this appendix are collected the equipment information to carry out the measurement campaign. Thus, we include every device and connections characteristics necessary to understand the interaction of these items with the measured magnitude.

In addition, the measurement equipment configuration is defined as well to have a better idea about the performance to obtain the data from a real Mobile Communication Network.

E.1 Measurement Equipment

DEVICE	DESCRIPTION
Antenna SWA-0859	Omnidirectional antenna (6 dBi) at 2.6 m
ANT-TSMW connection	Coaxial cable (0.87 dB Attenuation)
GPS Antenna	Antenna to obtain measurement global position
R&S TSMW	Radio Network Scanner
TSMW-Laptop connection	LAN cable
Laptop	Fujitsu Lifebook E7800

Table E.1: Equipment description used for the measurements.

Every electronic device has its own characteristics which Manufacturers always give it with extended information. So, next sections summaries the relevant ones for this project.

E.1.1 HUBER&SUHNER SWA-0859/360/4/10/V

Omnidirectional antenna designed by HUBER & SUHNER [24]. Table E.2 contains the specifications given by the manufacturer for this antenna.

In this particular case, it is an ultra broad band antenna that allows final users to measure different technologies as GSM (900 & 1800), CDMA, UMTS, WIFI, WLAN (2400 & 5600), WiMax or LTE between others. Hence, its antenna gain has a variation in order of 2 dBi (5-7 dBi) dependent on the frequency range/technology where it is being measuring.

PARAMETER	VALUE
Model	1399.17.0037
Frequency range	806 MHz to 5875 MHz
Impedance	50 Ω
VSWR	$< \pm 1.5$
Polarization	Vertical
Gain	≈ 6 dBi for UMTS
-3 dB Beamwidth (H)	360°

Table E.2: SWA-0859 data specifications.



Figure E.1: SWA-0859 Omnidirectional Antenna.

E.1.2 R&S TSMW

TSMW is a radio network scanner manufactured by RHODE & SCHWARZ [25]. It allows to perform measurements from two different inputs with different antennas but they can not be measured at the same time. Furthermore, this device is capable to measure on different technologies like WCDMA or GSM as well as LTE.

Another important characteristic is that it can demodulate 3G Broadcast information.

PARAMETER	VALUE
Frequency rate	30 MHz to 6 GHz
Input bandwidth	20 MHz
Sampling rate	up to 200 <i>samples/s</i>
WCDMA Sensitivity	up to -123 dBm
WCDMA dynamic range	up to 30 dB
Level measurement uncertainty (30 MHz to 2.5 GHz)	$< \pm 1$ dB

Table E.3: TSMW specifications.



Figure E.2: TSMW radio network scanner.

E.1.3 Cables

For this configuration we used just one connection cable between the omnidirectional antenna and radio network scanner. This cable was calibrated thanks to a signal generator and a spectrum scanner obtaining an attenuation factor of 0.87 dB.

E.2 Measurement Setup

The use of a vehicle is completely necessary, due to the fact that it represents the medium to mount all devices like antennas and Network scanner. Specifically for this project was used a van from the Center for Personkommunikation (CPK) of aalborg University where mount all the equipment.

Figure E.3 and Figure E.4 relate the structure of the van with the metrics of the antenna height and a schematic configuration image to understand better this setup.

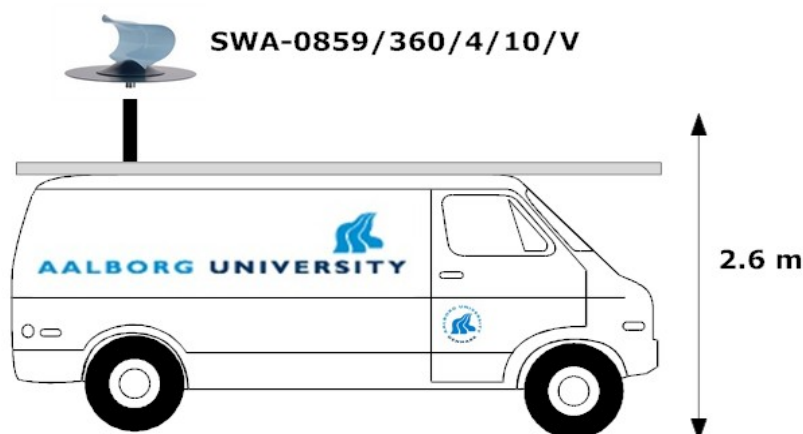


Figure E.3: Antenna layout on the van.

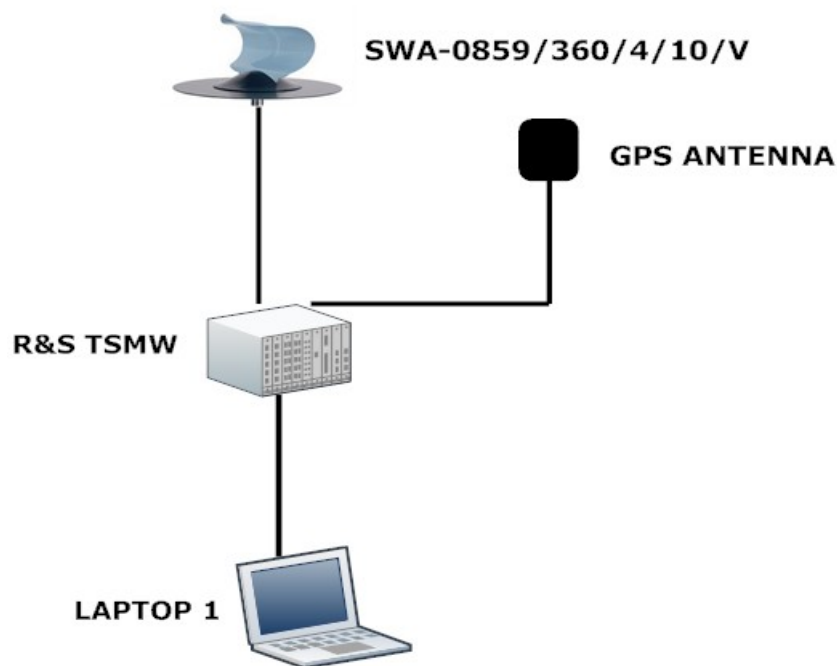


Figure E.4: Schematic connection for measurement equipment.

Finally, you can see some real pictures of the van with all of the equipment at the end of this section. It is possible to watch here all the connectivity systems used to carry out the measurement campaign.



Figure E.5: Real van which we carried out the measurement campaign.



Figure E.6: Connections between the equipment.

Appendix F

Datasheets

This appendix focuses on technical aspects in relation to the equipment where we found some useful data for the current project. Everything related to devices that we used such as antennas, structures where antennas were mounted, network scanner analyser, etc.

F.1 katherin-scala 742215 Antenna



742 215

65° Panel Antenna

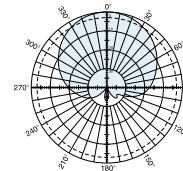
Kathrein's X-polarized adjustable electrical downtilt antennas offer the wireless carrier the ability to tailor polarization diversity sites for optimum performance. Using variable downtilt, only a few models need be procured to accommodate the needs of widely varying conditions. Remotely controlled downtilt is available as a retrofitable option.

- 0-10° downtilt range.
- DC Grounded metallic parts for impulse suppression.
- No moving electrical connections.
- Wideband vector dipole technology.
- Optional remote downtilt Control.
- Will accommodate future 3G / UMTS applications.

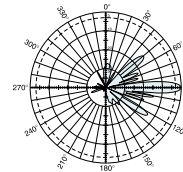
General specifications:

Frequency range	1710–2200 MHz
Impedance	50 ohms
VSWR	< 1.5:1
Intermodulation (2x20w)	IM3: < -150 dBc
Polarization	+45° and -45°
Front-to-back ratio (180° ±30°)	>30 dB (co-polar) >25 dB (total power)
Maximum input power	300 watts per input (at 50°C)
Electrical downtilt continuously adjustable	0–10 degrees
Connector	2 x 7-16 DIN female
Isolation	>30 dB
Cross polar ratio	
Main direction 0°	25 dB (typical)
Sector ±60°	>10 dB
Weight	13.7 lb (6.2 kg)
Dimensions	51.7 x 6.1 x 2.8 inches (1314 x 155 x 70 mm)
Wind load	at 93 mph (150kph)
Front/Side/Rear	79 lbf (350 N) / 21 lbf (90 N) / 79 lbf (350 N)
Wind survival rating*	120 mph (200 kph)
Shipping dimensions	62.8 x 6.8 x 3.6 inches (1595 x 172 x 92 mm)
Shipping weight	17 lb (7.7 kg)
Mounting	Fixed mount options are available for 2 to 4.6 inch (50 to 115 mm) OD mast.

See reverse for order information.



Horizontal pattern
±45°- polarization



Vertical pattern
±45°- polarization



Specifications:	1710–1880 MHz	1850–1990 MHz	1920–2200 MHz
Gain	17.7 dBi	17.9 dBi	18 dBi
+45° and -45° polarization horizontal beamwidth	68° (half-power)	66° (half-power)	64° (half-power)
+45° and -45° polarization vertical beamwidth	7.1° (half-power)	6.8° (half-power)	6.4° (half-power)
Vertical Pattern—sidelobe suppression for first side-lobe above main beam	0° 4° 8° 10° 18 18 17 17 dB	0° 4° 8° 10° 18 18 17 17 dB	0° 4° 8° 10° 18 18 17 17 dB



*Mechanical design is based on environmental conditions as stipulated in EIA-222-G (April 2007) and/or ETS 300 019-1-4 which include the static mechanical load imposed on an antenna by wind at maximum velocity. See the Engineering Section of the catalog for further details.

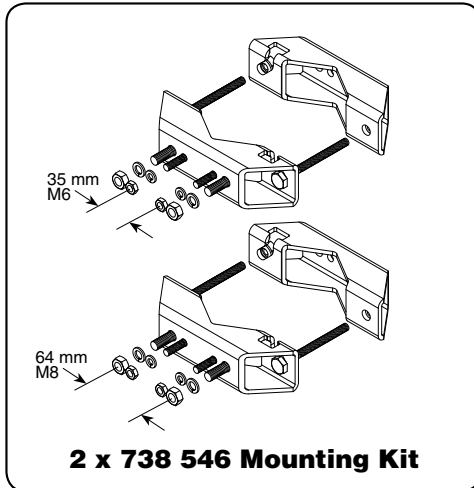
10822-G
936.3439/d

Kathrein Inc., Scala Division Post Office Box 4580 Medford, OR 97501 (USA) Phone: (541) 779-6500 Fax: (541) 779-3991
Email: communications@kathrein.com Internet: www.kathrein-scala.com



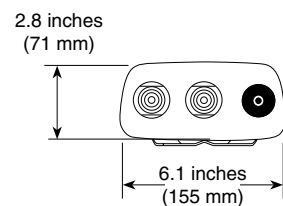
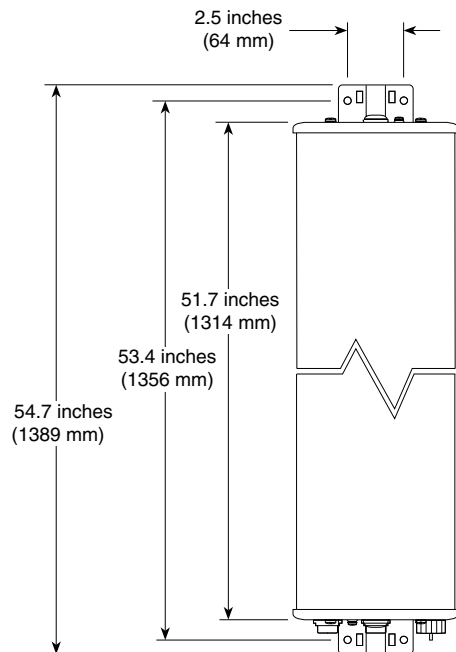
742 215

65° Panel Antenna



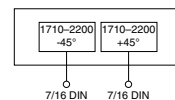
Mounting Options:

Model	Description
2 x 738 546	Mounting Kit for 2 to 4.6 inch (50 to 115 mm) OD mast.
850 10013	Locking Tilt Mount Kit 0–13 degrees downtilt angle.



Order Information:

Model	Description
742 215	Antenna with 7-16 DIN connectors 0°–10° adjustable electrical downtilt



All specifications are subject to change without notice. The latest specifications are available at www.kathrein-scala.com.

Kathrein Inc., Scala Division Post Office Box 4580 Medford, OR 97501 (USA) Phone: (541) 779-6500 Fax: (541) 779-3991
 Email: communications@kathrein.com Internet: www.kathrein-scala.com

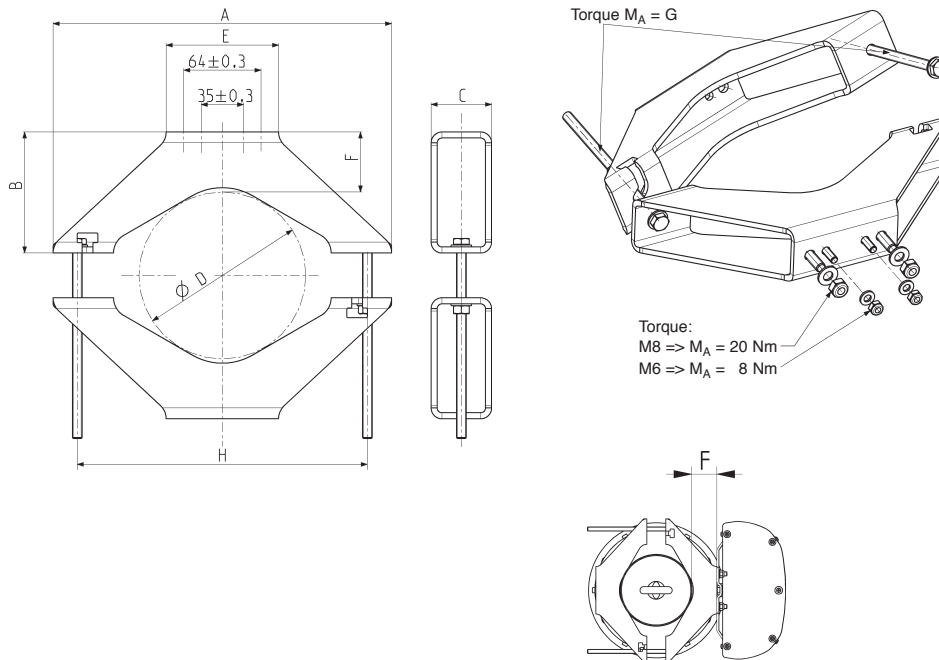
F.2 Panel accessory mounting hardware 738546

Panel Accessories Mounting Hardware Clamps

KATHREIN
Antennen · Electronic

Clamps

Type No.	731651	738546	85010002	85010003
Suitable for mast diameter	28 – 60 mm	42 – 115 mm	110 – 220 mm	210 – 380 mm
Antenna – mast distance F	40 – 44 mm	37 – 44 mm	47 – 56 mm	48 – 69 mm
Number of pieces	1 clamp	1 clamp	1 clamp	1 clamp
Material – Clamp	Hot-dip galvanized steel	Hot-dip galvanized steel	Hot-dip galvanized steel	Hot-dip galvanized steel
– Screws	Hot-dip galvanized steel/ Stainless steel	Hot-dip galvanized steel/ Stainless steel	Hot-dip galvanized steel/ Stainless steel	Stainless steel
– Nuts	Stainless steel	Stainless steel	Stainless steel	Stainless steel
Weight	0.8 kg	1.1 kg	2.7 kg	4.8 kg



Type No.	A	B	C	D	E	F	G	H
731651	116 mm	40 mm	40 mm	28– 60 mm	93 mm	40–44 mm	20 Nm	84 mm
738546	152 mm	40 mm	40 mm	42–115 mm	93 mm	37–44 mm	25 Nm	125 mm
85010002	280 mm	100 mm	50 mm	110–220 mm	93 mm	47–56 mm	35 Nm	240 mm
85010003	442 mm	150 mm	50 mm	210–380 mm	150 mm	48–69 mm	35 Nm	392 mm

Please note: Kathrein does not recommend to use counter nuts.
The additional nuts supplied are only meant as spares.

F.3 Rfd world 206516L Antenna

Product Data Sheet

APX18-206516L-CT6



Optimizer® Dual Polarized Antenna, 1710-2170, 65deg, 17.5/18.0dBi, 1.3m, FET, 6deg

Product Description

Dense urban networks where site aspect is essential.

Features/Benefits

- Very broadband design operating from GSM1800 up to 3G-UMTS.
- Reduction of visual impact by gathering 3 antennas in a cylindrical volume.
- Reduction of site dimensions will ease site acceptance.
- Possible camouflage solution on demand.
- Wind load thrust highly reduced.
- Compatible with usual base stations with 35 dB typical isolation between ports.
- Effective polarization diversity ensured by high cross polar discrimination.
- Optimized suppression of side lobes allows strong mechanical tilt.



Technical Specifications

Electrical Specifications

Frequency Range, MHz	1710-1900	1900-2170
Horizontal Beamwidth, deg	67	62
Vertical Beamwidth, deg	7	6.5
Electrical Downtilt, deg		6
Gain, dBi (dBd)	17.5 (15.4)	18 (15.9)
1st Upper Sidelobe Suppression, dB	>22	>18 (typ 20)
Front-To-Back Ratio, dB		>27
Polarization	Dual pol +/-45°	
VSWR	< 1.4:1	
Isolation between Ports, dB	>30 (typ 35)	
3rd Order IMP @ 2 x 43 dBm, dBc	>150, N/A	
7th Order IMP @ 2 x 46 dBm, dBc	N/A, >170	
Impedance, Ohms	50	
Maximum Power Input, W	300	
Lightning Protection	Direct Ground	
Connector Type	(2) 7-16 Long Neck Female	

Mechanical Specifications

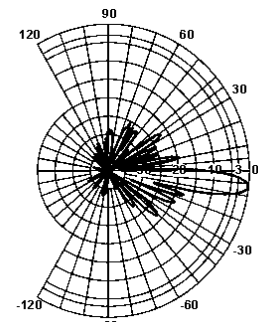
Dimensions - HxWxD, mm (in)	1349 x 169 x 80 (53.0 x 6.65 x 3.15)
Weight w/o Mtg Hardware, kg (lb)	8.5 (18.7)
Survival Wind Speed, km/h (mph)	200 (125)
Rated Wind Speed, km/h (mph)	160 (100)
Max Wind Loading Area, m² (ft²)	0.23 (2.46)
Front Thrust @ Rated Wind, N (lbf)	406 (91)
Maximum Thrust @ Rated Wind, N (lbf)	406 (91)
Wind Load - Side @ Rated Wind, N (lbf)	236 (53)
Wind Load - Rear @ Rated Wind, N (lbf)	196 (44)
Radome Material	Fiberglass
Radome Color	Light Grey RAL7035
Mounting Hardware Material	Diecasted Aluminum
Shipping Weight, kg (lb)	13.5 (30)
Packing Dimensions, HxWxD, mm (in)	1464 x 251 x 203 (57.64 x 9.88 x 7.99)

Ordering Information

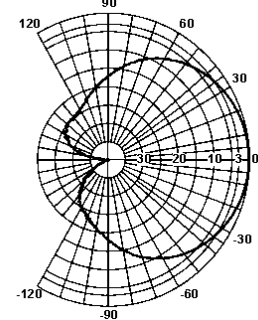
Mounting Hardware	APM40-2
Mounting Pipe Diameter, mm (in)	60-120 (2.36-4.72)
Mounting Hardware Weight, kg (lb)	3.4 (7.5)

Other Documentation

- [APM40 Series Datasheet](#)
- [APM40 Series Installation Instructions](#)



Vertical Pattern



Horizontal Pattern

All information contained in the present datasheet is subject to confirmation at time of ordering

RFS The Clear Choice ®

APX18-206516L-CT6

Rev: A1

Print Date: 14.06.2011

Please visit us on the internet at <http://www.rfsworld.com/>

Radio Frequency Systems

F.4 Panel accessory mounting hardware APM40-2

Universal Mount Kit		APM40 Series		RFS	
Installation and Ordering Instructions					
General Description					
<p>The RFS APM40 mounting kits are suitable for all base station antennas up to 2.6m in length.</p> <p>Benefits</p> <ul style="list-style-type: none"> • One mount kit fits all. This single mount kit can be used on the RFS range of CDMA800, GSM900, GSM1800, PCS1900, UMTS2100 and all multiband antennas. • Convenient, one handed adjustment. This new design incorporates self-captivated bolts to allow a rigger to easily adjust using one hand. • A single flexible mount system. The one system incorporates all options required for optimal adjustment flexibility. <p>Features</p> <ul style="list-style-type: none"> • A basic direct mount kit which can have added: Optional beam sliding tilt mount for mechanical downtilt Optional scissors tilt for fixed at mast (or wall) downtilt Optional azimuth adjustment independent of mast • All kits are fully upgradeable • Pipe diameter: 60-120 mm, or 30-60mm with optional adapter. • Wall mount option • Mechanical downtilt: 0-7.5° for 2.6m antennas 0-10° for 2m antennas 0-15° for 1.3m antennas • Azimuth adjustment up to +/-30° • Downtilt angle indicator • Suitable for industrial and marine environments 					
					
					
Antenna Ordering Information [eg: APX18-206516L-A (Antenna + Direct pipe mount)]					
Antenna Suffix	Type of Mounting	Mounting Kit			
A	Direct Pipe (no tilt)	APM40-1			
B	Azimuth upgrade	APM40-1 & APM40-E3			
C	Beam tilt	APM40-2 / APM40-3 / APM40-4 / APM40-5 / APM40-5D / APM40-5E / APM40-3HD*			
D	Beam tilt with azimuth upgrade	APM40-2 & APM40-E3			
E	Beam tilt with scissor upgrade	APM40-2 & APM40-E2			
F	Beam tilt with scissor and azimuth upgrades	APM40-2 & APM40-E2 & APM40-E3			
-	Direct to beam upgrade	APM40-E1			
-	Bracket interface for APM40	APM40-E4			
7	No mount kit	-			
-	Pipe adapter for 30-60mm pipes	APM40-E6			
* Model dependent					
Mechanical Specifications					
Weight of kit, kg (lb)		1.8 (4.0) Direct kit APM40-1 3.4 (7.49) Beam tilt kit APM40-2 5.4 (11.9) Beam tilt kit APM40-3, APM40-3HD 2.7 (5.95) Beam tilt kit APM40-4 13 (28.6) Beam tilt kit APM40-5 8 (17.6) Beam tilt kit APM40-5D 10.0 (22.0) Beam tilt kit APM40-5E			
Mounting kit material		Aluminum, Galvanized steel			
Packed size, H x W x D, mm (in)		1250 x 200 x 70 (49.2 x 7.9 x 2.7) Beam tilt kit 950 x 200 x 70 (37.4 x 7.9 x 2.8) APM40-4 Beam tilt kit 730 x 200 x 45 (28.7 x 7.9 x 1.8) direct kit			
Packaging material		Plastic sleeve			
Tools required		18mm (0.75") AF Socket (3/8" drive recommended), 10mm (0.4") AF spanner or socket			
RFS The Clear Choice®		Universal Mount Kit		ANAI-702 Iss8 Print Date: 13.1.2012	
Please visit us on the internet at http://www.rfsworld.com				Radio Frequency Systems	

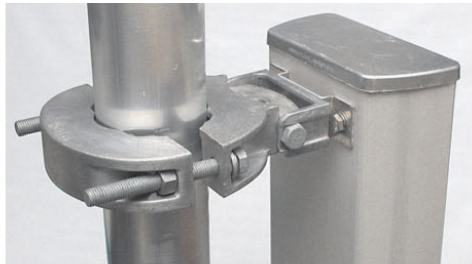
All information contained in the present sheet is subject to confirmation at time of ordering.

Universal Mount Kit

APM40 Series



Installation and Ordering Instructions



*APM40-1
Direct Mount configuration. Pole mounted.*



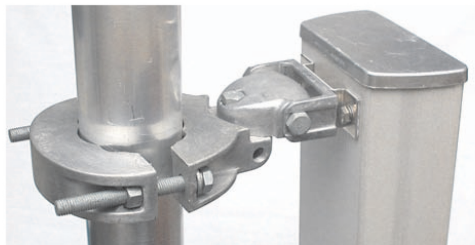
*APM40-2 or APM40-3
Beam tilt configuration at 0deg. Pole or Wall mount.*



*APM40-1 + APM40-E3
Direct Mount configuration with Azimuth adjustment.
Wall mounted.*



*APM40-2 + APM40-E2 + APM40-E3
Beam tilt configuration at 0deg with scissor kit and
azimuth adjustment. Pole or Wall mount.*



*APM40-1 + APM40-E3
Direct Mount configuration with Azimuth adjustment.
Pole mounted.*



*APM40-2 + APM40-E3
Beam tilt configuration at
0 deg with Azimuth
adjustment
Pole or Wall mount.*



*APM40-2 + APM40-E2 + APM40-E3
Beam tilt configuration at 6deg with scissor kit and
azimuth adjustment. Pole or Wall mount.*



*APM40-2 + APM40-E2
Beam tilt configuration
with scissor kit.
Pole or Wall mount.*



*APM40-E6
Adapter for 30-60mm pipe.*

All information contained in the present sheet is subject to confirmation at time of ordering.

RFS The Clear Choice®

Universal Mount Kit

ANA1-702 Iss8

Print Date: 13.1.2012

Please visit us on the internet at <http://www.rfsworld.com>

Radio Frequency Systems

F.5 HUBER&SUHNER

HUBER+SUHNER® DATA SHEET Sencity Art Antenna: 1399.17.0037

Rev.: AQ



SWA-0859/360/4/10/V

Description

Omnidirectional antenna for indoor DAS and In-Building Coverage
Ultra broad band antenna supporting AMPs, CDMA, PCS, UMTS1900, GSM 900, GSM 1800, UMTS, WiFi, WLAN 2400 and 5600, WiMax



Product Configuration

Technical Data

Electrical Data

	Band 1	Band 2	Band 3	Band 4
Frequency (MHz)	806 - 960	1710 - 2170	2400 - 5600	5600 - 5875
VSWR	1.5	1.5	1.5	2
Gain (dBi)	5	6	7	7

General Data

Nominal impedance	50 Ω
IMD level	143 dBc at carrier power 2x 30 dBm
Polarisation	vertical
Connector	N, jack (female), bottom
Composite power max.	300 W at ambient temperature 50 °C

Mechanical Data

Dimensions (mm)	91 x 200 (Height x Diameter)
Weight	0.3 kg
Windload	frontal: 18 N at km/h

Environmental Data

Environmental conditions	indoor
Operation temperature (°C)	-40 to 80
Storage temperature (°C)	-40 to 80
Transport temperature (°C)	-40 to 80
RoHS 2002/95/EC	compliant

Material Data

Radome colour	
Back plate/base plate material	Aluminium

Related Products

9091.99.0095 Ceiling Bracket_SencityArt

Related Documents

Mounting instruction	DOC-0000197543
Painting instruction	DOC-0000256180
Security instruction	DOC-0000278984
Outline drawing1	DOU-00061284.1

HUBER+SUHNER is certified according to ISO 9001 and ISO 14001

WAIVER!

It is exclusively in written agreements that we provide our customers with warrants and representations as to the technical specifications and/or the fitness for any particular purpose. The facts and figures contained herein are carefully compiled to the best of our knowledge, but they are intended for general informational purposes only.



HUBER+SUHNER AG
RF Industrial
9100 Herisau, Switzerland
Phone +41 (0)71 353 41 11
Fax +41 (0)71 353 45 90
www.hubersuhner.com

HUBER+SUHNER – Excellence in Connectivity Solutions

Document: DOC-0000329321 W

Issued: 07.09.11

Uncontrolled Copy

Page 1/1

F.6 R&S TSMW Universal Network Radio Scanner

Specifications

Specifications		
RF characteristics		
Frequency range		30 MHz to 6 GHz
Reference frequency	internal	1×10^{-6} aging per year
Level measurement uncertainty	S/N > 16 dB, 30 MHz to 2.5 GHz	< 1 dB
	S/N > 16 dB, 2.5 GHz to 6 GHz	< 1.5 dB
Maximum permissible input level		5 dBm/0 V DC
Noise figure	3.5 GHz, preamplifier ON	typ. 7 dB
	3.5 GHz, preamplifier OFF	typ. 19 dB
Intermodulation-free dynamic range	level 2 \times -45 dBm, 3.5 GHz, preamplifier ON	typ. -65 dBc (-12.5 dBm TOI)
	level 2 \times -35 dBm, 3.5 GHz, preamplifier OFF	typ. 70 dBc (0 dBm TOI)
RF receive paths	independent	2
VSWR	30 MHz \leq f \leq 2.5 GHz	typ. 1.5
	2.5 GHz \leq f \leq 6 GHz	typ. 1.7
Preselection channels		5 per RF path, 3 used as tracking filters
LTE characteristics		
Frequency bands supported		no restrictions
Measurement modes		LTE-FDD and TD-LTE
Measurement speed	automatic detection of all 504 physical cell IDs	max. 200 measurements/s
Physical decoding accuracy		
Sensitivity for initial physical cell ID decoding		-123 dBm
Sensitivity after successful physical cell ID decoding		-127 dBm
SINR dynamic range		max. 42 dB
WiMAX™ characteristics		
Frequency bands supported		no restrictions
Measurement speed	automatic detection of all 114 preamble indices	5 measurements/s
Preamble decoding accuracy	frame duration 5 ms; FFT size 1024; bandwidth 10 MHz; 2.5 GHz	± 1 dB (-30 dBm to -109 dBm)
Sensitivity for initial preamble decoding	RSSI	< -97 dBm
Sensitivity after successful preamble decoding	RSSI	< -112 dBm
SINR dynamic range		-20 dB to +40 dB
GSM characteristics		
Frequency bands supported		no restrictions
Measurement modes		SCH code power, TCH total in-band power, timeslot power, BCH demodulation for all system information types
Measurement speed		500 channels/s
Sensitivity		-118 dBm
Measurement accuracy		typ. ± 1 dB
BSIC decoding accuracy		98% for C/I > +2 dB
BSIC decoding dynamic range		
Sensitivity for initial BSIC detection		C/I > -18 dB
Sensitivity after successful BSIC detection		C/I > -29 dB
BCCH decoding dynamic range		C/I > 0 dB
WCDMA characteristics		
Frequency bands supported		no restrictions
Number of RF carrier frequencies		max. 12
Measurement speed	high speed/high dynamic range automatic detection of all 512 scrambling codes	100 Hz/12 Hz, with BCH demodulation
Scrambling code detection sensitivity		
Sensitivity for initial SC detection	high speed/high dynamic range	-112 dBm/-121 dBm
Sensitivity after successful SC detection	high speed/high dynamic range	-118 dBm/-123 dBm

Specifications		
Scrambling code detection accuracy	RSCP	typ. < 1 dB
	$E_c/I_0 > -12$ dB	typ. < 1.5 dB
Scrambling code false detection (ghost code)		< 10^{-9}
Dynamic range E_c/I_0		-22 dB/-30 dB
Min. BCH demodulation threshold E_c/I_0		> -17 dB
CDMA2000® characteristics		
Frequency bands supported		no restrictions
Number of RF carrier frequencies		max. 18
Measurement speed	automatic detection of all 512 PN	10 Hz
PN detection sensitivity		-119 dBm
Dynamic range	E_c/I_0	29 dB
1xEV-DO characteristics		
Frequency bands supported		no restrictions
Number of RF carrier frequencies		max. 18
Measurement speed		10 Hz
PN detection sensitivity		-120 dBm
Dynamic range	E_c/I_0	33 dB
TETRA characteristics		
TETRA bands supported		no restrictions
Number of RF carrier frequencies	within a 10 MHz downlink band	max. 400
Channel resolution		25 kHz (QPSK)
Measurement speed		max. 8000 channels/s, 20/s for a 10 MHz block
Sensitivity	RSSI measurements	-120 dBm
	TETRA BSCH decoding (BSCH decoding for channels with an SNR > 9.5 dB)	-115 dBm
I/Q characteristics (requires R&S®TSMW-K1)		
Digital filter bandwidth, burst		800 kHz to 20 MHz
Digital filter bandwidth, streaming	hardware requirements: Gbit LAN link, jumbo frames, hard disk transfer rate 80 Mbyte/s	max. 22 Msample/s
Resampling rate		1 Msample/s to 21.94 Msample/s
Demodulation bandwidth		20 MHz
I/Q buffer size		200 Mbyte
Gbit LAN I/Q interface		
Data format	14 bit ADC resolution	8, 12, 16 or 20 bit
R&S®Digital I/Q interface (additionally requires R&S®TSMW-B1¹⁾		
Interface	clock rate	71.4 MHz, fix
	level	LVDS
	connector	26-pin MDR
Data format	channel link protocol: clock rate max. 22.1 MHz	20 bit
Source	interface mode 1 (enable mode)	frontend 1 and 2
RF power scan		
Frequency range		30 MHz to 6 GHz
Resolution bandwidths		140 Hz to 1.438 MHz
Sensitivity	22.4 kHz RBW, RMS, at 900 MHz	
	preamplifier OFF	-107 dBm
	preamplifier ON	-116 dBm
	140 Hz RBW, RMS, at 900 MHz	
	preamplifier OFF	-129 dBm
	preamplifier ON	-138 dBm
Scan speed	180 kHz resolution, 100 MHz span, 20 MHz bandwidth ²⁾	130 Hz
	11.23 kHz resolution, 10 MHz span, 10 MHz bandwidth ²⁾	690 Hz
	140 Hz resolution, 1 MHz span, 1 MHz bandwidth ²⁾	64 Hz